THE UNIVERSITY
of EDINBURGH

THE UNIVERSITY
of EDINBURGH

Investigating mechanisms of RNAi-dependent heterochromatin establishment in *Schizosaccharomyces pombe*

Ekaterina Kapitonova

Submitted for the degree of Doctor of Philosophy

University of Edinburgh

October 2019

Table of Contents

Declaration

I declare that the work presented in this thesis was conducted by myself, except where it is explicitly stated otherwise. This work has not been submitted for any other degree or professional qualification.

Signed,

Ekaterina Kapitonova

Acknowledgments

First, I want to thank my supervisor Dr Elizabeth Bayne for giving me such a challenging and exciting project to work on. I also want to thank her for critically reading and suggesting corrections for this thesis. I want to thank my colleagues for their support and friendship. I especially want to thank Jo Strachan for multiple scientific discussions and her continuous help during my project. Her critical input was crucial for the progression of this thesis. I want to thank Elliott Chapman for discussing my results and for helping me to improve my experiments. Special thanks go to Ana Arsenijević: our coffee breaks and adventures beyond work made me a happier person. I am truly grateful to find such an amazing friend. I want to thank Jerko Roško for all the jokes and laughter we had. I also want to thank Dmitry Degtev for always being ready for fun and for organizing Christmas lunches with me. I am eternally grateful to my parents, Irina Kapitonova and Sergey Kapitonov, for their unconditional love and support.

I would like to specially thank Pedro Almada, whose love, wisdom and patience made me a better person. His constant encouragement and support in all endeavours helped me to become who I am now.

Finally, I want to dedicate this thesis to my childhood angel, my dog Sherry, who is no longer with us, but who left an unforgettable imprint on all of my family.

Lay summary

Cells contain genetic information in form of DNA. Information stored in DNA has to be retrieved and interpreted for cells to function normally, and it has to be passed on to the daughter cells during cell division. The retrieval of information from DNA and inheritance depend on DNA organization. Different types of DNA organization are achieved by interaction of DNA with proteins called histones to form a complex called chromatin. Chromatin can be compressed to form a tightly packaged DNA:protein structure called heterochromatin, which prevents information retrieval from DNA. Chromatin can also be loosely organized in euchromatin, which is an open chromatin configuration required for genetic information retrieval. These various states of chromatin organization are crucial for correct information retrieval from DNA, and they are frequently perturbed in such diseases as cancer. Thus it is essential to study the mechanism of chromatin organization in order to understand how healthy and diseased organisms work.

My thesis investigated the process of heterochromatin establishment at the centromeres of yeast *Schizosaccharomyces pombe*, which is a crucial for normal cell division. Centromeric heterochromatin formation in *S. pombe* depends on RNA interference (RNAi). RNAi relies on the association of RNA with the target chromatin region,

leading to the recruitment of multiple protein complexes that drive heterochromatin formation. Once established, heterochromatin is maintained from one generation to the next. Currently we know fairly well how heterochromatin is maintained, but establishment is not yet well understood. Recent discoveries indicate that there are factors that are required specifically for the establishment phase, but not maintenance. However it is not clear how many of these factors exist. It is also not yet clear in what order the already known factors act. During my project I developed two assays that aimed to efficiently detect potential establishment factors present in the genome. I tested these assays using sixteen mutant strains lacking preselected candidate factors. Using various molecular biology techniques and genetic assays I was able to characterize two potential establishment factors, as well as to reveal previously unseen heterochromatin establishment dynamics. In the process of assay characterization, one of the assays (called cross-based assay) was shown to be more suitable for studying heterochromatin formation. Thus in the future, the cross-based assay can be further used to advance our knowledge about heterochromatin establishment.

Abstract

Heterochromatin is a condensed conformation of eukaryotic DNA, which plays an essential role in genome homeostasis. In depth research across various species showed that RNA interference (RNAi) is one of the pathways that is important for heterochromatin formation. To date RNAi-driven heterochromatin assembly has been extensively studied in the fission yeast *Schizosaccharomyces pombe.* At centromeres in *S. pombe*, RNAi is required for heterochromatin establishment and maintenance. Unlike heterochromatin maintenance, RNAi-driven heterochromatin establishment at the centromeres is not very well understood. The interconnectedness between the RNAi and chromatin modification pathways that are required to establish heterochromatin makes it difficult to elucidate which pathway acts first. Recent studies also showed that heterochromatin establishment requires additional factors dispensable for maintenance. Thus exploring novel factors required for the *de novo* heterochromatin formation can help us to understand the order and the mechanism of heterochromatin establishment. In this study I developed and tested two assays — plasmid-based and cross-based assays — designed to identify novel establishment-specific factors genome-wide. While the plasmid-based assay proved unreliable, the cross-based establishment assay was shown to effectively identify establishment-specific factors. It

also provided new insights into heterochromatin establishment dynamics.

Abbreviations

ARC – Argonaute siRNA chaperone

CLRC – CLr4-Rik1-Cul4 complex

CMT3 – Chromomethylase

DNMT3a – DNA methyltransferase 3 Alpha

dsRNA – Double stranded RNA

exo-siRNA – Exogenous siRNA

HAT – Histone acetyltransferase

HDAC – Histone deacetylase

HKMTs – Histone lysine methyltransferase

HP1 – Heterochromatin protein 1

JmjC – Jumonjii C

lncRNA – long non coding RNA

miRNA – microRNA

NFR – Nucleosome-free region

PEV – Position effect variegation

PH – Pleckstrin homology

piRNA –PIWI-interacting RNA

PRC2 – Polycomb repressive complex 2

PTGS – Posttranscriptional gene silencing

PTM – Post-translational modifications

RdRP – RNA-dependent RNA polymerase

RDRC – RNA-directed RNA polymerase complex

RISC – RNA-induced silencing complex

RITS – RNA-induced transcriptional silencing

RNAi – RNA interference

TGS – transcriptional gene silencing

SAM – S-adenosylmethionine

sRNA – small RNA

siRNA – small interfering RNA

XCI – X chromosome inactivation

Chapter 1 — Introduction

1.1 Epigenetics

The term "epigenetics" was coined by Conrad Waddington, for whom it was the study of developmental processes that allow phenotype to arise from genotype (Waddington, 1942). He then developed this idea further, proposing a concept of "epigenetic landscape", which illustrates different developmental pathways that a cell can undergo toward different differentiated states (Waddington, 1957). Since then the definition of epigenetics has undergone many refinements. For example, Arthur Riggs and colleagues proposed a definition of epigenetics as "the study of mitotically and/or meiotically heritable changes in gene function that cannot be explained by changes in DNA sequence'' (Russo, Martienssen and Riggs, 1996). The definition by Riggs and colleagues thus focuses on what epigenetics is not, without suggesting potential mechanisms at work. Mark Ptashne, in turn, put forward a definition of epigenetics as a study of heritable changes in gene expression without changes in the underlying DNA sequences that can be maintained by positive feedback loops without the initiating signal (Ptashne, 2013). Adrian Bird, however, questioned the necessity of heritability as an important component of epigenetics. He defined epigenetics as "the structural adaptation of chromosomal regions so as to register, signal or perpetuate altered activity states" (Bird, 2007). This definition includes both

transient and stable changes with the focus on chromosomes and genes. A lot of current studies in eukaryotes focus on how DNA and chromatin modifications regulate gene expression. Thus in this context epigenetics is a study of chromatin modifications regulating gene expression (Allshire & Madhani, 2018).

Hermann Muller was one of the first to observe the effect of chromatin state affecting gene activity. By using X Rays to induce mutations in *Drosophila melanogaster*, he observed a variegating eye colour phenotype where eyes had red and white patches due to translocation of the *white* gene close to the pericentric silent heterochromatin (Elgin & Reuter, 2013; Muller, 1930). This phenomenon was called position effect variegation (PEV) since the variegating phenotype was caused by the change in gene position. This was one of the earliest experiments that showed the complexity of cellular data storage and retrieval: the phenotype depends not only on data stored in genes, but also on context-dependent data extraction and processing of it into meaningful information.

D. melanogaster is not the only model organism where PEV was observed. For example, in *Schizosaccharomyces pombe* PEV allowed us to advance our understanding of how chromatin modifications regulate gene expression (Allshire & Ekwall, 2015). Many of the

mechanisms that establish and maintain repressive chromatin environments are conserved between *S. pombe* and higher eukaryotes, making *S. pombe* an important model organism to study chromatin-based epigenetics.

1.2 Chromatin

In eukaryotic nuclei DNA is organized by histone and non-histone proteins into an organized structure called chromatin (Jenuwein & Allis, 2001). The basic unit of chromatin is the nucleosome, where DNA is wrapped twice around a core histone octamer in a superhelical structure (Fig 1-1). X Ray examination of nucleosome structure showed that histone octamers consist of four histone pairs: two H2A-H2B dimers and one H3-H4 tetramer (Luger, et al. 1997). Nucleosomes are connected to each other via linker DNA, thus forming the ~11-nm "beads on a string" fibre (Felsenfeld & Groudine, 2003). Nucleosomal position and histone modifications can further fold the "beads on a string" structure into a 30-nm chromatin fibre leading to around 50-fold DNA compaction. Finally, chromatin can be further compacted into higher-order structures, as well as undergo nuclear compartmentalization (Zhou, Goren, & Bernstein, 2011).

Chromatin compaction was first observed by Emil Heitz, who showed that compact chromatin, which he called heterochromatin, stained differently from decondensed chromatin, which he called euchromatin (Heitz, 1928). Euchromatin is more accessible and transcriptionally active, whereas heterochromatin is inaccessible and a more compact structure, that can be further classified into constitutive and facultative heterochromatin (Grewal & Jia, 2007). Constitutive heterochromatin describes gene-poor regions of permanent gene silencing such as at telomeres and centromeres, whereas facultative heterochromatin is found at genes that are silenced in a regulated manner during development (Bannister & Kouzarides, 2011).

Formation of qualitatively different chromatin states, such as heterochromatin or euchromatin, largely depends on nucleosome modifications and nucleosome occupancy (Allis & Jenuwein, 2016). Nucleosome modifications allow distinct epigenetic states to assemble, that can be read and translated into different biological outputs.

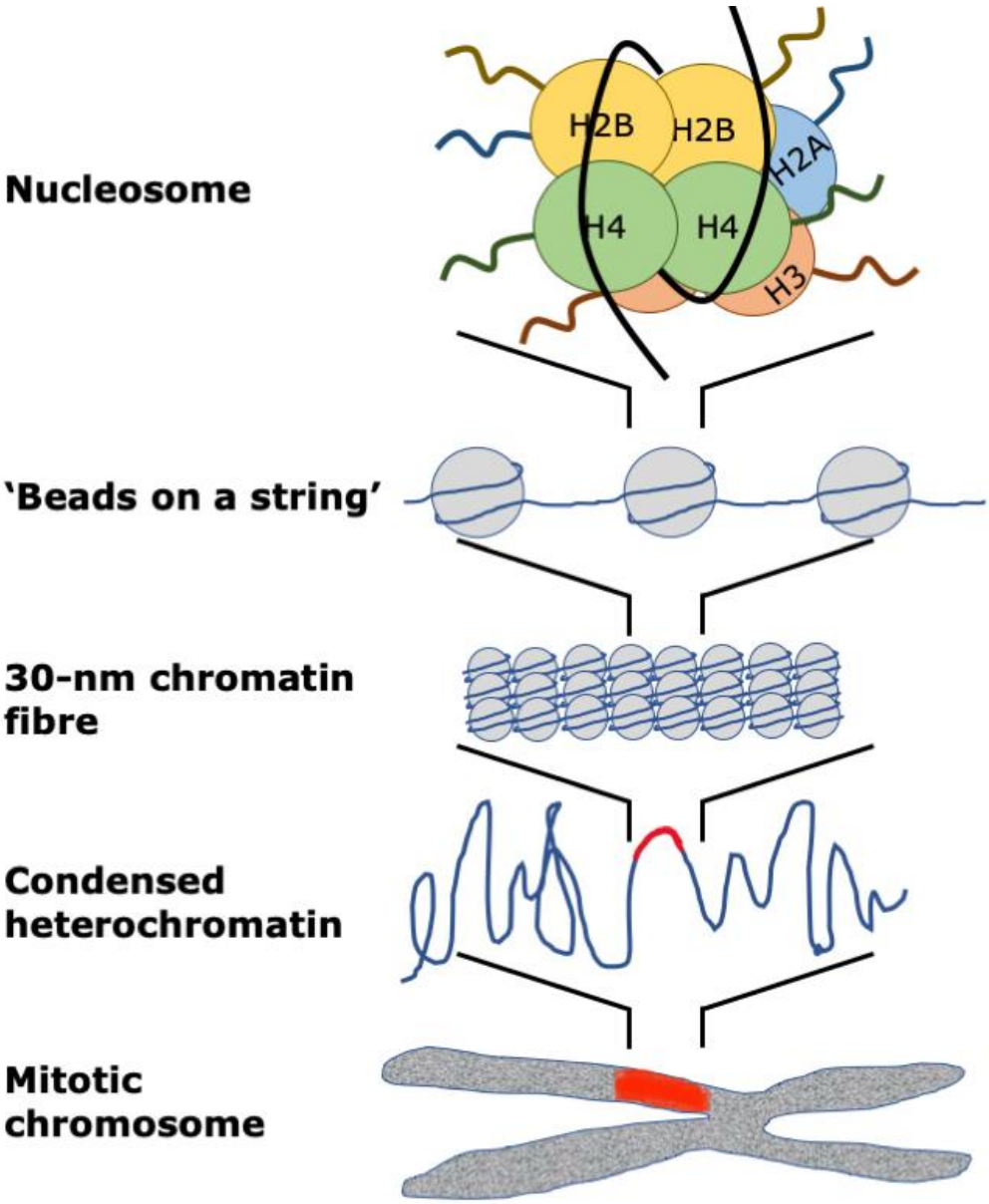

Figure 1-1 Chromatin organization. Schematic diagram of chromatin organization starting from a core nucleosome to a fully condescend mitotic chromosome.

1.2.1 Histone posttranslational modifications (PTMs)

Nucleosomes have protruding N-terminal histone tails that can be covalently modified, which, in turn, influences their interactions with neighbouring nucleosomes (Bannister & Kouzarides, 2011). The discovery that these modifications can be recognized by specific protein domains led to development of a "histone code" hypothesis (Allis & Jenuwein, 2016; Dhalluin et al., 1999). According to the "histone code" hypothesis, the modifications, introduced by various histone-modifying enzymes or "writers", can then be read by downstream effector proteins or "readers", as well as removed by "erasers".

1.2.1.1 Acetylation

Vincent Allfrey and colleagues were first to discover histone acetylation in 1964 (Allfrey, Faulkner, & Mirsky, 1964). Now we know that lysine acetylation is a dynamic process controlled by histone acetyltransferases (HATs) and histone deacetylases (HDACs) (Bannister & Kouzarides, 2011). HATs can be divided into type-A and type-B. The type-B HATs, such as Hat1 or KAT1, are highly conserved and acetylate free H3 and H4 histones, which ensures their deposition into nucleosomes (Parthun, 2007; Wapenaar & Dekker, 2016). In contrast to the type-B HATs, type-A HATs acetylate histones within the N-terminal tail. They are less

conserved than the type-B HATs, and according to their conformation and amino-acid sequence homology they can be classified into CBP/p300, GNAT and MYST families (Bannister & Kouzarides, 2011). HATs modify multiple sites in both the globular histone core and histone tails. Acetylation acts to neutralize the positive charge of lysine residues, which results in weakened interactions between histones and negatively-charged DNA (Musselman et al., 2012). Weakened histone-DNA interactions lead to chromatin adopting a more open confirmation, which generally correlates with transcriptional activity (Musselman et al., 2012).

HDAC enzymes have an opposing function to HATs, whereby they restore the positive charge of lysine residues by removing acetyl marks (Bannister & Kouzarides, 2011). This leads to strengthening of DNA-histone interactions, which makes HDACs transcriptional repressors. HDACs are organised into four classes: classes I and II, which include enzymes related to Rpd3 and Hda1 in budding yeast; class III or sirtuins, which encompasses enzymes homologous to budding yeast Sir2; and class IV, which has a single member, HDAC11. Single HDAC enzymes can deacetylate multiple histone lysine residues depending on the complex they are associated with, suggesting that HDACs have low inherent substrate specificity (Bannister & Kouzarides, 2011).

Apart from destabilizing DNA-histone interactions, acetyl-lysine marks can be read by effector proteins. The best characterized reader of acetyl-lysine marks is the bromodomain, which was discovered 35 years after histone acetylation itself (Dhalluin et al., 1999; Musselman, Lalonde, et al., 2012). Two other known readers are the PHD finger (Zeng et al., 2010) and the pleckstrin homology (PH) domain (Su et al., 2012). These domains are commonly present in transcriptional activators, thus linking acetylation with transcription. Apart from transcription, proteins containing these domains contribute to such processes as DNA damage response (Su et al., 2012) and mRNA splicing (Musselman, Lalonde, et al., 2012).

1.2.1.2 Methylation

Histone methylation, discovered together with histone acetylation (Allfrey et al., 1964), is one of the most ubiquitous histone modifications. Methylation, unlike acetylation, does not change histone protein charge. It can occur on lysine and arginine residues, where lysines can be mono-,di- and tri-methylated and arginines can be mono- and di-methylated (Bannister & Kouzarides, 2011).

The first histone lysine methyltransferases (HKMTs) discovered were human SUV39H1, and its murine homolog *Suv39h1* (Rea et al.,

2000). These enzymes were shown to specifically mediate methylation of lysine 9 in the N-terminus of histone H3 (H3K9me), a mark associated with heterochromatin. Proteins with a SET domain, including SUV39H1, mediate methylation of lysines within the N-terminal histone tails (Bannister & Kouzarides, 2011; Rea et al., 2000). Dot1 family proteins lack the signature SET domain and methylate lysines within the globular histone core (Feng et al., 2002). Arginine methylation is mediated by the PRMT family (Greer & Shi, 2014). Regardless of their function, all HMTs require S-adenosylmethionine (SAM) as a methyl group donor (Bannister & Kouzarides, 2011).

When half-lives of lysine and arginine methyl marks were examined, it was concluded that methylation, unlike acetylation, is irreversible (Byvoet et al., 1972). However in 2004 the first histone demethylase, named LSD1, was identified, thus providing evidence that methylation is, in fact, a dynamic process (Shi et al., 2004). Demethylases are highly conserved enzymes, that were classified into two families: enzymes with a Jumonji C (JmjC) domain, and the amine oxidases (Greer & Shi, 2014). Demethylases, like methylases, are substrate-specific and are sensitive to whether the substrate is mono-,di- or tri-methylated.

The diversity of methylation states (i.e. mono- ,di-, and tri-methylation) is associated with a variety of different effector proteins reading them. These effectors are structurally related and belong to the Royal superfamily (Musselman, Lalonde, et al., 2012). Specificity for mono-, di-, or tri-methylation arises from the size of the aromatic cage that all of these enzymes use for binding methyl-lysine, whereas specificity for a particular methyl mark position is determined by interaction with neighbouring residues (Musselman, Lalonde, et al., 2012).

The functional diversity of histone lysine methylation illustrates the complexity of this PTM. Lysine methylation is involved in both gene activation and gene repression (unlike acetylation, which is only associated with transcriptional activity). For example, H3K4me is generally involved in gene activation, with actively transcribed genes enriched for H3K4 trimethylation at their 5' termini (Musselman, Lalonde, et al., 2012). The TAF3 subunit of the basal transcription factor TFIID binds H3K4me3 via a PHD finger domain, thus linking histone methylation with RNA polymerase II-mediated transcription (Vermeulen et al., 2007). However, if H3K4me3/2 is recognized by the PHD finger domain of ING family proteins, it leads to the recruitment of HDAC1 repressor complex, thus linking H3K4me3/2 to gene repression (Shi et al., 2006).

Lysine methylation is also involved in constitutive heterochromatin formation in multiple species. For example, in *Schizosaccharomyces pombe* binding of Swi6 and Chp2 to H3K9me recruits eraser complexes that remove acetylation, as well as Swi6 acts concertedly with H3K9 methyltransferase Clr4 (SU(VAR)3-9 homolog), leading to heterochromatin formation at centromeres, telomeres and mating-type loci (Allshire & Madhani, 2018; Haldar et al., 2011). A Similar mechanism is present in *Drosophila melanogaster*, where H3K9me2/3 provides binding sites for HP1 protein (Swi6 homolog) that interacts with H3K9 methyltransferase SU(VAR)3-9 (Elgin & Reuter, 2013). In *Arabidopsis thaliana* H3K9me2 provides binding sites for Chromomethylase 3 (CMT3), which induces cytosine methylation (Pikaard & Scheid, 2014). Cytosine methylation then recruits SUVH4, which can further methylate H3K9, thus linking DNA methylation and histone modification to generate a repressive chromatin environment.

1.2.1.3 Phosphorylation and other modifications

Phosphorylation is another dynamic post-translational modification process controlled by kinases and phosphatases, that occurs on tyrosine, threonine and serine residues (Bannister & Kouzarides, 2011). Kinase-mediated phosphate transfer from ATP makes

histones negatively charged, thus disrupting histone-DNA interactions. Phosphorylation of histone H2AX at S139 in mammals and H2A at S129 in yeast is one of the best-characterized phosphorylation marks, which occurs in response to DNA damage (Musselman, Lalonde, et al., 2012). S129/S139 phosphorylation contributes to the recruitment of HATs, such as NuA4, and chromatin remodelers, such as Ino80, to make chromatin more accessible to the DNA repair machinery (Foster & Downs, 2005). Histone phosphorylation is also important in mitosis, where phosphorylation of pericentromeric H3 serine 10 by Aurora B displaces HP1 bound to H3K9me, a process potentially required for chromosome segregation (Hirota et al., 2005)

Apart from methylation, acetylation and phosphorylation, histones can undergo ADP ribosylation (Palazzo et al., 2019); O-GlcNAc glycosylation, which potentially links nutrition with cancer and epigenetics (Dehennaut, Leprince, & Lefebvre, 2014); and ubiquitination and sumoylation, which are generally associated with gene activation and gene repression, respectively (Gill, 2004).

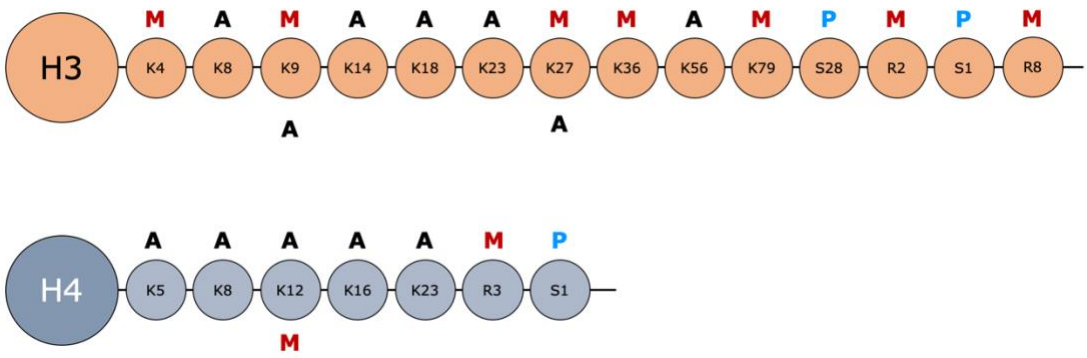

Figure 1-2. Posttranslational modifications of H3 and H4 histones.
M – methylation; A – acetylation; P – phosphorylation (Kouzarides, 2007).

1.2.1.4 Histone modifications crosstalk

In addition to acting alone, histone modifications can interact with each other, further increasing the complexity of information retrieval and processing (Bannister & Kouzarides, 2011). This so-called histone modification crosstalk can happen via multiple mechanisms. There might be competition between modifications for the same site, where one modification antagonizes the other. One such example is modifications of H3K27. H3K27 can be both methylated and acetylated (Cao et al., 2002; Creyghton et al., 2010). In *Drosophila* embryos, H3K27 acetylation by histone acetyltransferase CBP and methylation by methyltransferase E(Z) from the Polycomb repressive complex (PRC2) are antagonistic, and the knockdown of E(Z) or overexpression of CBP decreases H3K27me and increases H3K27ac (Tie et al., 2009). Modifications can also be co-dependent. Ubiquitylation of histone H2B within the HS4 insulator, a sequence element which is located at the boundary between heterochromatin and the *β-globin* gene cluster in chicken, is required for the presence of active chromatin marks, such as H3K4 methylation and H3, H4 and H2A.Z hyperacetylation (Ma et al., 2011). A modification present on one residue can sometimes prevent protein binding to a modification on an adjacent residue. For examples, HP1 protein cannot bind to methylated lysine 9 of histone H3 if the neighbouring serine 10 is phosphorylated (Fischle et al., 2005). In addition, a

single effector protein may bind several modifications within the same histone tail at the same time. This phenomenon was initially reported for $TAF_{II}250$ (subunit of TFIID transcription factor), which can bind to multiple acetylation marks on histone H4 via its double bromodomain (Jacobson et al., 2000). Finally, multiprotein complexes can include multiple subunits with domains capable of recognizing different histone modifications. For example the PRC2 complex has subunits containing Tudor, PHD finger and WD40 repeat domains that modulate methyltransferase activity of this complex (Musselman, Lalonde, et al., 2012). Binding to different trimethylated histones by the WD40 domain of the core PRC2 subunit EED regulates PRC2 activity: EED binding to H3K27me3 promotes PRC2 methyltransferase activity, whereas binding to H1K26me3 inhibits PRC2-driven methylation (Xu et al., 2010). Similarly PHD finger protein (PHF1), which is a PRC2-associating protein, was shown to bind to H3K36me3 and inhibit PRC2-driven H3K27 methylation (Musselman, Avvakumov, et al., 2012). This ability to generate a network of various interactions allows increased specificity.

1.2.2 Histone variants

Diversification of the canonical histones — H2A, H2B, H3 and H4 — into variants, specifically H3 and H2A histone variants, provides

another mechanism for differentiation of chromatin states (Henikoff & Smith, 2015). Histone variants, unlike core histones, are incorporated into chromatin throughout the cell cycle by replacement of a pre-existing histone or nucleosome. Switching between canonical and non-canonical histones, which can also alter the pattern of pre-existing PTMs, can specialize chromatin regions. For example, CENP-A is an H3 histone variant, which specifically localizes to the centromeres (Palmer et al., 1991). CENP-A is essential for kinetochore assembly, and it is in general considered to define centromeres (Amor et al., 2004). In most eukaryotes H3.3 is another H3 variant, which is present in transcriptionally active chromatin. Upon induction of gene expression, H3 can be rapidly lost and replaced by H3.3, whose deposition happens continuously while genes are transcribed (Schwartz & Ahmad, 2005). The role of H3.3 in transcription is not yet clear. In *Drosophila,* H3.3, unlike H3, was shown to be deficient for H3K9me, and enriched for histone modifications associated with active transcriptions (McKittrick et al., 2004) . Moreover H3.3 was shown to constitute ~25% of the total H3 histone amount, which is similar to the percentage of active transcription occurring in *Drosophila* cell culture (~26%), suggesting that all of the actively transcribed gene can potentially be packaged using H3.3 histone variant (McKittrick et al., 2004). H2AZ is another histone variant associated with active transcription, where Swr1

complexes catalyse the replacement of H2A in the H2A/H2B dimer (Narlikar,Sundaramoorthy &Owen-Hughes,2013). H2A nucleosomes together with free H2AZ/H2B dimers stimulate the ATPase activity of Swr1, which leads to H2A/H2B eviction and H2AZ/H2B deposition. This happens most commonly adjacent to the nucleosome-free regions of active promoters, thus activating transcription and preventing heterochromatin spreading (Luk et al., 2010).

1.3 Heterochromatin

As mentioned above, heterochromatin is a compact form of chromatin. Characteristic features of heterochromatin are histone hypoacetylation, presence of specific methyl marks and association of repressive proteins such as heterochromatin protein 1 (HP1) (Bernstein & Allis, 2005). The main function of heterochromatin is to maintain genome homeostasis by silencing highly repetitive DNA elements, such as transposable elements and satellite repeats (Allshire & Madhani, 2018). Since these regions are condensed throughout most of the cell cycle (it briefly becomes accessible during DNA replication), they are referred to as constitutive heterochromatin. Heterochromatin is also crucial for regulating developmental genes, and these regions are referred to as facultative heterochromatin (Grewal & Jia, 2007). Finally heterochromatin has an important structural role, where packaged

DNA occupies discrete nuclear regions, allowing short and long-range chromatin interactions, as well as centromere function (Pidoux & Allshire, 2004; Pombo & Dillon, 2015).

A hallmark of constitutive heterochromatin in many eukaryotes, is methylation on lysine 9 of histone 3 (H3K9me) (Allshire & Madhani, 2018). H3K9 methylation is mediated by well conserved proteins: Suv39 methyltransferases in mammals and fruit fly (Rea et al., 2000), and Clr4 in *S. pombe* (Ivanova et al., 1998). All these proteins have a catalytic SET domain for lysine methylation, and a chromodomain that binds to H3K9me. They are therefore able to both 'read' and 'write' the methyl mark. Methylation by Suv39/Clr4 creates a binding site for HP1 (Swi6 in *S. pombe*), which in turn recruits other complexes, such as Sir2, Clr3 and Clr6, that remove acetylation and promote H3K9me spreading (Lachner et al., 2001; Zhang et al., 2008). This leads to formation of a positive-feedback loop that facilitates maintenance of heterochromatin domains in *cis*. In plants and mammals H3K9 methylation can also be coupled with DNA methylation (Allshire & Madhani, 2018). Cytosine methylation is crucial for mammalian development, and recruitment of both H3K9 and DNA methyltransferases allows to reinforce DNA compaction (Jones & Liang, 2009).

How do cells know where to establish heterochromatin? It can be hypothesised that underlying DNA sequence determines heterochromatin location. In *S. pombe* Atf1 and Pcr1 bind to the REIII sequence element at the mating type locus, where they recruit Clr4 and Swi6 and contribute to heterochromatin establishment and maintenance together with the RNAi pathway, discussed in 1.4 (Jia, Noma, & Grewal, 2004). Heterochromatin formation can also be mediated by long noncoding RNAs. For example X chromosome inactivation (XCI) in mammals involves heterochromatin formation at one of the X chromosomes, where long noncoding RNA (lncRNA) *Xist* localises to the future inactive X chromosome and initiates silencing (Wutz, 2011). *Xist* binds to several regions within the X chromosome with no single conserved binding motif, suggesting that potentially several regions might act additively or synergically to mediate *Xist* binding (Wutz, 2011). Purification of proteins associated with *Xist,* along with subsequent gene knockdowns, showed that XCI is perturbed in the absence of SAF-A, SHARP and LBR (McHugh et al., 2015). SAF-A had already been shown to be important for Xist localization to the X chromosome (Wutz, 2011), and McHugh and colleagues confirmed that without SAF-A *Xist* localization is diffuse (McHugh et al., 2015). *Xist* interaction with SHARP was shown to be important for Pol II depletion from the *Xist*-coated territory. Upon the knockdown of SHARP, SMRT or HDAC3,

where HDAC3 is a deacetylase that interacts with SHARP through SMRT co-repression complex, Pol II depletion is abolished and X chromosome silencing is perturbed (McHugh et al., 2015). The effect of HDAC3 on XCI fits with previous observations that inactivated X chromosomes are hypoacetylated (Keohane et al., 1996). By interacting with SHARP, *Xist* recruits PRC2, which mediates H3K27 methylation, and this recruitment is abolished upon SHARP and HDAC3 knockdown (McHugh et al., 2015). X chromosome inactivation also involves DNA methylation (Bernstein & Allis, 2005). After DNA methylation has been established, it can be maintained without SHARP or other initiating factors (Allshire & Madhani, 2018)

Small ncRNAs can also initiate heterochromatin formation (Grewal & Jia, 2007). Repetitive elements, such as telomeric and centromeric repeats, are targets for the machinery responsible for heterochromatin formation. One mechanism that has been shown to play an important role in silencing of repetitive elements in multiple eukaryotes, is RNA-interference (RNAi) (Bernstein & Allis, 2005).

1.4 RNA-interference (RNAi)

The process of double-stranded RNA (dsRNA) driving gene silencing of homologous sequences was independently discovered in plants and nematodes (Fire et al., 1998; Hamilton & Baulcombe, 1999).

Later this gene silencing mechanism was named RNA-interference (RNAi) and it was identified in many eukaryotes, including mammals and fission yeast (Martienssen & Moazed, 2015).

Nowadays RNAi can be broadly defined as gene silencing by small RNAs (sRNAs) associated with proteins from the Argonaute family (Ghildiyal & Zamore, 2009). There are three known classes of sRNAs: short interfering RNAs (siRNAs), microRNAs (miRNAs) and PIWI-interacting RNAs (piRNAs) (Fig 1-3). Apart from interaction with Argonaute proteins, the common trait between all three classes is size, which ranges from ~20 to 30 nucleotides. Argonaute-sRNA complexes can drive silencing by degrading target RNAs or blocking their translation (posttranscriptional gene silencing or PTGS) or by inducing formation of heterochromatin (transcriptional gene silencing or TGS) (Martienssen & Moazed, 2015)

1.4.1 siRNAs

siRNAs are generated by processing of double-stranded RNA (dsRNA) (Martienssen & Moazed, 2015). siRNAs can be produced from exogenous dsRNA, such as viruses, and thus these are called exo-siRNAs; siRNAs can also derive from endogenous transposons or repetitive sequences, in which case they are termed endo-siRNAs (Ghildiyal & Zamore, 2009). Endogenous dsRNAs can be produced

by bidirectional transcription, or synthesised by an RNA-dependent RNA polymerase (RdRP). RdRP is present in plants, many fungi and *C. elegans* (but not Drosophila and mammals) (Sijen et al., 2001). In fission yeast and plants, RdRP makes dsRNA that is further processed into siRNAs, whereas in *C. elegans* RdRP makes siRNAs directly (Martienssen & Moazed, 2015; Sijen et al., 2001). dsRNA acts as a substrate for a class III nuclease, called Dicer, that cleaves the dsRNA precursor into ~22-nucleotide duplex siRNAs (Bernstein et al.,2001). After being cleaved by Dicer, one strand of the duplex siRNA is degraded, and the other strand, called the guide RNA, associates with an Argonaute protein in a complex such as the RNA-induced silencing complex (RISC) (Song et al., 2004). The guide RNA can then base-pair with any complementary RNA, thus initiating PTGS, whereby the associated Argonaute protein can 'slice' the target sequence. Alternatively, siRNAs can associate with an RNA-induced transcriptional silencing (RITS) complex, thus inducing TGS through recruitment of factors required for heterochromatin formation (Andre Verdel et al., 2004).

TGS has been extensively studied in *S. pombe* (Allshire & Ekwall, 2015). Since TGS in *S. pombe* is the subject of this thesis, more details about it will be provided in section 1.5.3. RNAi-driven TGS was also observed in plants, where siRNAs can be either endogenous

or exogenous (from viruses) (Borges & Martienssen, 2015). siRNAs are amplified by the action of RdRP and Dicer and then associate with Argonaute proteins to drive DNA and chromatin methylation (Borges & Martienssen, 2015). In *C. elegans*, TGS can also be triggered by both exogenous and endogenous dsRNAs. Introducing exogenous dsRNAs with food leads to an increase in H3K9me and a decrease in RNA polymerase II at the target loci, dependent on components of the nuclear RNAi pathway (NRDE) and RDRP. In addition, mutations in some *nrde* genes lead to a reduction in H3K9me at many genes that are silenced by endo-siRNAs, suggesting that endogenous siRNAs can drive heterochromatin formation (Burkhart et al., 2011; Castel & Martienssen, 2013). The role of endo-siRNAs in *Drosophila* is not yet clear*,* however a study by Fagegaltier and colleagues showed that recruitment of Su(var)3-9 and HP1 to centromeres relies on endogenous siRNAs, Dicer2 and Ago2 (Fagegaltier et al., 2009). In mammals not much is known about siRNA-driven TGS. However, in human cell culture exogenous siRNAs were shown to interact with AGO1 and AGO2, DNA methyltransferase 3 Alpha (DNMT3a) and histone deacetylase 1 (HDAC1), ultimately driving H3K9me2 and H3K27me3 at gene promoters (Kim et al., 2006; Weinberg & Morris, 2016).

1.4.2 miRNAs

Gene regulation by miRNAs is common in most eukaryotes (Treiber, Treiber, & Meister, 2019). miRNAs are encoded in the genome and are transcribed by RNA polymerase II into primary miRNA transcripts (pri-miRNAs) that are polyadenylated and capped (Lee et al., 2004). Then miRNA maturation occurs, where pri-miRNAs are first cut by an RNAse III nuclease called Drosha releasing a stem loop intermediate called the precursor miRNA (pre-miRNA) (Lee et al., 2003). Then the pre-miRNA interacts with Exportin-5, which mediates pre-miRNA export to the cytoplasm (Lund et al., 2004). In the cytoplasm Dicer performs a second processing step, cutting both strands of the stem loop intermediate, thus generating a mature miRNA duplex with 5' and 3' overhangs (Figure 1-2) (Bartel, 2004; Ketting et al., 2001). After maturation the miRNA, similarly to siRNAs, is loaded onto the RISC complex where together with Argonaute it can drive PTGS (Bartel, 2004). miRNA complementarity to its target sequence determines the type of PTGS that will take place: full complementarity (which is rare in animals) leads to AGO2-driven cleavage of mRNA, whereas partial complementarity (common in animals) leads to translational repression (O'Brien et al.,2018). Plant miRNAs are mostly fully complimentary to their target mRNA, and together with AGO1 they mostly induce PTGS by RNA cleavage (Ghildiyal & Zamore, 2009). MiRNAs have important

roles during development, and many cancers are associated with deregulated miRNA expression (Treiber et al., 2019).

1.4.3 piRNAs

Together with PIWI proteins, piRNAs have a conserved role across the animal kingdom in silencing transposons (Siomi et al., 2011). Unlike miRNAs and siRNAs, piRNAs are generated independent of Dicer (Luteijn & Ketting, 2013). Multiple studies in flies and mice identified two piRNA biogenesis mechanisms: a primary processing pathway that generates primary piRNAs responsible for silencing in somatic cells; and the 'ping-pong' amplification loop that is responsible for primary piRNA amplification in the germ-line cells (Siomi et al., 2011). In *C. elegans* primary piRNA are encoded by separate genes (Luteijn & Ketting, 2013), whereas in Drosophila piRNAs originate from piRNA clusters or piRNA loci that reside in the heterochromatic telomeric and pericentromeric regions (Brennecke et al., 2007). piRNA precursors are transported to the cytoplasm, where they undergoes 5' processing (Luteijn & Ketting, 2013). In both *Drosophila* and mice the 5' end is processed by a nuclease called Zucchini (PLD6 in mammals) (Nishimasu et al., 2012), whereas the nuclease responsible for 5' processing in *C. elegans* is unknown (Luteijn & Ketting, 2013). Apart from Zucchini , *Drosophila* utilizes two helicases — Armitage and Yb — for primary RNA

processing (Olivieri et al., 2010). Armitage is a 5'-3' helicase that unwinds piRNA precursors (Pandey et al., 2017). Armitage association with piRNA precursors is mediated by Yb, with deletion of Yb leading to promiscuous Armitage binding to RNA (Ishizu et al., 2019). The unwound precursor potentially serves as a substrate for Zucchini that cleaves the piRNA precursor to generate the 5' end of the mature piRNA (Nishimasu et al., 2012). piRNAs then associate with PIWI, Aubergine and Ago3 in Drosophila, and with MILI, MIWI and MIWI2 in mice (Ghildiyal & Zamore, 2009). After PIWI loading, piRNAs undergo 3' processing (Luteijn & Ketting, 2013). First the 3' end is trimmed by 3'-5' exonuclease Trimmer (Izumi et al., 2016), and then it is methylated by Hen1 (Kawaoka et al.,2011).

The 'ping-pong' cycle involves the Aubergine and Ago3 proteins that possess 'slicer' activity. Cycles of RNA slicing followed by 3'end trimming (Figure 1-2) generate more piRNAs in an amplification mechanism that is proposed to adjust the population of piRNAs to target active transposons (Siomi et al., 2011). Apart from PTGS driven by Aubergine and Ago3, PIWI can drive TGS. In *Drosophila* PIWI was shown localize to H3K9me2-rich regions and a yeast two-hybrid assay showed that PIWI specifically interacts with HP1 (Brower-Toland et al., 2007). Further studies in *Drosophila* showed that PIWI is required for H3K9me and HP1 localization at a subset of

transposons: PIWI knockdown leads to depletion of both HP1 and H3K9me from transposons in the germ line (Wang & Elgin, 2011).

How do piRNA loci within transposons, whose transcription is required for silencing, avoid being silenced themselves? In *Drosophila* transcription of piRNA loci depends on HP1-homolog Rhino, which associates with many piRNA clusters (Klattenhoff et al., 2009). Rhino binds to H3K9me and recruits Moonshiner, which is a paralogue of transcription factor TFIIA-L, which, in turn, recruits TFIID2 core variant TRF2, thus initiating piRNA transcription (Andersen et al.,2017).

In worms, the piRNA biogenesis pathway differs from the one present in flies and mice. As mentioned before, in worms piRNAs (called 21U RNAs) are produced from individual genes. Unlike Drosophila piRNAs, which can be 26-30nt long, 21U RNAs are exactly 21nt long with uridine 5'-monophosphate at the 5' end (Ghildiyal & Zamore, 2009). 21U RNAs associate with the PIWI protein PRG-1 and act as a template for RdRP to synthesise 22G RNAs. These 22G RNAs are then loaded onto WAGO-9, which is worm-specific Argonaute protein, and translocate to the nucleus, where together with NRDE proteins they can drive TGS (Luteijn & Ketting, 2013).

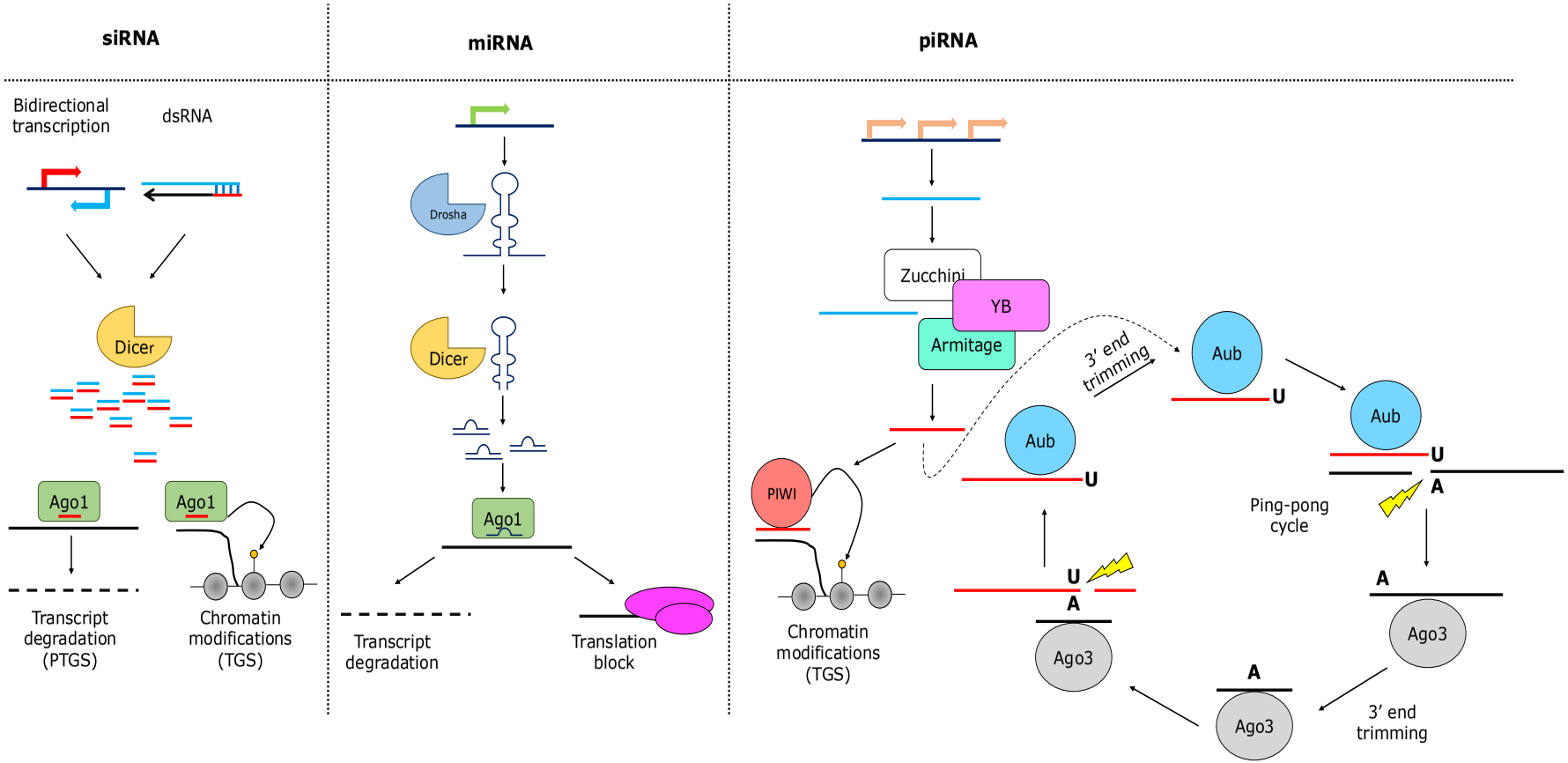

Figure 1-3. small RNAs biogenesis and silencing mechanisms. Schematic diagram showing the biogenesis of siRNA, miRNA and piRNA and their mechanisms of silencing.

1.5 RNAi-mediated heterochromatin formation in *S. pombe*

1.5.1 *S. pombe* as a model system for studying RNAi-dependent co-transcriptional heterochromatin formation

Fission yeast *S. pombe* is a haploid unicellular ascomycete yeast that has been used to study TGS since the discovery of PEV in *Drosophila* (Allshire & Ekwall, 2015; Hoffman, Wood, & Fantes, 2015). In *S. pombe* co-transcriptional heterochromatin formation occurs at centromeres, telomeres and mating-type loci. Silencing depends on histone-modifying enzymes and components of the RNAi machinery, which in *S. pombe* are present in single copy and, in many cases, conserved to higher eukaryotes (Allshire & Ekwall, 2015). In addition, fission yeast centromeres are similar in structure to the large repetitive centromeres present in metazoans, comprising domains of CENP-A chromatin and heterochromatin, which makes *S. pombe* a valuable system to study heterochromatin formation and centromere organization (Hoffman, Wood, & Fantes, 2015)

1.5.2 Constitutive heterochromatin in *S. pombe*

There are four loci of constitutive heterochromatin in *S. pombe*: centromeres, telomeres, mating-type and partially heterochromatic rDNA loci (Allshire & Ekwall, 2015). Centromeres consist of the central domain, which consist of the central core (*cnt*) and innermost repeats (*imr*), flanked by the outer repeats (*otr*) (Fig1-4) (Allshire & Ekwall, 2015). The central domain contains the centromere-specific histone variant CENP-A and is the region of kinetochore formation, whereas the outer repeats are regions of heterochromatin (Kniola et al., 2001). The outer repeats consist of 4.4-kb *dg* and 4.8-kb *dh* repeats, with a 1,780bp segment of the *dg* repeat being 97% identical among the three centromeres. *imr* repeats contain tRNA genes that act as boundary elements separating heterochromatin and CENP-A chromatin (Pidoux & Allshire, 2005). Centromeres II and III are also flanked by tRNA clusters that prevent heterochromatin spreading into euchromatin (Wood et al., 2002). Centromeres I and III are also flanked by *IRC* elements that also have a heterochromatin boundary function (Noma et al.,2006). Apart from the tRNA genes, centromeres are gene-void. tRNA genes at *imr* were showed to be nucleosome-free regions (NFRs), creating a chromatin 'gap' that potentially cannot be crossed by chromatin 'readers' and 'writers', thus preventing heterochromatin spreading (Garcia et al.,2010). Heterochromatin can also recruit factors that actively

inhibit heterochromatin spreading. Swi6 was shown to recruit a JmjC domain protein Epe1, deletion of which leads to heterochromatin spreading beyond its normal domain (Zofall & Grewal, 2006). Later it has been shown that Epe1 localization to heterochromatin boundaries is regulated by the action of ubiquitin ligase Cul4-Ddb1^{Cdt2} that induces ubiquitination and degradation of Epe1 specifically at the heterochromatin borders (Braun et al., 2011).

The mating-type region of *S. pombe* consists of three linked loci — mat1, mat2-P and mat3-M (Fig1-4) (Beach & Klar, 1984; Grewal, 2000). The mating-type is determined by the expressed *mat1* locus, which bears the information copied from *mat2*-P or *mat3*-M loci. *mat2*-P and *mat3*-M reside in a heterochromatin domain, which spans ~20kb (Grewal & Jia, 2007). The *mat2*-P and *mat3*-M loci are separated by a ~15kb recombinational 'cold spot' called the K-region (Grewal & Klar, 1997). Heterochromatin formation at *mat2*-P and *mat3*-M depends on the *cenH* element present in the K-region, which has homology to the centromeric *dg* and *dh* elements (Grewal & Jia, 2007; Grewal & Klar, 1997). The K-region also contains the REIII region, which is a binding site for Atf1/Pcr1 proteins that drive RNAi-independent heterochromatin formation (Jia et al., 2004). As with centromeric heterochromatin, the mat heterochromatic domain

is flanked by boundary elements — IR inverted repeats — preventing heterochromatin spreading (Grewal & Jia, 2007).

S. pombe telomeres consist of a ~300bp array of short tandemly repeated sequence capping each chromosome (Fig1-4) (Dehé & Cooper, 2010). The subtelomeric regions, adjacent to the telomeric repeats, and rDNA clusters present at the subtelomeric regions of chromosome III, are heterochromatic (Dehé & Cooper, 2010). Subtelomeres also have a *cenH*-like element embedded in the open reading frame of RecQ family putative telomere-linked helicase (Tlh) genes (Hansen, Ibarra, & Thon, 2006). Normally the mRNA level of *tlh* is low due to the presence of heterochromatin, however it increases in cells during telomere crisis. As with the mating-type locus, both RNAi-dependent and RNAi-independent mechanisms contribute to heterochromatin formation at the telomeres. Taz1 from the telomere-protein complex binds the telomeric repeats and drives RNAi-independent heterochromatin formation, whereas the RNAi machinery is recruited to the dh-like sequence (Grewal & Jia, 2007).

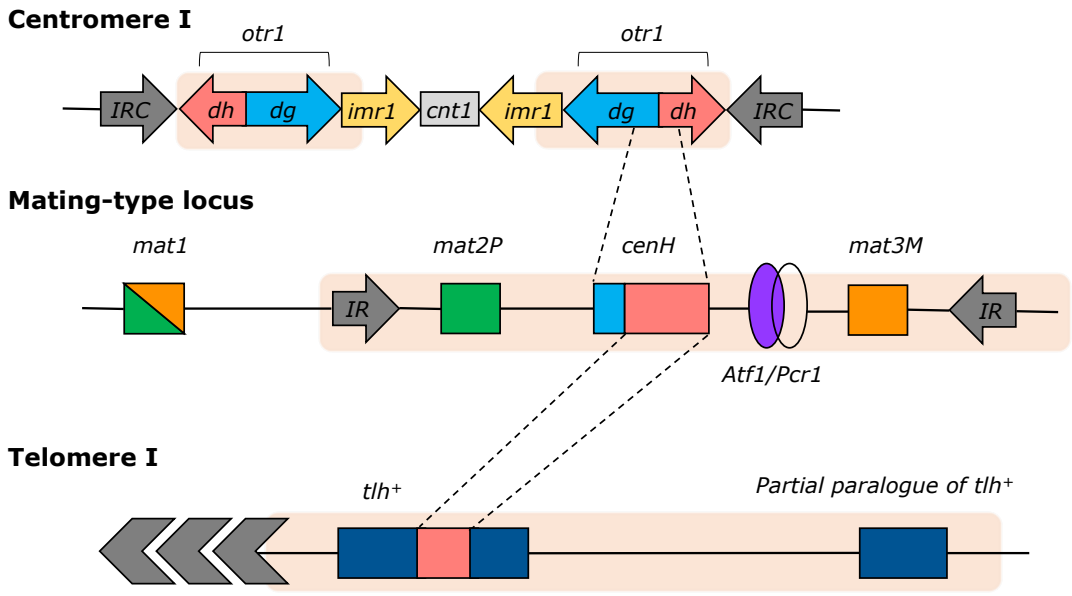

Figure 1-4. Loci of constitutive heterochromatin in *S. pombe*. Schematic diagram of centromere, mating-type and telomere loci in *S. pombe*. Peach-coloured boxes indicate regions of heterochromatin.

1.5.3 RNAi-dependent heterochromatin formation in *S. pombe*

All of the heterochromatin regions described above have sequence with homology to *dg-dh* repeats that drive RNAi-mediated silencing (Grewal & Jia, 2007). In parallel to RNAi, heterochromatin formation can be nucleated by RNAi-independent mechanisms involving Taz1 at telomeres and Atf1/Pcr1 at the mating-type locus (Grewal & Jia, 2007; Jia et al., 2004). Heterochromatin nucleation at the centromeres, however, seem to exclusively depend on the RNAi machinery, which makes centromeres a good model system to study RNAi-dependent TGS.

To date the fundamental mechanisms driving heterochromatin formation at the centromeres of *S. pombe* are fairly well understood (Allshire & Ekwall, 2015; Grewal & Jia, 2007; Martienssen & Moazed, 2015). RNA polymerase II (Pol II) transcribes pericentromeric repeats during S-phase, with the Pol II subunit Rpb7 being required to initiate the transcription of the pre-siRNAs (Djupedal et al., 2005). Pre-siRNAs are then converted to dsRNA by the enzyme Rdp1 from the RNA-directed RNA polymerase complex (RDRC) (Martienssen & Moazed, 2015). The dsRNA is then cleaved by Dicer, which generates ~23-nt duplexes with each strand bearing 3’ 2-nt overhangs (Bernstein et al., 2001; Martienssen & Moazed, 2015). siRNA

duplexes then associate with the Argonaute siRNA chaperone (ARC) complex that consists of Argonaute (Ago1), Arb1 and Arb2 proteins (Buker et al., 2007). The slicer activity of Ago1, which is regulated by Arb1, is required for the release of one of the two strands from the dsRNA duplex. Ago1, associated with a mature single stranded siRNA, can then be incorporated into the RNA-induced transcriptional silencing (RITS) complex. The RITS complex consists of Ago1, chromodomain protein Chp1 and targeting complex subunit 3 (Tas3) (Verdel et al., 2004). RITS localizes to chromatin in a siRNA-dependent manner, as RITS does not associate with centromeric loci in a *dcr1+* deletion background (Cam et al., 2005; Verdel et al., 2004).

RITS binding to centromeric loci leads to the recruitment of other complexes that are required to establish heterochromatin (Figure 1-4). RITS physically interacts with the RNA-directed RNA polymerase complex (RDRC) (Motamedi et al., 2004). RDRC consists of the RNA-directed RNA polymerase (Rdp1), helicase required for RNAi-mediated heterochromatin assembly (Hrr1) and a protein from the polyA polymerase/2'-5'oligoadenylate synthetase enzyme family, Cid12. Rdp1 synthesises the dsRNA and Hrr1 potentially increases Rdp1 processivity, while Cid12 is essential for Hrr1 and Rpd1 association (Motamedi et al., 2004). It was shown that in the

absence of RDRC no siRNAs associate with RITS, and RITS cannot localise to its target loci. Apart from RDRC, RITS also recruits the Clr4 complex (CLRC), which is required for methylation of lysine 9 on H3 (H3K9me) (Martienssen & Moazed, 2015). The methyltransferase subunit of CLRC is Clr4, which mediates H3K9me via its SET domain (Nakayama et al., 2001; Zhang et al., 2008). Other components of CLRC are Rik1, Cul4, Raf1 and Raf2, which together form an E3 ubiquitin ligase (Hong et al.,2005; Horn, Bastie, & Peterson, 2005; Jia, Kobayashi, & Grewal, 2005; Nakayama et al., 2001). RITS subunit Chp1 physically interacts with Rik1, thus it was proposed that this interaction could mediate RNAi-dependent recruitment of CLRC to chromatin (Zhang et al., 2008). However later it was shown that Stc1 is an adaptor protein that physically interacts with both Ago1 and CLRC and is required for centromeric silencing (Bayne et al., 2010). Stc1 tethering to chromatin can recruit CLRC without the RNAi machinery, supporting the hypothesis that Stc1 is a link between CLRC and RITS. Despite the fact that RITS recruits CLRC, CLRC is also required for RITS chromatin binding. Chp1 binding to H3K9me via its chromodomain is required to stabilize RITS, and Chp1 cannot localize to chromatin in *clr4Δ* cells (Noma et al., 2004). Moreover Clr4 is required for siRNA production, as well as RITS interaction with RDRC (Motamedi et al., 2004). H3K9 methylation by CLRC creates binding sites for other proteins that

contribute to the formation of heterochromatic domains (Martienssen & Moazed, 2015). H3K9me recruits Chp2 and Swi6, which are homologous to HP1 protein (Motamedi et al., 2008). Chp2 associates with the deacetylase complex SHREC, which mediates H3K14 deacetylation required for heterochromatin formation (Motamedi et al., 2008). Swi6, in turn, interacts with Ers1, which then stabilizes RITS and RDRC at heterochromatin (Rougemaille et al., 2012).

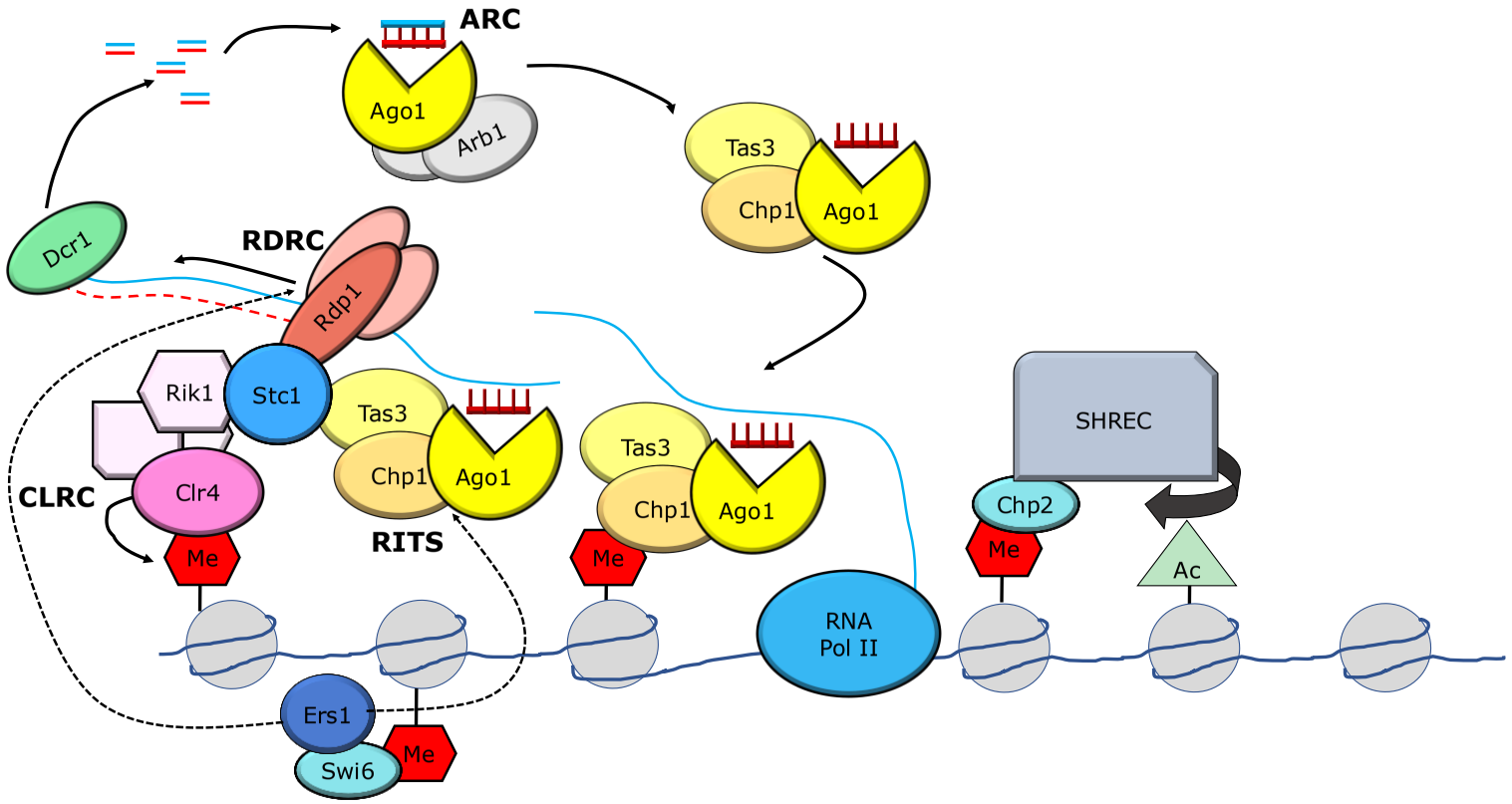

Figure 1-5. RNAi-mediated heterochromatin formation in *S. pombe.* Schematic diagram of the RNAi-dependent co-transcriptional gene silencing in *S. pombe.* Black-dotted arrows indicate physical interactions.

One of the counterintuitive features of heterochromatin is that to establish transcriptional gene silencing, transcription, mediated by RNA Pol II, has to take place. Indeed mutations in the Rpb7 and Rpb2 subunits of RNA Pol II leads to a reduction in H3K9 methylation and Swi6 accumulation at centromeres (Allshire & Ekwall, 2015; Djupedal et al., 2005). One explanation for this paradox is that Pol II-mediated transcription happens during a short period of time in the S phase of the cell cycle (Chen et al., 2008; Kloc, et al., 2008). During S phase, heterochromatin undergoes decondensation, which leads to a burst of RNA Pol II activity. This Pol II-driven burst of transcription is associated with increased siRNA production resulting in the recruitment of factors required to assemble heterochromatin. Another study suggested that the apparent paradox might be explained by different methylation states. H3K9me can be either di- or tri-methylated, and the level of methylation defines two distinct heterochromatin states (Jih et al., 2017). Unlike H3K9me3 domains, H3K9me2 domains are transcriptionally permissive, and are also quicker to establish. Thus it was suggested that early-forming H3K9me2 domains are potentially permissive to RNAi and RNA Pol II-mediated H3K9me spreading, with the establishment of silent H3K9me3 domains following later.

1.5.4 Heterochromatin establishment

Heterochromatin formation can be divided into two parts: initial heterochromatin establishment with subsequent maintenance. During heterochromatin establishment, RNAi and chromatin-modifying machineries have to be targeted to the locus *de novo.* Then heterochromatin has to be maintained, whereby such signals as Swi6 bound to H3K9me allow heterochromatin to be stabilized and spread (Grewal & Jia, 2007). One of the questions that remains to be answered is how exactly heterochromatin formation is initiated. RNAi and CLRC functions are interconnected, with deletion of a component from either pathway affecting both siRNA production and H3K9me (Volpe et al., 2002). This makes it hard to evaluate which pathway acts first. One model proposes that an initial pool of siRNAs associated with RITS base-pair with nascent transcripts, thus recruiting the machinery to target loci for heterochromatin establishment with no prior H3K9me being present (Allshire & Ekwall, 2015). Tethering RITS subunit Tas3 to the *ura4+* RNA transcript was shown to result in *ura4+* silencing, consistent with the idea that RITS can initiate heterochromatin formation (Bühler, Verdel, & Moazed, 2006). However the source of the initial siRNAs that could associate with RITS and induce heterochromatinization is not clear. One hypothesis is that primal RNAs (priRNAs) can potentially play the initiating role. priRNAs are Dicer-independent

small RNAs that are degradation products of centromeric transcripts (Halic & Moazed, 2010). Halic and Moazed put forward a model whereby priRNAs associated with Ago1/Tas3 subcomplex (but not Chp1) can base-pair with the bidirectionally transcribed centromeric transcripts, leading to recruitment of RDRC and Dicer that can then mediate initial siRNA production, independent of H3K9 methylation. An alternative model suggests that the initial small RNAs could be made by Dicer cleavage of RNA Pol II transcripts that fold into double-stranded hairpin-like structures (Djupedal et al., 2009). These hairpin-derived small RNAs would not require RITS, RDRC or CLRC for their production, thus they might serve as the initiating signal to induce heterochromatin formation *de novo*.

Another model suggests that H3K9me is the initiating signal, required for RITS stability at the target loci (Martienssen & Moazed, 2015; Noma et al., 2004). This model is supported by experiments with mutant Tas3 that cannot interact with Ago1, but can still interact with Chp1 (Shanker et al., 2010). This Tas3 mutation ($Tas3^{WG}$) does not perturb maintenance of heterochromatin, supposedly because RITS can remain associated at the centromeres via Tas3-Chp1 interaction with H3K9me and Ago1 interaction with siRNA and nascent RNA. However if H3K9me is perturbed via $clr4^{+}$ deletion, heterochromatin cannot be re-establish upon $clr4^{+}$ re-

introduction in the Tas3^{WG} background. Re-establishment of heterochromatin upon deletion and reintroduction of an RNAi gene is not affected by the Tas3^{WG} mutation, and it has been suggested that this is due to low levels of H3K9me that persist in RNAi deletions (Shanker et al., 2010). Based on these data the authors proposed that H3K9me is the signal required to start heterochromatin formation. However Djupedal and colleagues showed that in the presence of a point mutation in histone H3 (H3K9R), which prevents H3K9me, siRNAs can still be produced, thus arguing against this model (Djupedal et al., 2009).

Apart from the lack of clarity over the order in which RITS and CLRC act, it is also not clear what additional factors are required for heterochromatin establishment. A study by Marasovic and colleagues identified Triman as an establishment-specific factor (Marasovic, Zocco, & Halic, 2013). Triman is a 3'-5' exonuclease that trims long (~25-nt to 65-nt long) Ago1-bound siRNA precursors to their mature ~22-nt length. Without trimming, long siRNAs do not stably associate with Ago1, which impairs RITS association with the target locus. An RNA-associated factor named Mkt1 was also shown to be specifically involved in establishment and dispensable for maintenance of heterochromatin (Bayne lab, unpublished data). Previously Mkt1 was shown to interact with Mtl1, which is a subunit

of the NURS/MTREC complex (Egan et al., 2014). Together with Red1, Mtl1 forms a core module of the MTREC complex, which mediates meiotic RNA, ncRNA and cryptic transcript degradation (Lee et al., 2013). Interaction of Mkt1 with Mtl1 might potentially indicate that Mkt1 functions alongside Mtl1 in RNA surveillance pathway. Consistent with this , Mkt1 was shown to interact with the ribosomal proteins that interact with Cid14 (Keller et al., 2010; Bayne lab, unpublished data). Poly(A) polymerase Cid14 is a subunit of the TRAMP complex, which adds poly(A) tails to target RNAs, thus initiating RNA degradation by the exosome (Houseley, LaCava, & Tollervey, 2006; Martienssen & Moazed, 2015). Cid14 was shown to be important for centromeric silencing, where it potentially targets centromeric transcripts for exosome-driven degradation or proper processing by RDRC (Bühler et al.,2007).

1.6 Study aims

Heterochromatin formation is a conserved process across eukaryotes, essential for genome homeostasis (Grewal & Jia, 2007). Extensive studies of the role of heterochromatin in maintaining genome stability in *S. pombe* have elucidated many aspects of heterochromatin formation. However, despite the multitude of studies, there are still some gaps in our understanding of heterochromatin assembly. In particular, more work is required to understand how heterochromatin is established.

In this study I aimed to investigate early steps in RNAi-dependent heterochromatin formation at the centromeres in *S. pombe*. I developed two assays — plasmid-based and cross-based — to detect defects in heterochromatin establishment, with a view to screening for novel establishment-specific factors genome-wide. I validated these assays using sixteen candidate deletion mutants. While the plasmid-based assay proved unreliable, the cross-based assay was shown to effectively detect establishment-specific factors. The cross-based assay also provided novel insights into heterochromatin establishment dynamics that can potentially help us to better understand the mechanism of *de novo* heterochromatin establishment.

Chapter 2 — Materials and methods

2.1 *S. pombe* growth

2.1.1 *S. pombe* media and selection

S. pombe strains were cultured in either nutrient rich media (YES) or synthetic minimal media (PMG), where both YES and PMG can be either liquid or solid (agar). In order to induce mating, cells were plated on malt extract (ME) agar plates.

YES liquid: 3.0% (w/v) glucose, 0.5% (w/v) yeast extract, 200mg/l adenine, 200mg/l histidine, 200mg/l arginine, 200mg/l lysine, 200mg/l uracil,200mg/l leucine.

YES agar: Same as above, but with 2% (w/v) agar added. For YES low adenine plates 1/10th (20mg/l) of adenine was added.

PMG liquid: 2% (w/v) glucose, 14.7mM potassium hydrogen phthalate, 3.75g/l glutamic acid ,15.5mM Na_2HPO_4, 1x vitamins, 1x minerals, 1x salts. The media was supplemented with 200mg/l uracil, adenine, arginine leucine, lysine and histidine as required.

PMG agar: Same as above, but with 2% (w/v) agar added.

ME agar: 3% (w/v) Bacto-malt extract, 2% agar, 200mg/l adenine, 200mg/l histidine, 200mg/l arginine, 200mg/l lysine, 200mg/l uracil,200mg/l leucine.

50x Salts: 14.1mM Na_2SO_4 , 4.99mM $CaCl_2$, 670mM KCl, 260mM $MgCl_2$.

10,000x Minerals: 47.6mM citric acid, 1.60mM CuSO, 2.47mM molybdic acid ,6.02mM KI , 13.9mM $ZnSO_4$, 7.40mM $FeCl_2$, 80.9mM boric acid, 23.7mM $MnSO_4$.

1000x Vitamins: 40.8µM biotin, 4.20mM pantothenic acid , 55.5mM inositol 81.2mM nicotinic acid.

Salts, vitamins and mineral were added to both YES and PMG media.

Drugs were supplemented to YES and PNG agar as required at the following final concentrations:

Nourseothricin (clonNAT) (WERNER BioAgents): 0.1mg/ml.

Geneticin (G418) (Gibco): 0.1mg/ml.

Thiabendazole (TBZ) (Sigma-Aldrich): 15µg/ml in DMSO.

5-Fluorootic Acid (5-FOA) (Melford Laboratories): 1g/l.

2.1.2 Cell culture

S. pombe cells were cultured in conical flasks at variable culture volumes. Cultures were grown at 32$_o$C with shaking at 180rpm. Cells were counted using a haemocytometer.

2.1.3 Genetic crosses

S. pombe were crossed on low nitrogen ME agar plates, as fission yeast haploids require nitrogen starvation to undergo conjugation with subsequent sporulation (Forsburg & Rhind, 2006). Cells of opposite mating types (h- and h+) were mixed in approximately 1:1 ratio, and incubated at 25 $_0$C for 2-3 days. After the incubation period, asci containing four spores were detected microscopically. A blob (5mm in diameter) of cross mixture was suspended in 300µl 1/100 glusulase (203,682 units/ml of glucuronidase and 9,084 units/ml of sulfatase) in dH_2O (Perkin Elmer), and incubated either at 25 $_0$C overnight or at 32 $_0$C for ~five hours. After the glusulase treatment, cells were spun down at 4000rpm for 2 min, and glusulase was replaced with dH_2O. The release of spores was validated microscopically. Spores were diluted either 1/5 or 1/10 depending on the spore concentration and plated on selective agar plates. The plates were incubated at 32 $_0$C until the F1 colonies become clearly visible.

2.1.4. Spotting assay

A small patch of cells or a single colony were resuspended and thoroughly mixed in 100μl sterile dH_2O in a 96-well plate. Cell suspension was serially diluted 1:10 four times. A 48-prong replicator was sterilized by immersing it in EtOH and passing by a flame. The pinner was then cooled down at room temperature, immersed into the 96-well plate, and transferred to a dried selective plate to transfer cells.

2.1.5 *S. pombe* storage

After achieving a correct *S. pombe* genotype, a patch of cells was thoroughly mixed by vortexing with 50% (v/v) glycerol in sterile dH_2O in 1.8ml Nunc® CryoTubes® (Sigma-Aldrich). The CryoTubes were then stored at -80^{o}C.

2.2 *S. pombe* transformation and genotyping

2.2.1 Lithium Acetate (LiAcTE) transformation

Transformation was performed using LiAc method (Kawai, Hashimoto, & Murata, 2010). For the transformation, 50 ml of YES culture was grown to log phase (exponential growth phase), where $6x10^6$ cells/ml was enough for two transformations. Cells were spun down at room temperature (3000rpm/2min) and washed once with dH_2O. Cells were then resuspended in 10 ml of 0.1M LiAc in TE buffer (10mM Tris(HCl) pH 8.0 and 1mM EDTA pH 8.0, autoclaved) pH4.95 and incubated at 32 ^{0}C for 1 hour with shaking. Cells were spun down, and resuspended in 0.1M LiAcTE pH 4.95 to a concentration of $1x10^9$ cells/ml. In an Eppendorf tube, 150µl of cells, 2µg of plasmid and 370µl of 50% PEG_{3350} (50% PEG_{3350} in TE, filter sterilized) were mixed, and incubated at 32 ^{0}C for 1 hours with. Then cells were heat-shocked at 42 ^{0}C for 20 min. After the heat shock, cells were spun down (4000rpm/1min) and resuspended in 300µl of dH_2O. For antibiotic selective marker transformation, cells were transferred to a 50ml Falcon tube with 10ml YES and incubated overnight at 25^{o}C with shaking. After the overnight incubation, cells were spun down (4000rpm/1min), resuspended in 100 µl and plated on the antibiotic selective plates. For auxotrophic marker selection cells were plated straight away to the selective media.

2.2.2 LiAcTE transformation optimized for 96-well plate

To use LiAcTE method for multiple simultaneous transformations, I optimized a microtiter plate transformation protocol originally devised for *S. cerevisiae* (Gietz & Schiestl, 2007). All the reagents were used as in subsection 2.2.3. First, using a 96-prong replicator imprints were made on a YES agar plate. The strains were plated onto the imprints using toothpicks and incubated overnight at 32$_{o}$C. Using toothpicks, overnight-grown strains were transferred to a 96-well plate containing 100 µl of sterile dH_2O per well. Plates were then centrifuged for 5 min at 1500g, 20$_{o}$C. Supernatant was removed by pipetting, and 50 µl of transformation mix (15µl LiAcTE, 20µl of 2mg/ml salmon sperm DNA, 1µg plasmid DNA and H_2O up to 50µl) was added to each well. Then 100 µl of PEG_{3350} was added into each well. Everything was mixed by pipetting. The plate was then sealed and incubated at 42 $_{0}$C for 1h. After the incubation, plates were centrifuged for 10 min at 1500g. Supernatant was removed and pellets were resuspended in 20µl, and 10µl were plated on non-selective and selective agar plates. Plates were then incubated for four days at 32 $_{0}$C. Data presented in figure 3 – 6 was scanned differently to the scanning protocol outlined in 2.7.1: the blue background was not included in the scanning process.

2.2.3 Colony PCR

A pinhead patch of cells was resuspended in 10µl 20mM NaOH. The Suspension was incubated at 95°C for 1h, mixed by vortexing and briefly spun down. 1µl of the supernatant was used for subsequent PCR using Taq DNA polymerase (Roche) upon manufacturer's instructions. Samples were subjected for the following cycling protocol:

95°C — 3 min

95°C — 30 sec
50°C — 30 sec
72°C — 1 min/kb
} 35 cycles

72°C —10 min

5µl of loading dye (5x: 100mM Tris-HCl pH7.5, 100mM EDTA pH8.0, 25%Ficoll-400, 1% OrangeG) was added to each reaction, and samples were subjected to gel electrophoresis as outlined in 2.3.5.

2.3 Molecular cloning and fragment construction

2.3.1 pREP-CD41 plasmid construction

To reintroduce wild type Clr4 and Dcr1, pREP-CD41 plasmid expressing WT *clr4*+ and *dcr1*+ under their endogenous promoters was constructed from p348 (pREP backbone, WT *clr4*+) and p474 (pJR1U backbone, WT *dcr1*+). These two plasmids were a gift from

the Halic lab (Marasovic et al., 2013). First, p348 plasmid was modified using QuikChange Lighting Site-Directed Mutagenesis Kit (Agilent Genomics) according to the manufacturer's manual. As shown in figure 3-3, a new SphI site was introduced inside the Nmt1 terminator sequence and the original SphI site was deleted from p348, producing pREP-CM2 plasmid. To generate REP-CD41 plasmid, the *dcr1+* cassette (*dcr1+* promotor_ *dcr1+* ORF_ *dcr1+* terminator) from the p474 plasmid was cloned into the nmt1 terminator site of p348 by restriction digest using SphI and SmaI restriction sites (Figure 3-4) .

For the construction of pREP-CD41 plasmid, the restriction digest proceeded as follows: 2µg of pREP-CM2 and p474 plasmids were first digested with 1 µl of SmaI enzyme (20units/µl, NEB) for 1,5 hours at 25 ^{0}C in 1x CutSmart buffer (NEB) (50 µl total reaction volume). For p474, 2.5µl of 1M NaCl was added to bring the salt concentration to 50mM. Then 2 µl of SphI (10units/µl) were added to both p474 and pREP-CM2 restriction mixes. Both reactions were incubated at 37 ^{0}C for 1,5 hours, and then the enzymes were deactivated for 20 min at 65 ^{0}C. Then both samples were run on an 0.8% agarose gel. Appropriate bands were cut from the gel, and purified using QIAquick Gel Extraction Kit (Qiagen) according to the manufacturer's manual.

The ligation was then performed using 2 µl T4 ligase buffer (NEB) and 1 µl T4 ligase (NEB) in 20 µl total reaction volume. The amount of pREP-CM2 backbone was 50ng, and the insert: backbone ratio was 3:1. The amount of insert was calculated using the following formula:

$$\left[\frac{insert(bp)}{vector(bp)}\ x\ 50ng\ of\ vector\right] x \frac{3}{1}$$

A control reaction to test for backbone recircularization was setup without adding the insert. After an overnight ligation at 4 ^{0}C *E.coli* transformation with subsequent plasmid mini-prep was performed as outlined in 2.2.3 and 2.2.4.

2.3.2 Preparation of competent *E. coli* cells

E.coli were freshly streaked, and 5 ml of LB was inoculated with a single colony to grow overnight with shaking at 37 ^{0}C. The next day the culture was diluted 1:200 into pre-warmed 100ml LB supplemented with 20nM $MgSO_4$. Cultures were grown at 37 ^{0}C with shaking until OD600 reached 0.48.Then cells were transferred to a chilled 250ml centrifuge bottle and incubated on ice for 10 min. Cells were pelleted by centrifugation for 5min at 5000rpm, 4 ^{0}C. Supernatant was decanted, and the pellet was gently resuspended in 40ml of cold TFB1 buffer (30mM KAc, 100mM $RuCl_2$, 10mM $CaCl_2$, 50m $MnCl_2$, 15% glycerol) per 100ml culture. The mixture was

incubated on ice for 5min, and then the cells were pelleted down at 300rpm, 10 min, 4 ^{0}C. Supernatant was decanted, and the pellet was gently resuspended in 4 ml of cold TFB2 buffer (10mM MOPS, 10mM $RuCl_2$, 75mM $CaCl_2$, 15% glycerol). The mixture was then incubated on ice for 15min, and 100 µl of cells were aliquoted into pre-chilled Eppendorf tubes. Aliquots were stored at -80 ^{0}C.

2.3.3 *E. coli* transformation

For the transformation, 50 µl of *E.coli* was mixed with 100ng of plasmid, and incubated on ice for 30 min. Then it was heat shocked at 42 ^{0}C for 2 min, and immediately cooled on ice for 1-2 min. After 1ml of L-Broth (15.5 g Luria Broth Base (Foremedium) suspended in 1L distilled water) was added, and the *E.coli* mixture was incubated for 1h at 37 ^{0}C with shaking. Cells were seeded on antibiotic-resistant plates at 37 ^{0}C overnight.

2.3.4 Plasmid miniprep and validation

Single bacterial colonies were inoculated into 5ml L-broth culture supplemented with an appropriate antibiotic. The liquid cultures were incubated overnight at 37 ^{0}C with shaking. Then plasmids were extracted with QIAprep MiniPrep or QIAprepc MaxiPrep Kits (Qiagen) following manufacturer's instructions.

To validate the ligation of the *dcr1+* construct, pREP-CD41 plasmid was digested with 1 µl EcoRV-HF (10 units/ µl) (NEB) for 15 min at 37$_{o}$C in 1xCutSmart buffer (50 µl total reaction volume). Then samples were run on 0.8% agarose gel.

2.3.5 Q5 PCR

Amplification of fragments for integrative transformation was performed by Q5® High-Fidelity DNA polymerase (NEB) as per manufacture's instructions. The DNA template was used at the following concentrations: 1µl of purified genomic DNA or 100ng of plasmid DNA. The following cycling times were used:

98$_{o}$C — 30 sec

98$_{o}$C — 10 sec
50$_{o}$C — 30 sec
72$_{o}$C — 30 sec/kb
} 35 cycles

72$_{o}$C —2 minutes

Amplification was verified by running 2µl of the reaction on an agarose gel. If successful, reactions were purified using QIAquick PCR Purification Kit (Qiagen).

2.3.6 Agarose gel electrophoresis

Agarose gel electrophoresis was used to visualize the presence of DNA after PCR amplification. To prepare 1% agarose gel, 1g of agarose was dissolved in 100ml TBE (2mM EDTA,90mM Tris-Borate). The agarose solution was boiled, and upon cooling 1% Ethidium Bromide (Sigma Aldrich) was added. Sample DNA was mixed with 1x loading dye. GeneRuler DNA Ladder Mix (Thermo Fisher Scientific) was used as a size marker. The gel was run at 100V for 40 min.

2.3.7 Gene replacement

To swap drug-resistance (*kan+, nat+* or *hyg+*) and prototrophic cassettes (*ura4+, arg3+, his3+* or *leu1+*) between each other, plasmids developed by Alexander Lorenz were used (Lorenz, 2015). A required cassette was amplified using cassette-specific primers as described in 2.3.5 and introduced by LiAcTE transformation outlined in 2.2.1.

2.3.8 Split marker fusion PCR

For genomic integration of the *ura4+* gene split marker fusion PCR was used (Fairhead et al. 1996; Yon & Fried, 1989). First two *ura4+* fragments with long regions of homology were generated. Primers used to generate these fragments are listed in table 2-1. First two

halves of *ura4+* — *ura4+* 5' and *ura4+* 3' — were amplified using Q5 PCR (described in 2.3.5) with U_5F + U_5R and U_3F+U_3R primer pairs (Fig 2-1A). These two fragments share a region of homology, which allows them to recombine and produce a wild-type *ura4+* gene upon transformation. Then two additional fragments were amplified from the genomic region at which *ura4+* was to be inserted. EL_5F+EL_5R amplified a region upstream of the *ura4+* insertion site ('endogenous locus 5' fragment) , and EL_3F+EL_3R amplified a region downstream ('endogenous locus 3' fragment) (Fig 2-1A). EL_5R and EL_3F primers contain 20bp overhangs homologous to the start and to the end of the *ura4+* gene, respectively. Then the 'endogenous locus -5' fragment was fused to the '*ura4+* 5' fragment and the 'endogenous locus -3' fragment was fused to the '*ura4+* 5' fragment (Fig 2-1B). Fusion PCR was performed in two following steps:

Reaction 1: 10 µl 5x Q5 buffer, 1µl dNTPs (10mM), 0.5µl Q5 polymerase, 10µl Q5 enhancer,2µl fragment 1 (100ng) and 2µl fragment 2(100ng), 24.5µl H_2O.

Reaction 2: 10 µl 5x Q5 buffer, 1µl dNTPs (10mM), 0.5µl Q5 polymerase, 10µl Q5 enhancer, 5µl forward primer and 5µl reverse primer, 18.5µl H_20. Forward and reverse primers are the primers complimentary to the beginning of the Fragment 1 and to the end of the Fragment 2 respectively.

Reactions 1 and 2 were prepared and reaction 1 was subjected to the following cycling protocol:

98°C — 30 sec

98°C — 10 sec
50°C — 30 sec
72°C — 30 sec/kb
} 5 cycles

4°C —Pause

98°C — 30 sec

98°C — 10 sec
50°C — 30 sec
72°C — 30 sec/kb
} 25 cycles

72°C — 2 min

When the programme paused, reaction 2 was added to the reaction 1, and the protocol was continued until completion. The success of the fusion was analysed by gel electrophoresis (2.3.5)

Two fused fragments were then introduced using lithium acetate transformation protocol (2.2.1) and cells were then plated on media lacking uracil. Recombination between the two *ura4+* fragments and thus generation of the wild-type *ura4+* gene allows the cells to grow on uracil-deficient media.

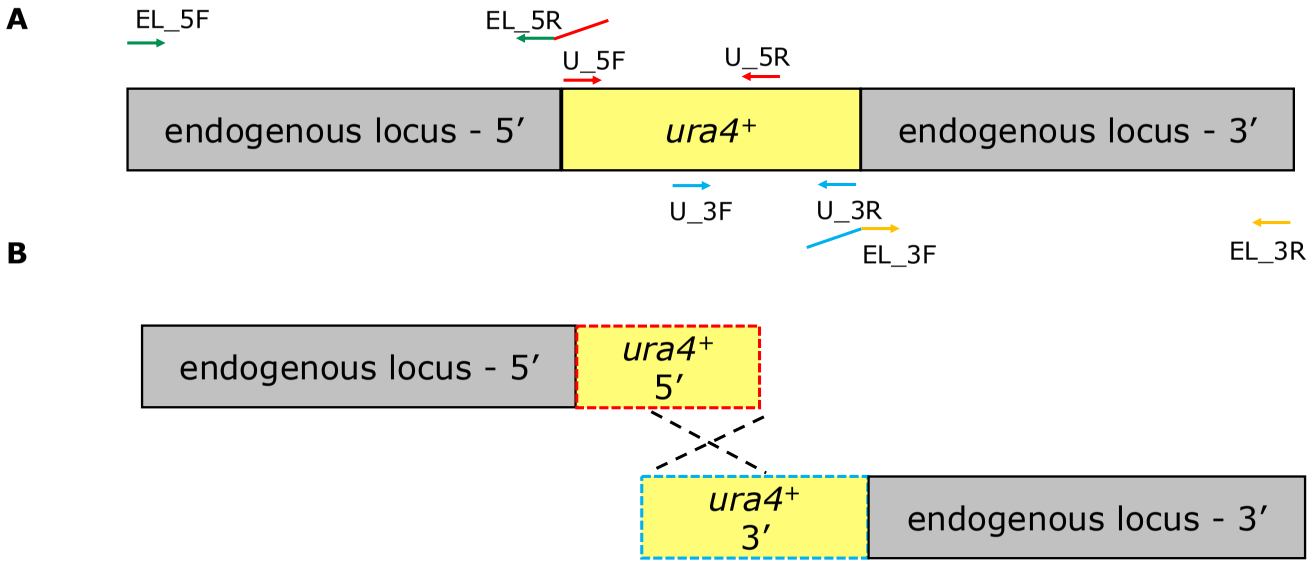

Figure 2-1. Split market fusion PCR. Schematic diagram of the split marker fusion PCR used to integrate *ura4*+ to the genome. See main text for the full description

2.4 RNA protocols

2.4.1 Total RNA extraction

Cells were grown in 5ml liquid cultures overnight until they reach mid-log phase (~$6x10_6$ cells/ml, counted using haemocytometer). 2ml of the overnight culture were then used for RNA extraction with MasterPure™ Yeast RNA Purification kit (Epicentre) according to the manufacturer's protocol. Quantification of RNA concentration was performed using NanoDrop 2000 spectrophotometer (Thermo Scientific).

2.4.2 small RNA extraction

Cells were grown in 50ml culture until they reach $1x10_7$ cells/ml concentration. Then cells were centrifuged at 3000rpm for 2 min, and the pellet was washed in 50ml dH_2O. The pellet was re-suspended in 500µl extraction buffer (100mM NaCl, 50mM Tris-HCl pH7.5, 10mM EDTA pH8.0m 1%SDS). Then 500µl phenol:chroloform (5:1, pH 4.3–4.7, Sigma Aldrich) was added together with 500µl acid-washed glass beads. Cells were lysed for 2x2min in a Mini-Beadbeater (BioSpec) at 4_oC. The bead-cell mixture was then spun at 13000rpm for 5min at 4_oC and the supernatant (~550 µl) was transferred to a new 1.5 ml Eppendorf. The RNA was extracted once with equal volume (~550 µl) phenol:chloroform (5:1), once with equal volume (~480 µl) phenol:chloroform:isoamyl alcohol

(25:24:1) and then with equal volume (~400 µl) of pure chloroform. After the series of extractions, the final volume was 350 µl. 100 µl of PEG_{8000} and 50 µl NaCl were added to the RNA mixture, with subsequent incubation on ice for 30 min. The sample was spun at 1300rpm for 10 min at 4^{o}C. The supernatant with the small RNA fraction was transferred to a fresh Eppendorf, and 3 volumes (~1ml) of EtOH and 50 µl of3M NaAc were added, and the RNA mixture was incubated at 20 ^{o}C overnight. After the overnight incubation the small RNA fraction was spun at 13000rpm for 10min at 4^{o}C. The RNA pellet was air-dried and re-suspended in 30 µl H_2O. RNA was then stored at -80^{o}C.

2.4.3 Reverse Transcription

1 µg of RNA extracted with MasterPure™ Yeast RNA Purification kit was mixed with 1µl TurboDNase and 1µl of 5x TurboDNase buffer in 10µl of DEPC-treated water (Sigma-Aldrich). Reactions were incubated at 37^{0}C for 1h. After the DNAse treatment, 2µl random hexamers (100ng/µl), 2µl dNTPs (10mM) and 12µl DEPC-treated water were added with subsequent incubation at 65^{o}C for 5 min. Then samples were incubated on ice for 5min. 2µl of DEPC-treated water, 2µl DTT (0.1M) and 8µl of 5x SuperScript III buffer were added, mixed by pipetting and split into 2x19µl aliquots. 1µl of SuperScript III RT enzyme was added to one of the aliquots, with

the remaining sample acting as a negative control. Both samples were incubated at 25^{o}C for 6min, 50^{o}C for 60min and 70^{o}C for 15min. After the incubation, both samples were diluted 1:4 in dH_2O for the subsequent qPCR.

2.4.4 qPCR

qPCR was performed using LightCycler © 480 SYBR Green I Mastermix and LightCycler © 96 system (Roche). 3μl of sample DNA was mixed with 5μl LightCycler Mastermix, 0.5μl Forward and 0.5μl Reverse primers (both at 10μM) and 1μl dH_2O. Primers were targeting gene exons. Primer sequences are presented in table 2-1. Each +RT sample was run in triplicates. Samples were subjected to the following cycling conditions:

95^{o}C — 2min

95^{o}C — 20 sec
55^{o}C — 20 sec
72^{o}C — 20 sec/kb
} 45 cycles

Differences between the samples were analysed as outlined in 2.7.3. Sample python code used for analysis is shown in appendix B.

Primer efficiencies for actin (qact F and qactR) and dg (qdg F and qdg R) primers were kindly provided to me by Elliott Chapman. The rest were calculated based on the slope of calibration curve (Rocha et al., 2016). The following formula was used:

$$Primer\ efficiency = 10^{(-\frac{1}{slope})}$$

Sample python code used for analysis is shown in appendix C.

2.4.5 Northern Blotting

12% Urea polyacrylamide gel was prepared from premade SequaGel reagents (National Diagnostics). For 1 gel 4.8ml Concentrate, 4.2ml Diluent, 1ml Buffer, 80μl 10%APS and 4μl TEMED were mixed, where APS and TEMED were added last. Small RNAs (10-100μg) were mixed 1:1 with 2xFDE sample buffer (100μl 0.5 EDTA pH8.0, 100mg bromophenol blue, 100mg xylene cyanol, to 10ml with 100% deiosined formamide). RNAs were then denatured at 95$_o$C for 3 min and cooled on ice. Urea was rinsed from the wells with 0.5xTBE, and the samples were loaded straight after. The gel was run using Mini=PROTEAN Tetra Cell (bio-Rad) in 0.5xTBE at 200V for 60min. RNAs were then transferred to Hybond NX membrane (Amersham) using Semiphor semi-dry apparatus. Membrane was pre-soaked in 0.5x TBE for 5min. Six cut pieces of Whatmann 3MM paper were quickly soaked in 0.5xTBE and the following stack was assembled:

3x3MM (Top)

Gel

Membrane

3x3MM (Bottom)

Small RNA transfer was performed at 250mA for 35min.

Membrane with transferred small RNAs was washed once in dH_2O. 3MM paper (9x11mm) was soaked in a crosslinking solution (75μl 1M HCl, 65μl 99% methylimidazole, 0.18g EDC and 5.860ml dH_2O). The membrane was placed on top of the saturated 3MM paper with small RNAs facing up. The membrane-paper stack was then wrapped in saran and foil and incubated at 50-60^oC for 2hrs. The membrane was washed once in dH_2O, and at this point it was either wrapped in saran and stored at -20^oC until required, or used for pre-hybridization.

For prehybridization membrane was incubated with 30ml of 42^oC Church buffer (1mM EDTA, 60mM Na_2HPO_4, 140mM NaH_2PO4, 7% SDS) inside a hybridization bottle for a minimum of 1h at 42^oC with rotation. During prehybridization, probe reactions were prepared on ice. siRNA probe reaction was prepared as follows: 1μl of IK8 (5'ATT CCT TTC TGA ACC TCT CTG TTA T), IK9 (5'TTT GAT GCC CAT GTT CAT TCC ACT TG) and IK10 (5' GGG AGT ACA TCA TTC CTA CTT CGA

TA) oligo mix (each at 4pmol/μl), 2ul dH_2O, 1μl 10x PNK buffer (NEB), 1μl T4 PNK(NEB) and 5μl γ^{32}P ATP. snoRNA58/5sRNA loading control probe was prepared as follows: 1μl snoRNA58/ 5S rRNA at 50pmol/μl, 1μl 10x PNK buffer, 1μl T4 PNK, 1μ γ^{32}P ATP, 6μl dH_2O. Probe reactions were incubated at 37^{o}C for 1h in a thermal cycler, after which 40μl of dH_2O was added. Probes were then passed through G50 ProbeQuant spin column (Amersham) at 3000rpm for 2 min to remove all unincorporated γ^{32}P ATP.

After finishing probe preparation, prehybridization Church buffer was removed, and 25ml of 42^{o}C fresh Church buffer was added to the hybridization bottle . Both siRNA and control probes were added to the bottle and left to hybridize overnight at 42^{o}C.

After the overnight incubation, hybridization solution was poured off and the membrane was washed twice for 20min at 42^{o}C in 100ml 2x SSC, 0.2% SDS solution (50ml 20x SSC, 5ml SDS,445ml dH_2O). Membrane was then placed on a piece of 3MM Whatmann paper , wrapped in saran and taped into an x-ray cassette. Blanked phosphoimager screen was then placed face down on top of the membrane and exposed for 6hr or a few days.

2.5 DNA protocols

2.5.1 Genomic DNA extraction

10ml cell cultures were grown overnight until they reached early stationary phase. Cells were centrifuged at 3000rpm for 2min, and the pellets was resuspended in 500μl SP buffer (1.2M sorbitol, 50mM $Na_2HPO_4*7H_2O$, 50mM sodium citrate, 40mM EDTA, pH5.6 with orthophosphoric acid) supplemented with 0.4mg/ml zymolyase 100T (10mg/ml in 50%glycerol). Samples were incubated at 37°C for 30-60min. Samples were centrifuged, and pellets were washed with 500μl SP buffer. Samples were centrifuged, and all the supernatant removed. Pellets were resuspended in 500μl TE and transferred to Eppendorf tube. 50μl of 50% SDS was added, mixed by vortexing and samples were incubated at 65°C for 5-10 min. 165μl 5M KOAc was added, samples were vortexed and incubated on ice for 30min. Then samples were spun at 13,000rpm for 10min at 4°C. Supernatant was transferred to fresh 2ml tube and 750μl isopropanol was added. Samples were then incubated either on dry ice for 10min or at -80°C for 30min. Samples were then spun at 13,000rpm for 10min at 4°C, supernatant was removed and pellets were air dried. Pellets were resuspended in 300μl TE and the DNA concentration was quantified using NanoDrop. DNA was subsequently used for PCR.

2.5.2 Sanger sequencing

DNA was sequenced using BigDye™ Terminator v3.1 Cycle sequencing Kit (Thermo Fisher Scientific). Sequencing reactions were prepared as follows: 2μl BigDye™ Terminator v3.1 Ready reaction mix, 2μl BigDye™ Terminator v3.1 Sequencing Buffer, 0.3μl primer (10μM), 300-400 ng DNA and 4.7μl dH_2O. Reactions were subjected to the following cycling conditions:

95°C — 5min

95°C — 30 sec
50°C — 20 sec
60°C — 4 min
} 25 cycles

60°C — 1 min

Samples were then processed by Edinburgh Genomics using a *3730xl* DNA Analyzer (Thermo Fischer Scientific).

2.6 Protein protocols

2.6.1 ChIP qPCR

Cells were grown in 100ml culture until they reach $5x10_6$ cells/ml concentration. Each cell culture was split into two 50ml Falcon tubes, and 1.35ml of 37% (1% final concentration) formaldehyde was added to each. Tubes were inverted several times and left on a rotating platform to fix for 15 min at room temperature. Fixed cells were then spun at 3500rpm for 2 min at 4_oC. Pellets were washed twice with 50ml ice-cold PBS, and were then transferred to round-bottom screw cap tubes. Cells were spun at 2700 rpm for 2min at 4_oC and the supernatant was removed. At this point cells were either stored at -80_oC or processed further.

350μl of ice-cold lysis buffer (100μl of 0.5M EDTA, 1.4ml of 5M NaCl, 2.5ml of 1M 50mM Hepes-KOH, pH7.5, 2.5ml of (w/v) sodium deoxycholate, 5ml of 10% (v/v) Triton X-100 and 38.5ml dH_20) with 3.5 μl of 100x yeast protease inhibitors and 3.5μl of 100x PMSF were added to each sample. 500μl of acid-washed glass beads were added, and cells were lysed using a Mini-Beadbeater for 2x2min with 1min incubation on ice between the two grinding sessions. Two holes were punched using a 0.5mmx16mm needle in each of the round-bottomed tubes. Each round-bottom tube was placed on top of an Eppendorf tube with the lid cut off. The stacked tubes were then

placed inside 15ml Falcon tubes and spun at 1000rpm for 1 min at 4^{o}C. The tubes were then removed from the Falcon tube using metal forceps, and the round-bottom tubes were discarded. The eppendorf tubes were closed with the cut-off lids and sonicated using Biotuptor Twin (Diagenode) for 4x5min cycles with 30 sec ON and 30 sec OFF. Samples were then spun at 13000rpm for 5min at 4 ^{o}C to pellet debris. Supernatant was transferred to a fresh tube, and spun again at 13000rpm for 15min at 4 ^{o}C. Supernatant was transferred to a fresh tube and kept on ice. During the centrifugation, Protein G agarose beads (Roche) mix was prepared. Beads were centrifuged at 2000rpm for 1 min, washed with 1ml lysis buffer 4 times and then resuspended in half the original volume taken of lysis buffer. Total volume of Protein G agarose is 50μl per ChIP. To pre-clear the lysate, 25μl of Protein G agarose solution was added and the samples were incubated for 1h at 4 ^{o}C. Samples were centrifuged at 2000 rpm for 2 min at 4 ^{o}C, and the lysates of the same strain were pooled into a clean Eppendorf tube. 30μl from each strain were transferred to a different Eppendorf tube and kept at -20 ^{o}C as an input sample. Pooled lysates were split into two ~300μl aliquots, where 25μl of remaining Protein G agarose were added to both. 1μl of anti-H3K9me2 Ab 5.1.1 (Nakagawachi et al., 2003) was added to one of the aliquots (the other aliquot is a negative control), and both aliquots were incubated overnight at 4^{o}C with rotation.

The next day the beads were centrifuged at 2000rpm for 4 min at 4^{o}C, and the supernatant was discarded. Beads were then washed with:

- 1 ml of lysis buffer
- 1ml of high salt lysis buffer (100µl of 0.5M EDTA, 5ml of 5M NaCl, 2.5ml of 1M 50mM Hepes-KOH, pH7.5, 2.5ml of (w/v) sodium deoxycholate, 5ml of 10% (v/v) Triton X-100 and 38.5ml dH_20) for 10min at 4^{o}C with rotation
- 1ml of wash buffer (12.5ml of 2% w/v) sodium deoxycholate, 6.25ml of 2M LiCl, 5ml of 5% NP-40, 0.5ml of 1M Tris-HCl, pH8, 100µl 0.5M EDTA, 25.65mls dH_2) for 10min at 4^{o}C with rotation
- 1ml TE buffer, pH8.0 (100µl of 0.5M EDTA, 0.5ml of 1M Tris-HCl, pH8, 49.4ml dH_2)

After the last wash the supernatant was removed and 100µl of 10% Chelex100 resin (BioRad) in dH_2O was added to each IP sample and to each input sample frozen earlier. Samples were boiled at 100^{o}C for 12 min, and then cooled at room-temperature for 5min. Samples were briefly spun, and 2.5µl of 10mg/ml proteinase K (Roche) was added to each. Samples were incubated at 55^{o} for 30 min with shaking at 1000rpm on ThermoMixer® (Eppendorf). Samples were then boiled at 100^{o}C for 10 min to inactivate proteinase K. Samples

were briefly spun and 50μl of supernatant (excluding resin) was removed to a fresh tube and stored at -20$_{o}$C . For qPCR IP samples were diluted 1:8 in sterile dH_2O and input samples were diluted 1:80. qPCRs and statistical analyses were performed as outlined in 2.4.4 and 2.7.3 respectively. Sample python code used for analysis is shown in appendix C.

2.7 Replication, plate scanning and statistical analysis

2.7.1 Plate scanning

Plates were scanned using Epson Perfection V33 scanner (4800 DPI x 9600 DPI, 48 Bits Colour). A sheet of blue carton board was added during scanning to improve the contrast of the scanned image.

2.7.2 Replication

2.7.2.1 Plasmid-based assay

After performing a single 96 – well transformation (section 2.2.2), 10-20 colonies grew per each strain transformed. All of these colonies were stored at -80^{0}C (section 2.1). For subsequent experiments, 10μl inoculation loops were used to plate a fraction of stored cells on YES agar plates. After incubating the plates for 2 days at 32 ^{0}C, 10μl inoculation loops were used to take a swab of different colonies for liquid cultures (section 2.1.2) for qPCR (section 2.4.4.), ChIP qPCR (section 2.6.1) and Northern blot (section 2.4.5) analyses. Three biological replicates were achieved by repeating the process of defrosting stored cells three times. Three technical replicates were performed per each qPCR and ChIP qPCR run.

2.7.2.2 Cross-based assay

After crossing the parental strains and plating the progeny on 5FOA media with limiting adenine (section 5.2), plates were imaged as described in section 2.1.4 and the proportion of red and white colonies was recorded. To generate independent replicas, this procedure was repeated four times.

2.7.3. Statistical analysis

The data were analysed using functions written in Python (PYTHON 3 Reference Manual), in Jupyter notebook (version 5.5.0, accessed through Anaconda Navigator) as an IDE. To analyse qPCR (section 2.4.4) and ChIP qPCR (section 2.6.1) data I used log2Fold Change (log2FC). Geometric mean was used to calculate mean fold changes. Cohen's d with associated 95% CI (Lakens, 2013) was used for evaluation in figure 5 – 4. When 95% CI did not include 0, then the difference was deemed significant.

Type	Name	Sequence
ER_5F	Hyg Fus_F	TCAATACACTACATGGCG
ER_5R	Ttef URA4Fus R	CCAGTGGGATTTGTAGCTAACAGTATAGCGACCAG CATTC
ER_3F	Clr4 URA4 Fus_F	GTTTCGTCAATATCACAAGCTTACAATTTGTTTTTCT CCAT
ER_3R	Clr4 Fus R	CTGATATAGCACTTCCCG
ER_5F	Nat Fus_F	ACCACTCTTGACGACACG
ER_5R	Ttef URA4Fus R	CCAGTGGGATTTGTAGCTAACAGTATAGCGACCAG CATTC
ER_3F	Dcr1 URA4 Fus F	GTTTCGTCAATATCACAAGCTGACTTGAAATATACA GTATT
ER_3R	Dcr1 Fus R	TGATCAAAACTCTCTCCG
ER_5F	Hyg Fus_F	TCAATACACTACATGGCG
ER_5R	Ttef URA4Fus R	CCAGTGGGATTTGTAGCTAACAGTATAGCGACCAG CATTC
ER_3F	Rik1 URA4 Fus F	GTTTCGTCAATATCACAAGCTTATCTTACACTTTATG GATC
ER_3R	Rik1 Fus R	CCCAGAGTTTACATACGTGC
ER_5F	Nat Fus_F	ACCACTCTTGACGACACG
ER_5R	Ttef URA4Fus R	CCAGTGGGATTTGTAGCTAACAGTATAGCGACCAG CATTC
ER_3F	Ago1 URA4 Fus F	GTTTCGTCAATATCACAAGCTAAATAGATATACGATT GACT
ER_3R	Ago1 Fus R	GATATCTCCCTTTTGCTGG
U_5F	spUra4_F	TTAGCTACAAATCCCACTGG
U_5R	spUra4-5Fusion_R	TTATGTAGTCGCTTTGAAGG
U_3F	spUra4-3Fusion_F	AATCCGAAATCTTAGAATTGG
U_3R	spUra4_R	AGCTTGTGATATTGACGAAAC
	HygR F	GAGAGCCTGACCTATTGC
	ura4_utr_R seq	GCAAGGGCATTAAGGCTTATTTACAG
	NSL-1	AAGGTGTTCCCCGACGACGAATCG
	ura4_utr_R seq	GCAAGGGCATTAAGGCTTATTTACAG
	Clr4 fus_check R	CCAATCAGTTGAACAAGC
	URA4_UTR_Fseq	CATGCTCCTACAACATTACCACAATC
	Ago1 fus_check R	GCGAATTGGAAGAGACCG
	URA4_UTR_Fseq	CATGCTCCTACAACATTACCACAATC

	Dcr1_3'UTR_R	CATTGACAATACCAGTTGC
	URA4_UTR_Fseq	CATGCTCCTACAACATTACCACAATC
	Rik1 fus_check R	TCTTCAATGATACGCACG
	URA4_UTR_Fseq	CATGCTCCTACAACATTACCACAATC
	Clr4-400(box 6)	GCTCTGAAATTGAACACATCGAC
	Clr4+600R (box6)	CTTAGATGGGTATAAGAGTCAAG
	Rik1+800F (box4)	CTCCTTTGAAAGGGCAAAAGATG
	Rik1_1300R (box4	GATGGGTCTAGCTCTAACTG
	Dcr1 F (box4)	CGAGACTGGTGCTTTACTCAC
	Dcr1 R (box4)	GTAAAGAGACGAAGCAACGTG
	Ago1_prb2_F	CAGATTGCTCGAACGTTAGAGAC
	ago1_prb2_R	CGAGCTGGAACTTCGAGCATC
	qRik1_F	TGGAATCGCAACGCGAAAAG
	qRik1_R	GGCCAGTTTTCAACCGTTC
	qStc1_F	ATTTGTTCGTGGGAGAACGGT
	qStc1_R	GAATCATGCTGTTTGGGCTGG
	qAgo1_F	TCCCACGAAAGCAATCCCAG
	qAgo1_R	CAACACATGCTTCGCCCATC
	qClr4_F	GGATGCTCAGAACTATGG
	qClr4_R	GGCTGAATGTCTTTGATGGC
	qDcr1_F	GTCTTTGGTTTGGGGAGC
	qDcr1_R	TCAATTGCCAGTTCCTCG
	qdg F	AATTGTGGTGGTGTGGTAATAC
	qdg R	GGGTTCATCGTTTCCATTCAG
	qact1 F	GGTTTCGCTGGAGATGATG
	qact1 R	ATACCACGCTTGCTTTGAG

Table 2-1. A list of primers used.

'Type' indicates the primer type from figure 2-1 for clarity.

Name	Source
p348	Marasovic et al., 2013
p474	Marasovic et al., 2013
pREP-81	Basi et al., 1993
pREP-CM1	This study
pREP-CM1	This study
pREP-CD41	This study

Table 2-2. A list of plasmids used.

strain no.	Genotype
3481	h+ otr1R(sph1):ade6 lys1::ura ade6-210 leu1-32 ura4-D18
3513	h+Clr4::hygR dcr1::NatR otr1R(sph1):ade6 lys::ura ade6-210 leu1-32 ura4-D18
3514	h-Clr4::hygR dcr1::NatR otr1R(sph1):ade6 lys::ura ade6-210 leu1-32 ura4-D18
3637	h-Clr4::hygR dcr1::NatR otr1R(sph1):ade6 lys::ura ade6-210 leu1-32 ura4-D18 pREP-CD41 (Clr4 WT Dcr1 WT)
3783	Tri::KanR Clr4::hygR dcr1::NatR otr1R(sph1):ade6 lys::ura ade6-210 leu1-32 ura4-D18
3833	h90 Clr4::hygR dcr1::NatR cycR otr1R(sph1):ade6 lys::ura ade6-210 leu1-32 ura4-D18
3854	tri1Δ::Kan Clr4::hygR dcr1::NatR cycR otr1R(sph1):ade6 lys::ura ade6-210 leu1-32 ura4-D19
3855	SPAC31G5.18c::kanR Clr4::hygR dcr1::NatR cycR otr1R(sph1):ade6 lys::ura ade6-210 leu1-32 ura4-D20
3856	SPAC12G12.07c::KanR Clr4::hygR dcr1::NatR cycR otr1R(sph1):ade6 lys::ura ade6-210 leu1-32 ura4-D21
3857	rim20c::KanR Clr4::hygR dcr1::NatR cycR otr1R(sph1):ade6 lys::ura ade6-210 leu1-32 ura4-D22
3858	rrg1::KanR Clr4::hygR dcr1::NatR cycR otr1R(sph1):ade6 lys::ura ade6-210 leu1-32 ura4-D23
3859	tfb2::KanR Clr4::hygR dcr1::NatR cycR otr1R(sph1):ade6 lys::ura ade6-210 leu1-32 ura4-D24
3860	arp8::KanR Clr4::hygR dcr1::NatR cycR otr1R(sph1):ade6 lys::ura ade6-210 leu1-32 ura4-D25
3861	hrp3::Kan Clr4::hygR dcr1::NatR cycR otr1R(sph1):ade6 lys::ura ade6-210 leu1-32 ura4-D26
3862	nrl1::KanR Clr4::hygR dcr1::NatR cycR otr1R(sph1):ade6 lys::ura ade6-210 leu1-32 ura4-D27
3863	tos4::KanR Clr4::hygR dcr1::NatR cycR otr1R(sph1):ade6 lys::ura ade6-210 leu1-32 ura4-D28
3864	SPBC21C3.12c::KanR Clr4::hygR dcr1::NatR cycR otr1R(sph1):ade6 lys::ura ade6-210 leu1-32 ura4-D29
3865	Nse5::KanR Clr4::hygR dcr1::NatR cycR otr1R(sph1):ade6 lys::ura ade6-210 leu1-32 ura4-D30
3866	SPCC126.13c::KanR Clr4::hygR dcr1::NatR cycR otr1R(sph1):ade6 lys::ura ade6-210 leu1-32 ura4-D31
3867	SPCC11E10.09c::KanR Clr4::hygR dcr1::NatR cycR otr1R(sph1):ade6 lys::ura ade6-210 leu1-32 ura4-D32
3868	snt2::KanR Clr4::hygR dcr1::NatR cycR otr1R(sph1):ade6 lys::ura ade6-210 leu1-32 ura4-D33
3869	msh3::KanR Clr4::hygR dcr1::NatR cycR otr1R(sph1):ade6 lys::ura ade6-210 leu1-32 ura4-D34
3870	SPCC645.13::KanR Clr4::hygR dcr1::NatR cycR otr1R(sph1):ade6 lys::ura ade6-210 leu1-32 ura4-D35
3871	SPAC589.05c::KanR Clr4::hygR dcr1::NatR cycR otr1R(sph1):ade6 lys::ura ade6-210 leu1-32 ura4-D36
3872	urm1::KanR Clr4::hygR dcr1::NatR cycR otr1R(sph1):ade6 lys::ura ade6-210 leu1-32 ura4-D37
3918	h+otr1R(sph1):ade6 lys1::ura cycR ade6-210 leu1-32 ura4-
3919	h- otr1R(sph1):ade6 lys1::ura cycR ade6-210 leu1-32 ura4-

3920	mkt1::Kan Clr4::hygR dcr1::NatR cycR otr1R(sph1):ade6 lys::ura ade6-210 leu1-32 ura4-D18
3921	h90 Clr4::hygR dcr1::NatR cycR otr1R(sph1):ade6 lys::ura ade6-210 leu1-32 ura4-D18 pREP-CD41
3922	tri1Δ::Kan Clr4::hygR dcr1::NatR cycR otr1R(sph1):ade6 lys::ura ade6-210 leu1-32 ura4-D19 pREP-CD41
3923	tfb2::KanR Clr4::hygR dcr1::NatR cycR otr1R(sph1):ade6 lys::ura ade6-210 leu1-32 ura4-D24+pREP-CD41
3924	tos4::KanR Clr4::hygR dcr1::NatR cycR otr1R(sph1):ade6 lys::ura ade6-210 leu1-32 ura4-D28+pREP-CD41
3925	SPBC21C3.12c::KanR Clr4::hygR dcr1::NatR cycR otr1R(sph1):ade6 lys::ura ade6-210 leu1-32 ura4-D29+pREP-CD41
3926	Nse5::KanR Clr4::hygR dcr1::NatR cycR otr1R(sph1):ade6 lys::ura ade6-210 leu1-32 ura4-D30+pREP-CD41
3940	h90 Clr4::hygR dcr1::NatR cycR otr1R(sph1):ade6 lys::ura ade6-210 leu1-32 ura4-D18 pREP-CD41
3941	mkt1::Kan Clr4::hygR dcr1::NatR cycR otr1R(sph1):ade6 lys::ura ade6-210 leu1-32 ura4-D18 pREP-CD41
3942	h90 Clr4::hygR dcr1::NatR cycR otr1R(sph1):ade6 lys::ura ade6-210 leu1-32 ura4-D18 pREP81(empty)
3968	h90 Clr4::hygR dcr1::NatR cycR otr1R(sph1):ade6 lys::ura ade6-210 leu1-32 ura4-D18 pREP-CD41
4152	Tos4::KanR otr1R(sph1):ade6 lys1::ura ade6-210 leu1-32 ura4-D18 (MIXED POPULATION)
4182	h-Dcr1::NATR otr1R(sph1):ade6 lys1::ura cycR his3D(?) arg3D(?) leu1-32 ade6-210 ura4-DS/D18
4380	h90 clr4::hygR dcr1::NATR cycR otr1R(Sph1):ade6+ ade6-210 leu1-32 ura4-D18 his3D1-(?)
4386	h+ otr1R(sph1):ade6 lys1::LEU1 ade6-210 leu1-32 ura4-D18
4411	h+ clr4::hygR:URA otr1R(Sph1):ade6+ his3D1- ade6-210 leu1-32 ura4-D18
4412	h+ clr4::hygR:URA otr1R(Sph1):ade6+ his3D1- ade6-210 leu1-32 ura4-D18
4479	tri1Δ::KanR clr4::hygR dcr1::NATR cycR otr1R(Sph1):ade6+ ade6-210 leu1-32 ura4-D18 his3D1-(?)
4480	mkt1::kanR clr4::hygR dcr1::NATR cycR otr1R(Sph1):ade6+ ade6-210 leu1-32 ura4-D18 his3D1-(?)
4481	rim20::KanR clr4::hygR dcr1::NATR cycR otr1R(Sph1):ade6+ ade6-210 leu1-32 ura4-D18 his3D1-(?)
4482	rrg1::KanR clr4::hygR dcr1::NATR cycR otr1R(Sph1):ade6+ ade6-210 leu1-32 ura4-D18 his3D1-(?)
4483	tfb2::KanR clr4::hygR dcr1::NATR cycR otr1R(Sph1):ade6+ ade6-210 leu1-32 ura4-D18 his3D1-(?)
4484	arp8::KanR clr4::hygR dcr1::NATR cycR otr1R(Sph1):ade6+ ade6-210 leu1-32 ura4-D18 his3D1-(?)
4485	hrp3::KanR clr4::hygR dcr1::NATR cycR otr1R(Sph1):ade6+ ade6-210 leu1-32 ura4-D18 his3D1-(?)
4486	nrl1::KanR clr4::hygR dcr1::NATR cycR otr1R(Sph1):ade6+ ade6-210 leu1-32 ura4-D18 his3D1-(?)
4487	tos4::KanR clr4::hygR dcr1::NATR cycR otr1R(Sph1):ade6+ ade6-210 leu1-32 ura4-D18 his3D1-(?)

4488	SPBC21C3.12c::KanR clr4::hygR dcr1::NATR cycR otr1R(Sph1):ade6+ ade6-210 leu1-32 ura4-D18 his3D1-(?)
4489	Nse5::KanR clr4::hygR dcr1::NATR cycR otr1R(Sph1):ade6+ ade6-210 leu1-32 ura4-D18 his3D1-(?)
4490	SPCC126.13c::KanR clr4::hygR dcr1::NATR cycR otr1R(Sph1):ade6+ ade6-210 leu1-32 ura4-D18 his3D1-(?)
4491	SPCC11E10.09c::KanR clr4::hygR dcr1::NATR cycR otr1R(Sph1):ade6+ ade6-210 leu1-32 ura4-D18 his3D1-(?)
4492	snt2::KanR clr4::hygR dcr1::NATR cycR otr1R(Sph1):ade6+ ade6-210 leu1-32 ura4-D18 his3D1-(?)
4493	msh3::KanR clr4::hygR dcr1::NATR cycR otr1R(Sph1):ade6+ ade6-210 leu1-32 ura4-D18 his3D1-(?)
4494	SPCC645.13::KanR clr4::hygR dcr1::NATR cycR otr1R(Sph1):ade6+ ade6-210 leu1-32 ura4-D18 his3D1-(?)
4495	SPAC589.05c::KanR clr4::hygR dcr1::NATR cycR otr1R(Sph1):ade6+ ade6-210 leu1-32 ura4-D18 his3D1-(?)
4496	urm1::KanR clr4::hygR dcr1::NATR cycR otr1R(Sph1):ade6+ ade6-210 leu1-32 ura4-D18 his3D1-(?)
4550	h- Ago1::NatR ade6-210 leu1-32 ura4-D18 otr1R (dg-glu) Sph1::ade6
4576	h+ clr4::hygR:URA4 otr1R(Sph1):ade6+ his3D1- ade6-210 leu1-32 ura4-D18
4579	h- rik1::HygR:URA4 otr1R:ade6+ ade6-210 leu1-32 ura4-D18 his3D
4580	h- Ago1::NatR:URA4 ade6-210 leu1-32 ura4-D18 otr1R (dg-glu) Sph1::ade6
4600	h 90 clr4::hygR:URA4 Ago1::NatR:URA4 otr1R(Sph1):ade6+ ade6-210 ura4-D18 leu1-32 his3D1(?)
4658	h+Dcr1::Nat:URA4 otr1R (dg-glu) Sph1::ade6ade6-210 leu1-32 ura4-D18
4659	h+Dcr1::Nat:URA4 otr1R (dg-glu) Sph1::ade6ade6-210 leu1-32 ura4-D18
4706	h- rik1::HygR:URA4 Dcr1::Nat:URA otr1R:ade6+ ade6-210 leu1-32 ura4-D18 his3D(?)
4707	h+ rik1::HygR:URA4 Dcr1::Nat:URA otr1R:ade6+ ade6-210 leu1-32 ura4-D18 his3D(?)
4782	dos2::kanMX6 rik1::HygR:URA4 Dcr1::Nat:URA otr1R:ade6+ leu1-32 ade6-210 ura4-D18 his3D1(?)
4783	mkt1::kanR rik1::HygR:URA4 Dcr1::Nat:URA otr1R:ade6+ ade6-210 leu1-32 ura4-D18 his3D(?)
4784	tri1Δ::KanR rik1::HygR:URA4 Dcr1::Nat:URA otr1R:ade6+ ade6-210 leu1-32 ura4-D18 his3D(?)
4785	rim20::KanR rik1::hygR:URA4 Dcr1::NatR:URA4 otr1R:ade6+ ade6-210 leu1-32 ura4-D18 his3D1(?)
4786	rrg1::KanR rik1::hygR:URA4 dcr1::NatR:URA4 otr1R:ade6+ ade6-210 leu1-32 ura4-D18 his3D1(?)
4787	tfb2::KanR rik1::hygR:URA4 Dcr1::NatR:URA4 otr1R:ade6+ ade6-210 leu1-32 ura4-D18 his3D1(?)
4788	arp8::KanR Rik1::hygR:URA4 Dcr1::NatR:URA4 otr1R:ade6+ ade6-210 leu1-32 ura4-D18 his3D1(?)
4789	hrp3::KanR rik1::hygR:URA4 dcr1::NatR:URA4 otr1R:ade6+ ade6-210 leu1-32 ura4-D18 his3D1(?)

4790	nrl1::KanR rik1::hygR:URA4 dcr1::NatR:URA4 otr1R:ade6+ ade6-210 leu1-32 ura4-D18 his3D1(?)
4791	tos4::KanR rik1::hygR:URA4 dcr1::NatR:URA4 otr1R:ade6+ ade6-210 leu1-32 ura4-D18 his3D1(?)
4792	SPBC21C3.12c::KanR rik1::hygR:URA4 dcr1::NatR:URA4 otr1R:ade6+ ade6-210 leu1-32 ura4-D18 his3D1(?)
4793	Nse5::KanR rik1::hygR:URA4 dcr1::NatR:URA4 otr1R:ade6+ ade6-210 leu1-32 ura4-D18 his3D1(?)
4794	SPCC126.13c::KanR rik1::hygR:URA4 dcr1::NatR:URA4 otr1R:ade6+ ade6-210 leu1-32 ura4-D18 his3D1(?)
4795	SPCC11E10.09c::KanR rik1::hygR:URA4 dcr1::NatR:URA4 otr1R(Sph1):ade6+ ade6-210 leu1-32 ura4-D18 his3D1(?)
4796	snt2::KanR rik1::hygR:URA4 dcr1::NatR:URA4 otr1R:ade6+ ade6-210 leu1-32 ura4-D18 his3D1(?)
4797	msh3::KanR rik1::hygR:URA4 dcr1::NatR:URA4 otr1R):ade6+ ade6-210 leu1-32 ura4-D18 his3D1(?)
4798	SPCC645.13::KanR rik1::hygR:URA4 dcr1::NatR:URA4 otr1R:ade6+ ade6-210 leu1-32 ura4-D18 his3D1(?)
4799	SPAC589.05c::KanR rik1::hygR:URA4 dcr1::NatR:URA4 otr1R:ade6+ ade6-210 leu1-32 ura4-D18 his3D1(?)
4800	urm1::KanR rik1::hygR:URA4 dcr1::NatR:URA4 otr1R:ade6+ ade6-210 leu1-32 ura4-D18 his3D1(?)
4803	dos2::kanMX6 clr4::hygR:URA4 Ago1::NatR:URA4 otr1R(Sph1):ade6+ leu1-32 ade6-210 ura4-D18 his3D1 (?)
4913	h+(?) clr4::hygR:URA4 Ago1::NatR:URA4 otr1R(sph1):ade6 lys1::LEU1 ade6-210 leu1-32 ura4-D18 his3D1(?)
4914	h- clr4::hygR:URA4 Ago1::NatR:URA4 otr1R(sph1):ade6 lys1::LEU1 ade6-210 leu1-32 ura4-D18 his3D1(?)
4915	h- rik1::HygR:URA4 Dcr1::Nat:URA otr1R(sph1):ade6 lys1::LEU1 ade6-210 leu1-32 ura4-D18 his3D(?)
4916	h+ rik1::HygR:URA4 Dcr1::Nat:URA otr1R(sph1):ade6 lys1::LEU1 ade6-210 leu1-32 ura4-D18 his3D(?)
5032	cid12-GFP-KanR rik1::HygR:URA4 Dcr1::Nat:URA otr1R:ade6+ ade6-210 ura4-D18 arg3D4? his3D1?leu1-32?
5033	cid12-GFP-KanR clr4::hygR:URA4 Ago1::NatR:URA4 otr1R(Sph1):ade6+ ade6-210 ura4-D18 arg3D4? his3D1?leu1-
5109	h90 clr4::NATR otr1R (dg-glu) Sph1::ade6 ade6-210 (his3?) leu1-32 ura4-D18
5110	h+ clr4::NATR otr1R (dg-glu) Sph1::ade6 ade6-210 (his3?) leu1-32 ura4-D18
5135	h+Ago1::NatR:URA4 ade6-210 leu1-32 ura4-D18 otr1R (dg-glu) Sph1::ade6
5136	h-Dcr1::Nat:URA4 otr1R (dg-glu) Sph1::ade6 ade6-210 leu1-32 ura4-D18
5240	h + Ago1::NatR:URA4 rik1::HygR:URA4 otr1R:ade6+ ade6-210 leu1-32 ura4-D18 his3D(?)
5241	h- Ago1::NatR:URA4 rik1::HygR:URA4 otr1R:ade6+ ade6-210 leu1-32 ura4-D18 his3D(?)
5242	h 90 Dcr1::Nat:URA4 clr4::hygR:URA4 otr1R(Sph1):ade6+ his3D1(?) ade6-210 leu1-32 ura4-D18
5244	dos2::kanMX6 Dcr1::Nat:URA4 clr4::hygR:URA4 otr1R(Sph1):ade6+ leu1-32 ade6-210 ura4-D18 his3D1(?)

5245	6D8 goi::kanR Dcr1::Nat:URA4 clr4::hygR:URA4 otr1R(Sph1):ade6+ his3D1(?) ade6-210 leu1-32 ura4-D18
5246	tri1Δ::KanR Dcr1::Nat:URA4 clr4::hygR:URA4 otr1R(Sph1):ade6+ his3D1(?) ade6-210 leu1-32 ura4-D18
5247	dos2::kanMX6 Ago1::NatR:URA4 rik1::HygR:URA4 otr1R(Sph1):ade6+ leu1-32 ade6-210 ura4-D18 his3D1(?)
5248	6D8 goi::kanR Ago1::NatR:URA4 rik1::HygR:URA4 otr1R(Sph1):ade6+ his3D1(?) ade6-210 leu1-32 ura4-D18
5249	tri1Δ::KanR Ago1::NatR:URA4 rik1::HygR:URA4 otr1R(Sph1):ade6+ his3D1(?) ade6-210 leu1-32 ura4-D18
5250	rim20::KanR Dcr1::Nat:URA4 clr4::hygR:URA4 otr1R(Sph1):ade6+ leu1-32 ade6-210 ura4-D18 his3D1(?)
5251	rrg1::KanR Dcr1::Nat:URA4 clr4::hygR:URA4 otr1R(Sph1):ade6+ leu1-32 ade6-210 ura4-D18 his3D1(?)
5252	tfb2::KanR Dcr1::Nat:URA4 clr4::hygR:URA4 otr1R(Sph1):ade6+ leu1-32 ade6-210 ura4-D18 his3D1(?)
5253	arp8::KanR Dcr1::Nat:URA4 clr4::hygR:URA4 otr1R(Sph1):ade6+ leu1-32 ade6-210 ura4-D18 his3D1(?)
5254	hrp3::KanR Dcr1::Nat:URA4 clr4::hygR:URA4 otr1R(Sph1):ade6+ leu1-32 ade6-210 ura4-D18 his3D1(?)
5255	nrl1::KanR Dcr1::Nat:URA4 clr4::hygR:URA4 otr1R(Sph1):ade6+ leu1-32 ade6-210 ura4-D18 his3D1(?)
5256	tos4::KanR Dcr1::Nat:URA4 clr4::hygR:URA4 otr1R(Sph1):ade6+ leu1-32 ade6-210 ura4-D18 his3D1(?)
5257	SPBC21C3.12c::KanR Dcr1::Nat:URA4 clr4::hygR:URA4 otr1R(Sph1):ade6+ leu1-32 ade6-210 ura4-D18 his3D1(?)
5258	Nse5::KanR Dcr1::Nat:URA4 clr4::hygR:URA4 otr1R(Sph1):ade6+ leu1-32 ade6-210 ura4-D18 his3D1(?)
5259	SPCC126.13c::KanR Dcr1::Nat:URA4 clr4::hygR:URA4 otr1R(Sph1):ade6+ leu1-32 ade6-210 ura4-D18 his3D1(?)
5260	SPCC11E10.09c::KanR Dcr1::Nat:URA4 clr4::hygR:URA4 otr1R(Sph1):ade6+ leu1-32 ade6-210 ura4-D18 his3D1(?)
5261	snt2::KanR Dcr1::Nat:URA4 clr4::hygR:URA4 otr1R(Sph1):ade6+ leu1-32 ade6-210 ura4-D18 his3D1(?)
5262	msh3::KanR Dcr1::Nat:URA4 clr4::hygR:URA4 otr1R(Sph1):ade6+ leu1-32 ade6-210 ura4-D18 his3D1(?)
5263	SPCC645.13::KanR Dcr1::Nat:URA4 clr4::hygR:URA4 otr1R(Sph1):ade6+ leu1-32 ade6-210 ura4-D18 his3D1(?)
5264	SPAC589.05c::KanR Dcr1::Nat:URA4 clr4::hygR:URA4 otr1R(Sph1):ade6+ leu1-32 ade6-210 ura4-D18 his3D1(?)
5265	urm1::KanR Dcr1::Nat:URA4 clr4::hygR:URA4 otr1R(Sph1):ade6+ leu1-32 ade6-210 ura4-D18 his3D1(?)
5266	rim20::KanR Ago1::NatR:URA4 rik1::HygR:URA4 otr1R(Sph1):ade6+ leu1-32 ade6-210 ura4-D18 his3D1(?)
5267	rrg1::KanR Ago1::NatR:URA4 rik1::HygR:URA4 otr1R(Sph1):ade6+ leu1-32 ade6-210 ura4-D18 his3D1(?)
5268	tfb2::KanR Ago1::NatR:URA4 rik1::HygR:URA4 otr1R(Sph1):ade6+ leu1-32 ade6-210 ura4-D18 his3D1(?)
5269	arp8::KanR Ago1::NatR:URA4 rik1::HygR:URA4 otr1R(Sph1):ade6+ leu1-32 ade6-210 ura4-D18 his3D1(?)
5270	hrp3::KanR Ago1::NatR:URA4 rik1::HygR:URA4 otr1R(Sph1):ade6+ leu1-32 ade6-210 ura4-D18 his3D1(?)

5271	nrl1::KanR Ago1::NatR:URA4 rik1::HygR:URA4 otr1R(Sph1):ade6+ leu1-32 ade6-210 ura4-D18 his3D1(?)
5272	tos4::KanR Ago1::NatR:URA4 rik1::HygR:URA4 otr1R(Sph1):ade6+ leu1-32 ade6-210 ura4-D18 his3D1(?)
5273	SPBC21C3.12c::KanR Ago1::NatR:URA4 rik1::HygR:URA4 otr1R(Sph1):ade6+ leu1-32 ade6-210 ura4-D18 his3D1(?)
5274	Nse5::KanR Ago1::NatR:URA4 rik1::HygR:URA4 otr1R(Sph1):ade6+ leu1-32 ade6-210 ura4-D18 his3D1(?)
5275	SPCC126.13c::KanR Ago1::NatR:URA4 rik1::HygR:URA4 otr1R(Sph1):ade6+ leu1-32 ade6-210 ura4-D18 his3D1(?)
5276	SPCC11E10.09c::KanR Ago1::NatR:URA4 rik1::HygR:URA4 otr1R(Sph1):ade6+ leu1-32 ade6-210 ura4-D18 his3D1(?)
5277	snt2::KanR Ago1::NatR:URA4 rik1::HygR:URA4 otr1R(Sph1):ade6+ leu1-32 ade6-210 ura4-D18 his3D1(?)
5278	msh3::KanR Ago1::NatR:URA4 rik1::HygR:URA4 otr1R(Sph1):ade6+ leu1-32 ade6-210 ura4-D18 his3D1(?)
5279	SPCC645.13::KanR Ago1::NatR:URA4 rik1::HygR:URA4 otr1R(Sph1):ade6+ leu1-32 ade6-210 ura4-D18 his3D1(?)
5280	SPAC589.05c::KanR Ago1::NatR:URA4 rik1::HygR:URA4 otr1R(Sph1):ade6+ leu1-32 ade6-210 ura4-D18 his3D1(?)
5281	urm1::KanR Ago1::NatR:URA4 rik1::HygR:URA4 otr1R(Sph1):ade6+ leu1-32 ade6-210 ura4-D18 his3D1(?)
5395	cid12-TAP-kanR Ago1::NatR:URA4 rik1::HygR:URA4 otr1R:ade6+ ade6-210 leu1-32 ura4-D18 / ura4-D18 his3D(?)
5396	cid12-TAP-kanR Dcr1::Nat:URA4 clr4::hygR:URA4 otr1R(Sph1):ade6+ his3D1(?) ade6-210 leu1-32 ura4-D18 / ura4-D18

Table 2-3. A list of *S. pombe* strains used.

Chapter 3 – Plasmid-based establishment assay

3.1 Introduction

The mechanism of RNAi-dependent heterochromatin formation has been extensively studied in *S. pombe* (Allshire & Madhani, 2018). Apart from characterizing the mechanism of action of core components, such as CLRC and RNAi, small-scale and genome-wide genetic screens identified multiple additional factors involved in heterochromatin maintenance, such as splicing proteins and COP9 signalosome components (Bayne et al., 2014; Rougemaille et al., 2008; Sugioka-Sugiyama & Sugiyama, 2011). However, how heterochromatin is established is not well understood. For example, it is not yet clear how a particular locus is targeted for heterochromatin formation. It is also not clear in what order RNAi and CLRC components act. So far two establishment-specific factors were characterized: primal RNAs (priRNAs) (Halic & Moazed, 2010) and Triman (Marasovic et al., 2013). Primal RNAs were proposed to initiate siRNA amplification. Triman, in turn, was shown to trim Argonaute-loaded small RNA precursors to generate mature priRNA and siRNA.

Thus in order to understand how heterochromatin formation is initiated, additional factors required for establishment have to be discovered. There are three main ways of assessing heterochromatin

establishment (Allshire & Madhani, 2018). One method is to delete a key chromatin modifier (such as H3K9 methyltransferase), thus perturbing heterochromatin. Then this gene is re-introduced, allowing heterochromatin to be re-established. However if an establishment factor is absent, heterochromatin cannot be re-established (Sadaie et al., 2004). Another method is to introduce a naïve DNA fragment, acting as a heterochromatin establishment platform, and to assess heterochromatin formation in the absence of a potential establishment factor (Buscaino et al., 2013). Finally heterochromatin can be perturbed by using inhibitors such as HDAC inhibitor Trichostatin A (TSA) (Ekwall et al., 1997). HDAC complexes, such as SHREC and Clr6, induce deacetylation, a process required for H3K9 methylation.

Since so little is known about the initial steps of heterochromatin formation, I aimed to develop an assay suitable for identifying multiple factors required for establishment genome-wide. Thus, the assay of choice has to be adaptable for high-throughput screening. Moreover, I wanted to use an assay that fully perturbs pre-existing heterochromatin, thus ensuring that the subsequent heterochromatin is established *de novo* and re-establishment is not accelerated by any remaining maintenance signal. Given this, I could not use assays involving TSA treatment or naïve DNA

introduction. Introduction of naïve DNA sequences is a complex multistep procedure that is hard to adapt for high-throughput screening. TSA treatment, in turn, is an indirect method of heterochromatin perturbation that can potentially lead to incomplete heterochromatin erasure. To overcome these issues, I adapted a plasmid-based establishment assay where essential factors are deleted and re-reintroduced on a plasmid (Figure 3-1A) Both *clr4+* (CLRC pathway) and *dcr1+* (RNAi pathway) are essential for heterochromatin establishment and maintenance at pericentromeres, and deleting one of them is enough to disrupt pericentromeric heterochromatin integrity (Allshire & Ekwall, 2015). However, we wanted to ensure that no residual signal that can potentially accelerate re-establishment is left. For this reason, we created a tester strain deleted for both *clr4+* and *dcr1+* to maximally disrupt the positive feedback loop that maintains pericentromeric heterochromatin. The tester strain is then crossed to a set of strains lacking potential establishment candidates (gene of interest deletion; *goiΔ)* The only other published study, where both RNAi and CLRC pathways were perturbed to test for heterochromatin establishment, is the study where Triman1 involvement in heterochromatin was tested (Marasovic et al., 2013). Subsequent re-introduction of *clr4+* and *dcr1+* allows us to test if *clr4+* and *dcr1+* are enough to drive heterochromatin re-establishment in the

absence of the gene of interest. I re-introduced *clr4+* and *dcr1+* on a plasmid, a method that was adapted for high-throughput transformations in *S. cerevisiae* (Gietz & Schiestl, 2007).

After *clr4+* and *dcr1+* reintroduction, there are several possible assays to assess heterochromatin presence. One of them uses an *ade6+* reporter inserted at a pericentromere (Fig 3-1B) (Allshire et al., 1994). In this assay, the *ade6+* gene is inserted in the pericentromeric region of chromosome 1 (cen1:*ade6+*), where it is silenced by heterochromatin. The endogenous gene copy, in turn, is inactivated by a point mutation (either *ade6-210* or *ade6-216*) (Allshire et al., 1994). Endogenous *ade6+* inactivation by a point mutation together with ectopic *ade6+* silencing by heterochromatin leads to cells appearing red on low adenine media due red pigment accumulation in the adenine biosynthesis pathway (Chaudhuri, Ingavale, & Bachhawat, 1997). If, however, pericentromeric heterochromatin is perturbed (e.g. by mutation in *clr4+*), ectopic *ade6+* (cen1:*ade6+*) is expressed. As a result, no pigment is accumulated and cells appear white on low adenine media. Another assay that allows assessment of heterochromatin integrity involves selection on media containing 5-fluoroorotic acid (5FOA) (Allshire et al., 1995). I will discuss this method in more detail in the Chapter 5, as it will be the basis of another assay I used.

In this chapter, I will discuss how I optimised a plasmid-based assay for high-throughput screening. The optimization included building a *clr4*+ *dcr1*+ plasmid and testing a high-throughput transformation protocol using sixteen deletion strains of *S. pombe.*

A

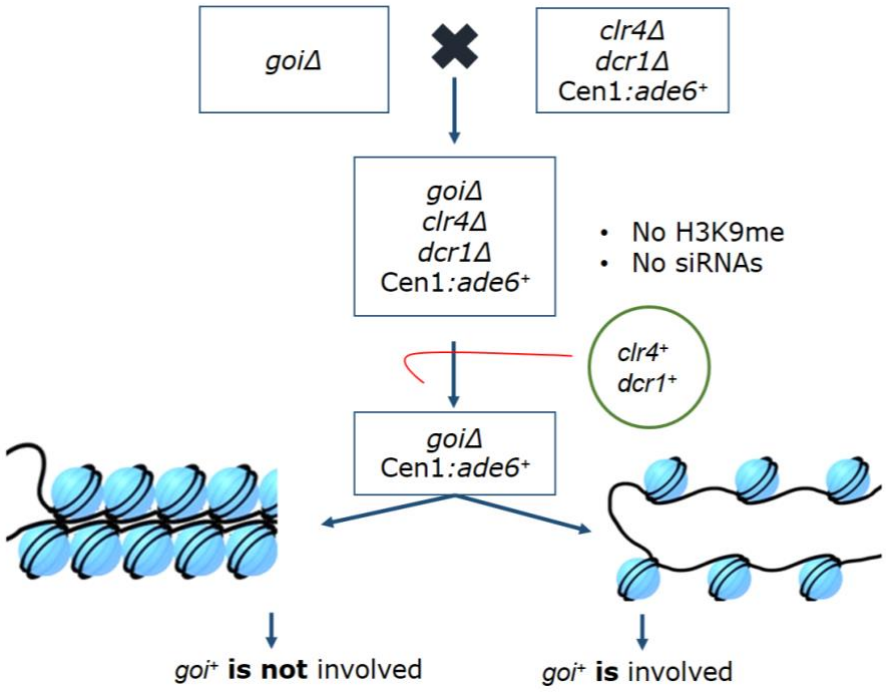
goiΔ
clr4Δ
dcr1Δ
Cen1:ade6+
goiΔ
clr4Δ
dcr1Δ
Cen1:ade6+
• No H3K9me
• No siRNAs
clr4+
dcr1+
goiΔ
Cen1:ade6+
goi+ is not involved
goi+ is involved

B

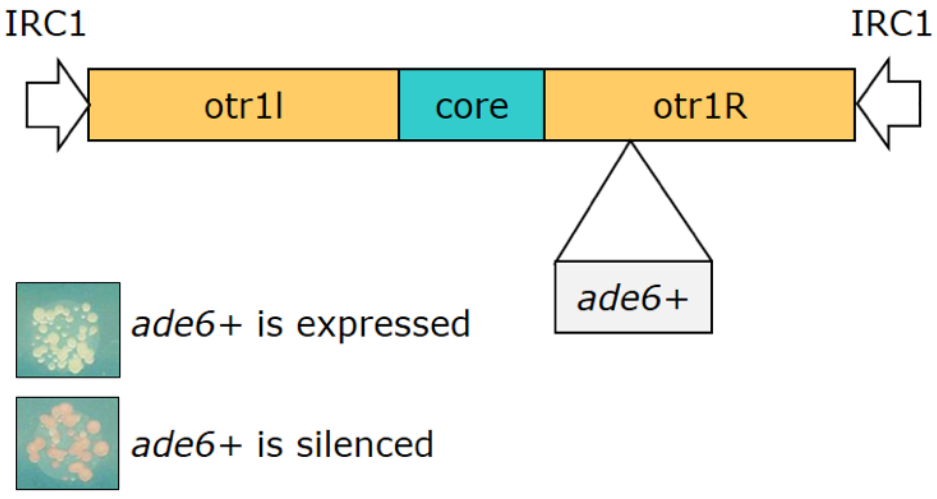
IRC1
IRC1
otr1l
core
otr1R
ade6+
ade6+ is expressed
ade6+ is silenced

Figure 3-1. Plasmid-based establishment assay principle. **(A)** In the plasmid-based approach, crosses are first performed to generate triple mutants, bearing deletions of *clr4+*, *dcr1+* and the gene of interest (*goi*), thus perturbing pericentromeric heterochromatin. The *clr4+* and *dcr1+* genes are then re-introduced on a plasmid, and heterochromatin re-establishment is assessed by the *ade6+* reporter assay. **(B)** Wild-type cells bearing an *ade6+* reporter in the outer repeat region of centromere I turn red on low adenine media. If, however, pericentromeric heterochromatin is perturbed, cells will turn white on low adenine media due to *ade6+* expression.

3.2 Optimization of plasmid-based establishment assay

3.2.1 pREP-CD41 construction

In order to rescue *clr4Δ* and *dcr1Δ* deletions, I designed a single plasmid, named pREP-CD41, expressing *clr4+* and *dcr1+* from their endogenous promoters. This plasmid was generated from two plasmids gifted from the Halic lab (Marasovic et al., 2013). Using a single plasmid was necessary due to there being only one remaining selection marker – *leu1+*. All other selection markers would be used to generate triple mutants.

The plasmids obtained from the Halic lab were p348, in which the *clr4+* gene is inserted in the pREP backbone, and p474, in which the *dcr1+* gene is inserted into pJR1 backbone. First, I sequenced the plasmids, since we had no plasmid map or sequence information. The open reading frame (ORF) of *clr4+* is 1473bp long, with 440bp of 5'UTR and 2579bp 3'UTR (Lock et al., 2019). Sequencing showed that the *clr4+* plasmid (p348) has an open reading frame with N-terminal triple Flag tag (3xFlag) (Fig3-2A). It also has full length 5'UTR with additional 556bp of upstream sequence. In terms of 3'UTR, it only has 987bp (38%) of endogenous sequence present. The ORF of *dcr1+* is 4125bp with 284bp 5'UTR and 1217bp 3'UTR (Lock et al., 2019). The *dcr1+* plasmid (p474) has the *dcr1+* ORF with full-length 5' and 3' UTRs. It also has 628bp of additional

sequence upstream of the 5'UTR and 625bp of sequence downstream of the 3'UTR (Fig 3-2B).

A

p348

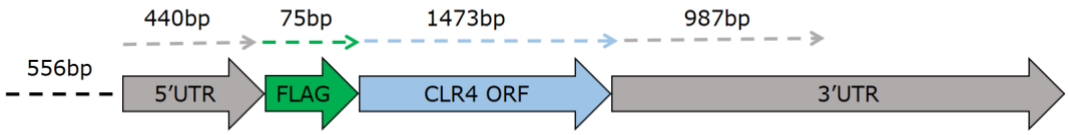

B

p474

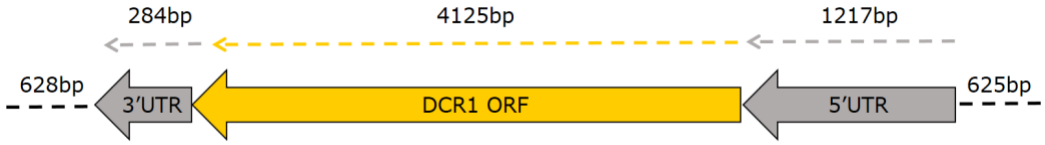

Figure 3-2. Diagram of *clr4*+ and *dcr1*+ sequences present in the respective plasmids, as determined by sequencing. Dotted lines represent the size of sequences present within the respective plasmid. **(A)** *The clr4*+ (p348) plasmid has *clr4*+ ORF present with a triple FLAG-tag at the 5' end. It also has a full-length 5'UTR sequence present with an additional 556bp sequence upstream. Only 987bp sequence of 3'UTR is present. **(B)** The *dcr1*+ (p474) plasmid has *dcr1*+ ORF present with full length 3'UTR and 5'UTR sequences. Around 620bp sequence is present upstream and downstream of the UTR regions.

To generate pREP-CD41, a single *clr4*+ *dcr1*+ expressing plasmid, I inserted the *dcr1*+ fragment from p474 into the *clr4*+ plasmid p348. In order to make this insertion I first had to modify p348 plasmid to reposition the SphI restriction site (Fig 3-3A). I first deleted the endogenous SphI site upstream of the *clr4*+ fragment, and then inserted a new SphI site into the plasmid-specific nmt1 promoter. Then, using SphI and XmaI restriction enzymes, I replaced the nmt1 promoter of the *clr4*+ plasmid p348 with the *dcr1*+ fragment from the p474 plasmid to generate a single pREP-CD41 plasmid (Fig 3-4A). Here, the function of nmt1 promoter is not required, since both ORFs are regulated by their endogenous promoters and terminators. To evaluate plasmid ligation, I performed restriction digest with EcoRV. Clone 3, unlike clone 1, generated the expected restriction digest pattern of four fragments of 8000bp, 6000 bp, 1600 and 1300bp sizes. (Fig3-4B).

A

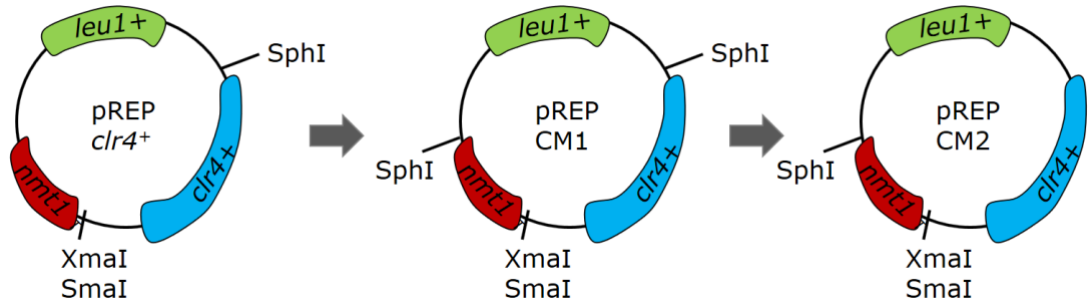

Figure 3-3. *clr4*+ plasmid(p348) modification. (A) A schematic diagram of p348 plasmid modifications. A new SphI restriction site was inserted upstream of the *nmt1* terminator sequence and the endogenous SphI site was deleted. Full plasmid maps are presented in appendix A.

A

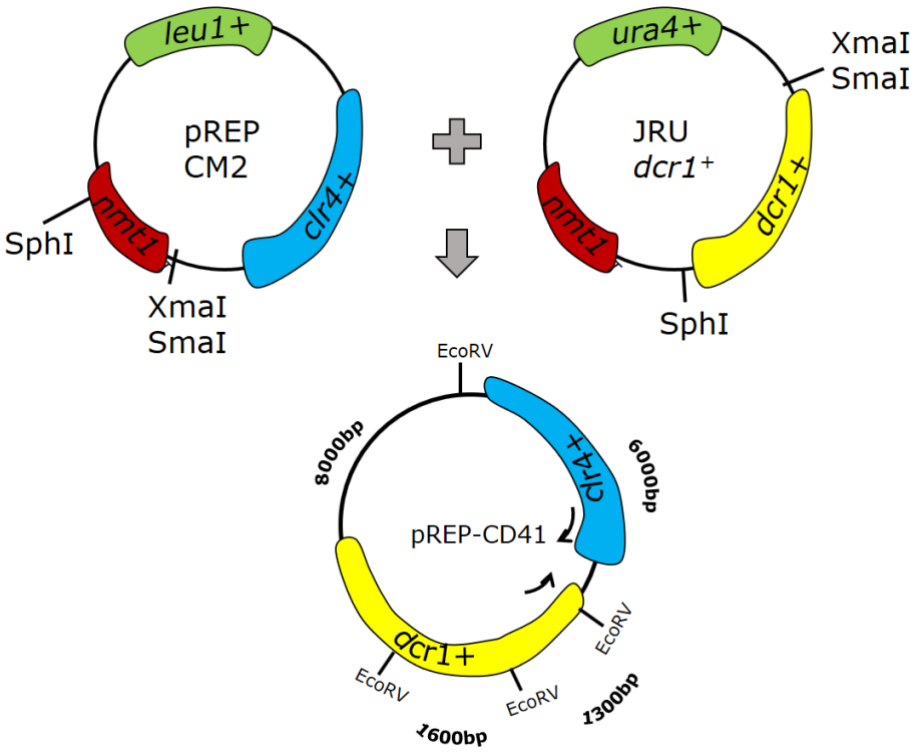

B

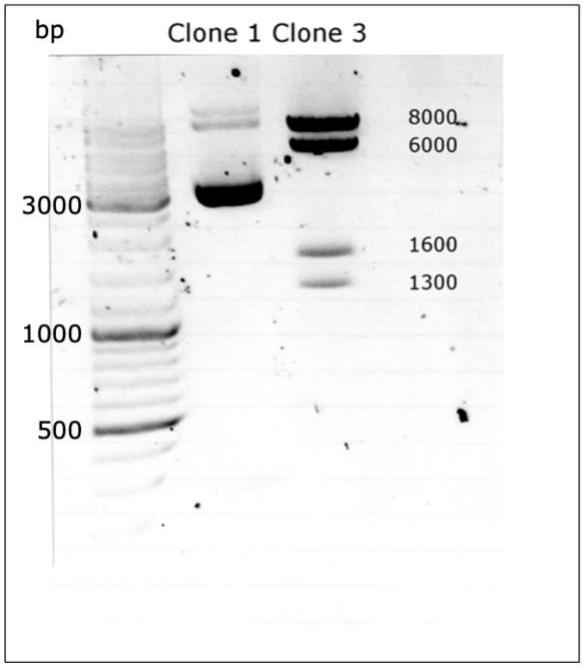

Figure 3-4. *clr4*$_+$*dcr1*$_+$ plasmid (pREP-CD41) construction. (A) A schematic diagram of pREP-CD41 plasmid construction, whereby the *dcr1*$_+$ fragment was excised from p474 plasmid with SphI and XmaI restriction enzymes and ligated into the similarly digested *clr4*$_+$ plasmid p348. **(B)** After diagnostic restriction digest with EcoRV of clones 1 and 3, clone 3, unlike clone 1, generated the right-sized restriction fragments as indicated in (A).

3.2.2 pREP-CD41 rescues centromeric silencing in a *clr4Δ dcr1Δ* deletion strains

After constructing the pREP-CD41 plasmid, I tested if its introduction into a *clr4Δ-dcr1Δ* deletion strain is sufficient to re-establish centromeric silencing. Using lithium acetate transformation protocol, I transformed a *clr4Δ-dcr1Δ* strain carrying the cen1:*ade6+* reporter, located at heterochromatic pericentromeres, with pREP-CD41. As controls I used *clr4+-dcr1+*, *clr4Δ-dcr1Δ* and *clr4+-dcr1+* cen1: *ade6+* strain with an empty pREP81 plasmid. As expected, *clr4+-dcr1+* strain was red and *clr4Δ-dcr1Δ* strain was white on low adenine media. After selecting for presence of the plasmid on media lacking leucine, cells turned red on low adenine media, suggesting that pREP-CD41 rescues the centromeric defects in *clr4Δ-dcr1Δ* deletions (Fig3-5). Selection on low adenine media lacking leucine prevents the red colour to develop as strongly as on low adenine media alone. Thus, I transformed a *clr4+-dcr1+* cen1: *ade6+* strain with an empty pREP81 plasmid as a control.

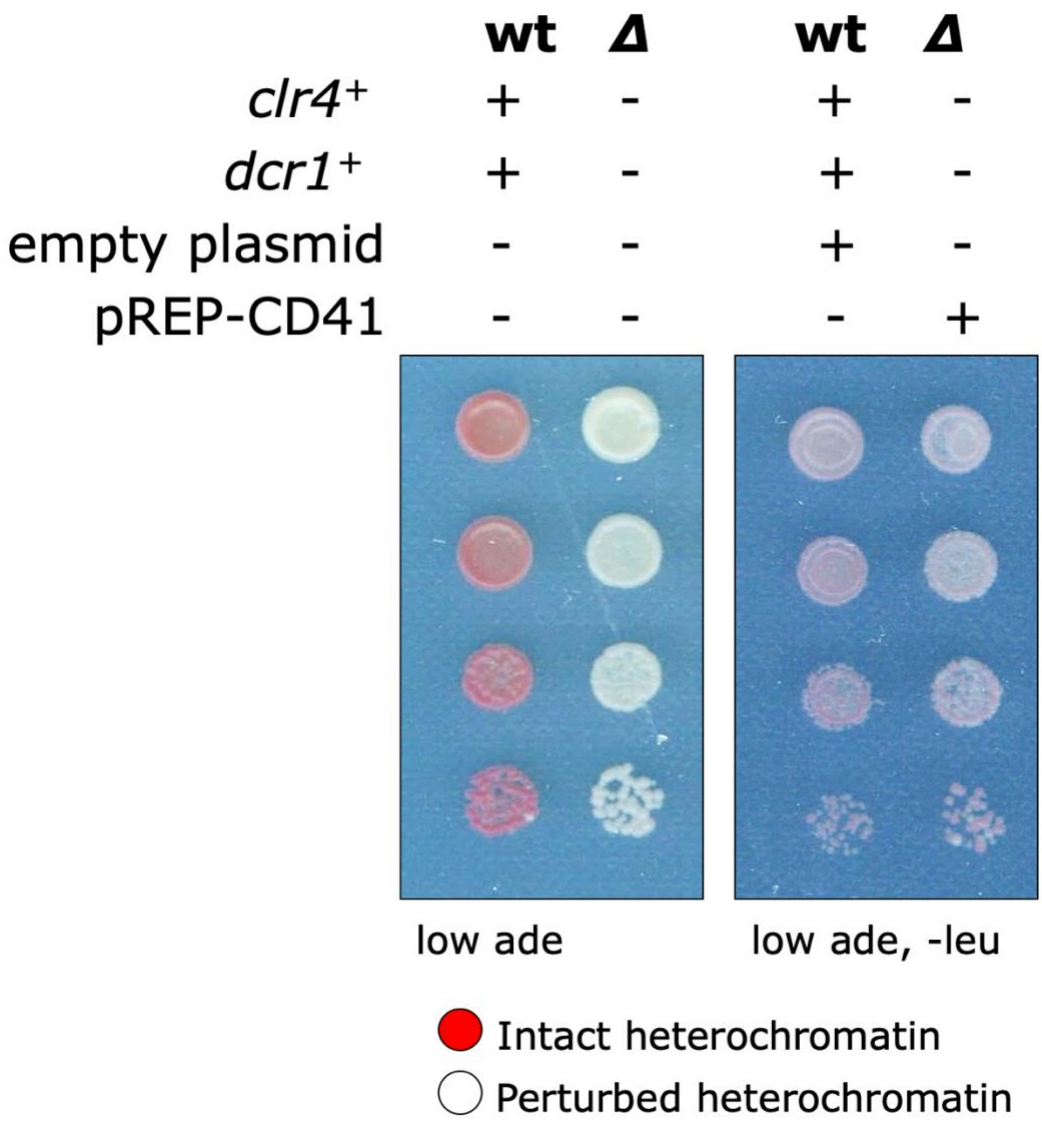

Figure 3-5. pREP-CD41 rescues silencing defect in a *clr4Δ dcr1Δ* deletion strain. On low adenine media wild type carrying the cen1:*ade6*+ reporter appear red due to *ade6*+ being silenced by heterochromatin (I). Strains with *clr4*+ and *dcr1*+ deletions appear white due to heterochromatin being perturbed and thus *ade6*+ being expressed (II). After introduction of the pREP-CD41, cells turned red on low adenine media lacking leucine (for selection of the plasmid),suggesting that heterochromatin was re-established at the centromeres (IV). Compared to the leucine-supplemented media, red colour does not develop as strong on media without leucine. Thus a *clr4*+ *dcr1*+ cen1:*ade6*+ strain transformed with an empty pREP81 plasmid is shown as a control (III).

3.2.3 Testing plasmid-based assay on sixteen candidates

After confirming that pREP-CD41 can rescue a *clr4Δ dcr1Δ* deletion strain, I tested if the plasmid transformation can be done in a high-throughput manner suitable for use in a genetic screen. I used a microtiter transformation protocol originally developed for *Saccharomyces cerevisiae* (Gietz & Schiestl, 2007). Instead of growing cells in 50-100ml liquid cultures with a subsequent multistep transformation procedure, this protocol relies on growing the cells on agar plates followed by a single-step incubation in the transformation mix. As a result, transformation can be done in a high throughput manner using a 48-prong replicator or a plating robot. I did the transformation almost exactly as it is described in the *S. cerevisiae* protocol apart from using lithium acetate at 0.1M concentration (instead of 1M) and plating all of the transformants on a single selective plate.

I used sixteen candidate deletion strains , pre-selected before by Dr Elizabeth Bayne, to test the microtiter protocol. These candidates were pre-selected based on three factors: (1) No effect on maintenance of silencing at centromeres; and (2) Homology with X chromosome-inactivating factors or; (3) Factors that showed a perturbed maintenance of centromeric silencing in a *clr3Δ* deletion

background, the information kindly provided to us by Dr Alessia Buscaino (Table 3-1). A *tri1Δ* strain was included as a control, since Triman was previously reported to be required for establishment (Marasovic et al., 2013).

After transforming sixteen *goiΔ-clr4Δ-dcr1Δ* strains with the pREP-CD41 plasmid using the optimized microtiter protocol and plating them on the low adenine media, four candidates remained white/light pink suggesting that heterochromatin was not re-established in these cells (Fig 3-6). These four candidates were characterized further, as described in the next chapter. Unexpectedly, heterochromatin was re-established in the *tri1Δ-clr4Δ-dcr1Δ* control strain upon the pREP-CD41 plasmid transformation.

Gene	**Systematic ID**	**Function** (Lock et al., 2019)
rim20	SPAC2G11.05c	Bro1 domain protein, vesicle-mediated transport
rrg1	SPCC338.11c	Putative methyltransferases
tfb2	SPBC13G1.13	Transcription factor ,TFIIH complex subunit
arp8	SPAC664.02c	Ino80 complex(chromatin remodeller) actin-like protein
hrp3	SPAC3G6.01	Atp-dependent DNA helicase
nrl1	SPBC20F10.05	NRDE2 homolog (nuclear RNAi in worms, splicing in humans), prevents DNA damage
tos4	SPAP14E8.02	Chromatin binding forkhead domain (many positive genetic interactions with RNAi genes)
SPBC21C3.12c		thioredoxin family protein, peroxidase
nse5	SPBC651.10	Smc5-6 complex non-SMC subunit
sap18	SPCC126.13c	Splicing factor (HDAC complex)
SPCC11E10.09c		Alpha-amylase homolog
snt2	SPAC3H1.12c	PHD finger subunit of Lid2 complex(histone demethylase)
msh3	SPAC8F11.03	MutS (mismatch repair) protein homolog 3
bye1	*SPCC645.13*	Predicted transcription elongation regulation (some homology to SPEN)
qtr3	*SPAC589.05c*	tRNA queuosine modification protein
urm1	SPCC548.04	ubiquitin-like protein modifier

Table 3-1. List of candidate establishment factors tested.

Screen for mutants that lose silencing of cen1:ade6 in combination with *clr3+* deletion
Homology to proteins found to bind human Xist RNA

A **B**

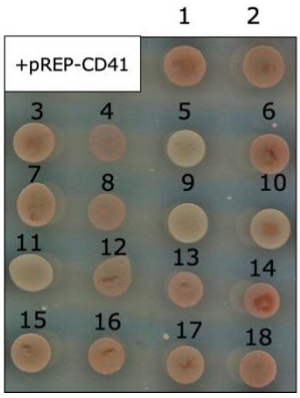

		1. *clr4Δdcr1Δ*	2. *tri1Δ*
3. *rim1Δ*	4. *rrg1Δ*	5. *tfb2Δ*	6. *arp8Δ*
7. *hrp3Δ*	8. *nrl1Δ*	9. *tos4Δ*	10.*SPBC21C3.12cΔ*
11. *nse5Δ*	12. *sap18Δ*	13. *SPCC11E10.09cΔ*	14. *snt2Δ*
15. *msh3Δ*	16. *bye1Δ*	17. *qtr3Δ*	18. *urm1Δ*

Figure 3-6. Candidate-gene approach revealed four potential establishment factors after transformation with pREP-CD41. (A) Sixteen *goiΔ-clr4Δ-dcr1Δ* triple mutant strains were transformed with pREP-CD41, and the transformants plates on media lacking leucine (for selection of the plasmid) and containing limiting adenine. Four of the strains display a white/pale colony colour, suggesting heterochromatin was not re-established in these cells. This plate was scanned without the blue background, which is different to the protocol in 2.7.1. **(B)** A key for the triple mutants deletion strains shown in A. All of the deletion strains numbered 2-18 have a *clr4Δ-dcr1Δ* background.

3.3 Discussion

Heterochromatin formation has been extensively studied using *S. pombe* as a model system. Both heterochromatin establishment and maintenance depend on the Clr4 complex (CLRC) and the RNA interference (RNAi) pathways. Unlike maintenance, establishment is not very well understood.

In this chapter, I describe a plasmid-based system that I developed to assess heterochromatin establishment. The system relies on perturbing heterochromatin maintenance by deleting *clr4+* and *dcr1+* and then assessing the contribution of non-essential factors to heterochromatin re-establishment. Re-establishment is induced by introducing *clr4+* and *dcr1+* on a plasmid.

First, I constructed a *clr4+ dcr1+* expressing plasmid, named pREP-CD41, and showed that it can induce heterochromatin re-establishment in *clr4Δ-dcr1Δ* cells. Then I introduced it to sixteen triple deletions, where deletion strains of *clr4+* and *dcr1+* are combined with deletion of one of sixteen candidate proteins potentially involved in establishment (Table 3-1).

Surprisingly, heterochromatin was re-established in the *tri1Δ* mutant background (*tri1Δ-clr4Δ-dcr1Δ* → *tri1Δ-clr4+-dcr1+).* Triman was

previously characterized as a factor, without which heterochromatin cannot be re-established (Marasovic et al., 2013). However, I was unable to reproduce this result. In their Triman characterization, Marasovic et al. used a less-direct method to assess heterochromatin formation. They used growth on thiabendazole (TBZ), a tubulin-destabilizing drug, as a readout for heterochromatin formation (Marasovic et al., 2013). Strains with perturbed pericentromeric heterochromatin, like *dcr1Δ* and *clr4Δ* mutants, have abnormal chromosome segregation pattern that results in hypersensitivity to TBZ (Hall, Noma, & Grewal, 2003). As a result, the mutants die on media with a TBZ concentration that is permissible for wild type strains. Thus, assaying growth of cells on TBZ-containing media tests for segregation defects which are indicative of compromised heterochromatin state. Therefore, testing only for TBZ-sensitivity can identify factors that are involved in segregation rather than heterochromatin formation. Inserting *ade6+* at the pericentromeres (cen1:*ade6+*) and assessing the colony colour on low adenine media is, however, directly indicative of how well *ade6+* is silenced by the pericentromeric heterochromatin. Thus, using *ade6+* reporter assay is a more direct method of assessing the heterochromatin state.

Among the sixteen factors tested, deletions of four were found to impair heterochromatin re-establishment according to the colony

colour assay: *tfb2Δ*, *tos4Δ*, *nse5Δ* and *SPBC21C3.12Δ.* I proceeded to evaluate the molecular characteristics of strains deleted for these factors as described in the next chapter.

Chapter 4 – Candidate characterization

4.1 Introduction

In the previous chapter I described a plasmid-driven establishment assay that allowed us to identify four factors that are potentially involved in establishment: Tos4, Tfb2, Nse5 and SPBC21C3.12. Tos4 is a transcription factor, regulated by Swi4-Swi6 cell cycle binding factor (SBF) in *Saccharomyces cerevisiae* (Horak et al., 2002). Tfb2 is one of the three core subunits of TFIIH, where TFIIH is essential for nucleotide excision repair and RNA polymerase II-driven transcription (Warfield et al., 2016). Nse5 is a member of the Smc5/6 complex from a structural maintenance of chromosome (SMC) family of proteins. It has been shown recently that Nse5 has multiple interactions with SUMO pathway, potentially acting as a scaffold for sumoylation in *S. cerevisiae* (Bustard et al., 2016). This makes Nse5 a particularly interesting candidate, since it was shown that multiple proteins essential for heterochromatin formation in fission yeast, such as Swi6, Chp2 and Clr4, interact with SUMO-conjugating enzyme and they can also be sumoylated themselves (Shin et al., 2005). Finally, *SPBC21C3.12* is an uncharacterized protein from the thioredoxin family of proteins.

Using the *ade6+* reporter assay, I showed that heterochromatin cannot be re-established without these factors, as indicated by the

pale colour of cells on the low adenine media (Fig 3-6). After looking at the effect of the deletion of these factors at the phenotypic level, in this chapter I describe assessment of their impact on heterochromatin re-establishment at the molecular level.

4.2 All candidates have a different molecular signature associated with perturbed heterochromatin

Deletion of *clr4+* and *dcr1+* leads to perturbed heterochromatin at the centromeres, which can be characterized by a decrease in H3K9 methylation and siRNA production at centromeres, and by an increase in non-coding RNA levels. (Allshire & Ekwall, 2015). Introducing wild-type copies of *clr4+* and *dcr1+* to the *clr4Δ-dcr1Δ* strain is expected to lead to increased levels of H3K9me and siRNAs and a decrease in levels of RNA levels. In contrast, if a true establishment factor is deleted alongside *clr4+* and *dcr1+* , H3K9me, siRNA and RNA levels should not be restored upon reintroduction of the wild-type *clr4+* and *dcr1+* genes. Thus I tested if the triple mutant strains (*goiΔ-clr4Δ-dcr1Δ*) lacking one of the factors identified earlier have these features after the pREP-CD41 plasmid introduction (*goiΔ-clr4Δ-dcr1Δ* +pREP-CD41$\rightarrow$ *goiΔ-clr4+-dcr1+*).

To assess the molecular characteristics of pericentromeric heterochromatin in the triple mutant cells after the pREP-CD41 plasmid introduction, I performed three assays: (1) Chromatin immunoprecipitation (ChIP) to assess methylation (H3K9me2) levels; (2) RT-qPCR to assess RNA transcription; (3) Northern blot to asses siRNA production. We hypothesised that compared to the WT strain, methylation and siRNA levels will be low, and ncRNA levels will be high when a true establishment factor is being tested in the re-establishment assay.

4.2.1 H3K9me2 is not re-established in the absence of Tos4 and Tfb2

First, I measured the H3K9me2 levels at the pericentromeres in the strains of interest using chromatin immunoprecipitation (ChIP). As expected H3K9me2 levels are severely downregulated in *clr4Δ-dcr1Δ* cells compared to the wild-type control (Fig 4-1). Introducing the pREP-CD41 plasmid to the *clr4Δ-dcr1Δ* cells leads to H3K9me2 accumulation comparable to the methylation levels in the WT controls ($0 < \log_2 FC < 1$). In contrast, after the pREP-CD41 plasmid introduction, methylation levels in the *tos4Δ-clr4Δ*-dcr1Δ cells did not increase to the levels observed in the *clr4Δ-dcr1Δ* +pREP-CD41 cells ($\log_2 FC = -7$) (Fig 4-1A). Likewise methylation in the *tfb2Δ-clr4Δ*-dcr1Δ + pREP-CD41 cells did not accumulate to the levels

observed in *clr4Δ-dcr1Δ* +pREP-CD41 cells (log_2FC = -1.8) (Fig 4-1B).

Methylation levels in the *SPBC21C3.12cΔ-clr4Δ-dcr1Δ* +pREP-CD41 cells were comparable to the levels observed in the *clr4Δ-dcr1Δ* +pREP-CD41 cells (log_2FC = 0.1) (Fig4-1C). Finally, H3K9me2 levels in *nse5Δ-clr4Δ-dcr1Δ* +pREP-CD41 cells were similar to those in the *clr4Δ*-dcr1Δ+pREP-CD41 cells(log_2FC=0.3)(Fig4-1D). Unexpectedly, combining *nse5Δ* with *clr4Δ-dcr1Δ* lead to methylation levels similar to the wild-type (log_2FC=0.2). In *clr4Δ-dcr1Δ* cells methylation levels are 9 fold less than in the wild type (log_2FC=-9.2). However, the difference between wild-type and the *nse5Δ-clr4Δ-dcr1Δ* triple mutant cells is reduced to 0.2 fold (log_2FC=0.2).

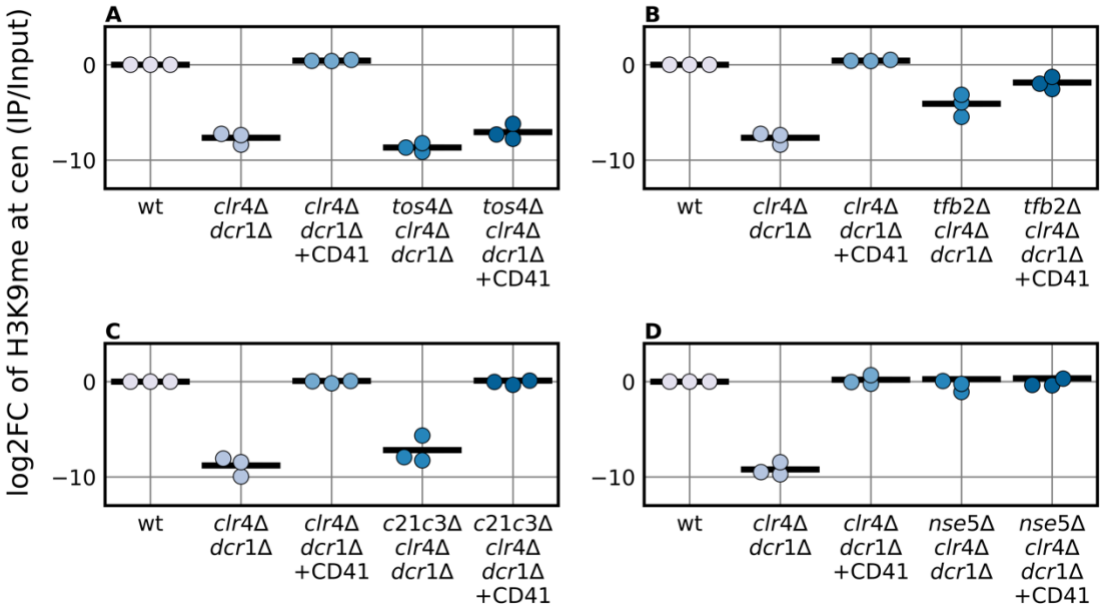

Figure 4-1: H3K9me2 profile differs among the candidate deletion strains. ChIP-qPCR analysis of H3K9me levels relative to input in the wild-type cells, *clr4Δ dcr1Δ* cells before and after introduction of the pREP-CD41 plasmid, and *goiΔ clr4Δ dcr1Δ* cells before and after introduction of the pREP-CD41 plasmid, where the gene of interest is *tos4Δ* **(A)**, *tfb2Δ* **(B)**, *SPBC21C3.12cΔ* **(C)** and *nse5Δ* **(D)** (n=3). Black horizontal lines represent geometric mean.

4.2.2 siRNA production does not decrease in the absence of Tos4 and Tfb2

Next I used Northern blotting to measure pericentromeric siRNA production before and after introducing the pREP-CD41 plasmid to the four pre-selected triple mutant strains. I hypothesised that the deletion of the 'true' establishment factor in the *clr4Δ-dcr1Δ* background will prevent siRNA production upon pREP-CD41 transformation.

As expected, siRNAs levels are high in the wild-type cells and undetectable in the *clr4Δ-dcr1Δ* cells (Fig 4-2). In triple mutant cells additionally deleted for *tos4+, tfb2+* and *SPBC21C3.12c+* siRNA levels are as low as in *clr4Δ-dcr1Δ* double mutant cells. In *nse5Δ-clr4Δ-dcr1Δ* cells, surprisingly, siRNA production is rescued.

Introducing pREP-CD41 to the *clr4Δ-dcr1Δ* strain induces siRNA production. In contrast, siRNAs were almost undetectable in *tos4Δ -clr4Δ-dcr1Δ* +pREP-CD41 cell, while in *tfb2Δ-clr4Δ-dcr1Δ* +pREP-CD41 cells low levels of siRNA were produced. In *SPBC21C3.12cΔ-clr4Δ-dcr1Δ* and *nse5Δ-clr4Δ-dcr1Δ* strains siRNA production was rescued and increased upon pREP-CD41 introduction.

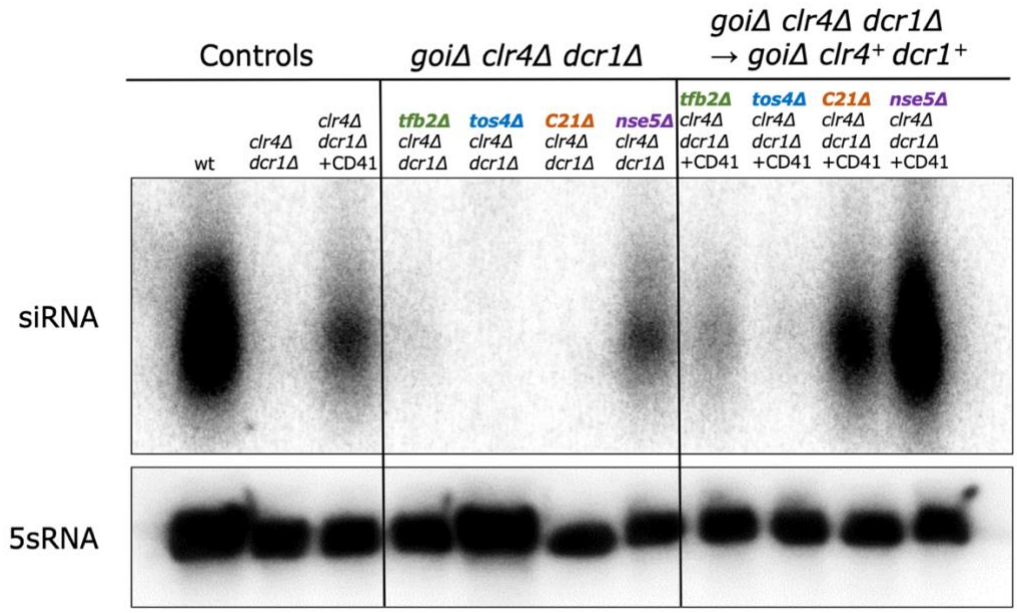

Figure 4-2: The levels of siRNA differ among the candidate deletion strains. Northern blot analysis of siRNA in the indicated strains before and after introduction of the pREP-CD41 plasmid. 5S rRNA is a loading control

4.2.3 The pREP-CD41 plasmid does not rescue pericentromeric RNA levels in *clr4Δ dcr1Δ* cells

I then used RT-qPCR to assess RNA expression from the *dg* sequence elements at the pericentromeres. We predicted that in *goiΔ-clr4Δ-dcr1Δ* strains, RNA expression will not be lowered to the same degree as in the *clr4Δ-dcr1Δ* cells upon the pREP-CD41 plasmid transformation.

As expected RNA levels were low in the wild-type cells and high in *clr4Δ-dcr1Δ* cells ($\log_2$FC = 4.4) (Fig4-3). Surprisingly transcript levels remained high after introducing the pREP-CD41 plasmid to the *clr4Δ-dcr1Δ*($\log_2$FC = 2.7). Thus transformation with the pREP-CD41 plasmid yields an intermediate RNA transcription state. As a result it is hard to quantitively asses the effect the candidate gene deletions might have on RNA expression during the heterochromatin re-establishment. *tos4Δ-clr4Δ-dcr1Δ*+pREP-CD41 and *SPBC21C3.12cΔ-clr4Δ-dcr1Δ*+pREP-CD41 strains had RNA transcript levels similar to *clr4Δ-dcr1Δ* alone (log2FC = 4.2) . RNA levels in *tfb2Δ-clr4Δ-dcr1Δ*+pREP-CD41 were comparable to *clr4Δ-dcr1Δ*+pREP-CD41 (log2FC = 2.8), and in *nse5Δ-clr4Δ-dcr1Δ*+pREP-CD41 cells RNA levels were comparable to the wild type cells (log2FC = 0.4).

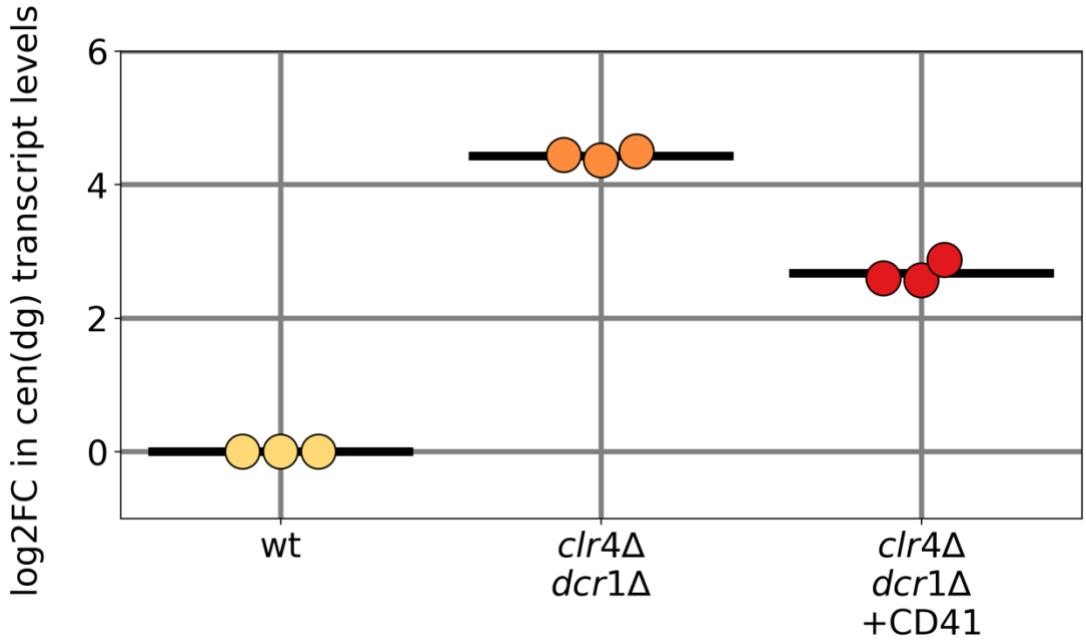

Figure 4-3: In the *clr4Δ-dcr1Δ* strain introduction of the pREP-CD41 plasmid does not reduce pericentromeric RNA levels to wild-type levels. RT-qPCR analysis of *cen*(*dg*) transcript levels relative to *act1*+ before and after the pREP-CD41 plasmid introduction (n=3). Black horizontal lines represent geometric means. Distribution of raw Ct values for *act1*+ is present in appendix D.

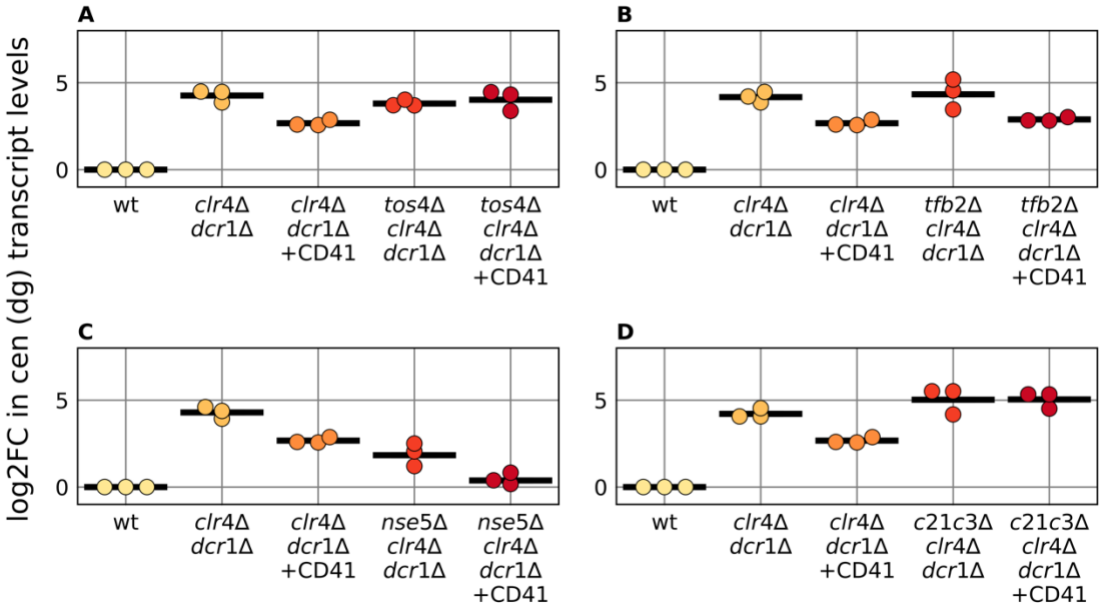

Figure 4-4. The difference in cen (dg) transcript levels is difficult to quantify due to incomplete rescue of centromeric transcription defect by the pREP-CD41 plasmid in the control *clr4Δ-dcr1Δ* strain. RT-qPCR analysis of *cen*(*dg*) transcript levels relative to *act1*+ in the wild-type cells, *clr4Δ dcr1Δ* cells before and after introduction of the pREP-CD41 plasmid, and *goiΔ clr4Δ dcr1Δ* cells before and after introduction of the pREP-CD41 plasmid, where the gene of interest is *tos4Δ* **(A)**, *tfb2Δ* **(B)**, *nse5Δ* **(C)** and *SPBC21C3.12cΔ* **(D)** (n=3). Black horizontal lines represent geometric means. Distribution of raw Ct values for *act1*+ is present in appendix E.

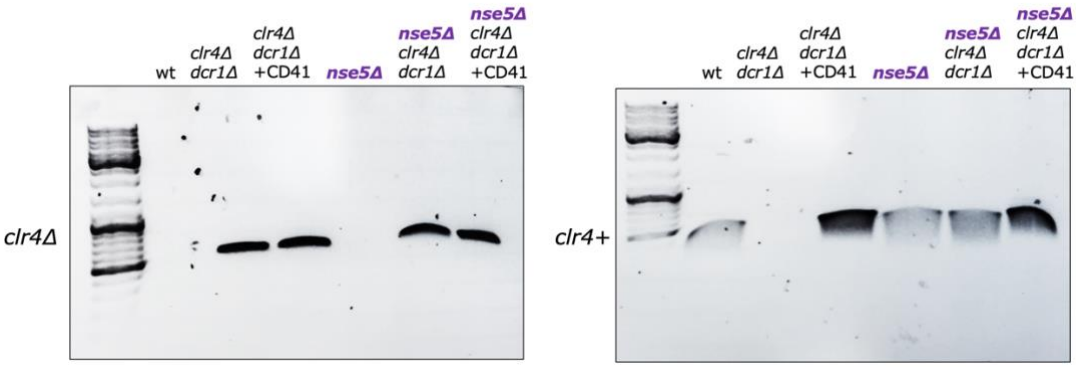

Figure 4-5: *nse5Δ-clr4Δ-dcr1Δ* strain has both *clr4+* and *clr4Δ* present. PCR analysis of *clr4+* and *clr4Δ* presence in the wild type and *clr4Δ-dcr1Δ* cells before and after pREP-CD41 introduction, and in nse5Δ and *nse5Δ-clr4Δ-dcr1Δ* before and after pREP-CD41 introduction.

4.3 Plasmid-induced heterochromatin re-establishment leads to inconsistent results

I decided to repeat the plasmid transformation procedure to ensure that no further optimization is required before starting a high-throughput screen. However repeating the protocol exactly as I did it the first time yielded different results (Figure 4-6A). Out of the four potential candidate deletion strains, only *nse5Δ-clr4Δ-dcr1Δ* +pREP-CD41 looked as white as after the first transformation. In contrast, *SPBC21C3.12cΔ-clr4Δ-dcr1Δ* +pREP-CD41 turned red, whereas both *tos4Δ-clr4Δ-dcr1Δ* and *tfb2Δ-clr4Δ-dcr1Δ* appeared mixed pink colour. The four candidates pre-selected after the original pREP-CD41 plasmid transformation look either white or pale pink. (Figure 4-5B).

A

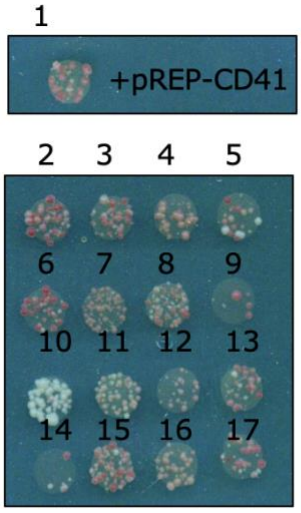

1	*clr4Δdcr1Δ*	**10**	*nse5Δ*
2	*rim1Δ*	**11**	*sap18Δ*
3	*rrg1Δ*	**12**	*SPCC11E10.09c Δ*
4	*tfb2Δ*	**13**	*snt2Δ*
5	*arp8Δ*	**14**	*msh3Δ*
6	*hrp3Δ*	**15**	*bye1Δ*
7	*nrl1Δ*	**16**	*qtr3Δ*
8	*tos4Δ*	**17**	*urm1Δ*
9	*SPBC21C3.12cΔ*		

B

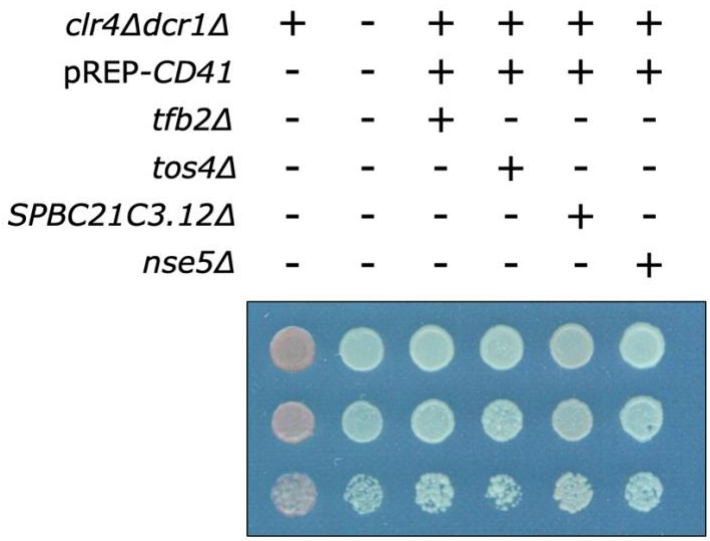

Figure 4-6: Second transformation of the sixteen triple deletion strains with pREP-CD41 plasmid did not replicate the results of the first transformation. (A) Transformants were plated on media lacking leucine (to select for the pREP-CD41 plasmid) and containing limiting adenine. Red colours indicate intact heterochromatin state, white colours indicate perturbed heterochromatin state. All the candidate deletions from 2-17 are in the *clr4Δ-dcr1Δ* background **(B)** Transformants from the first screen plated on media with limiting adenine and lacking leucine.

I then evaluated the expression levels of *clr4*+ and *dcr1*+ from the pREP-CD41 plasmid, which might potentially explain the inconsistent results seen in the transformation assay. RT-qPCR analysis revealed that when expressed from the pREP-CD41 plasmid, the mRNA levels of *clr4*+ (Fig 4-7A) and *dcr1*+(Fig 4-7B) genes are higher than in the WT strain (log2FC = 5.5 and log2FC =4.7 respectively), where both genes are expressed from their endogenous loci.

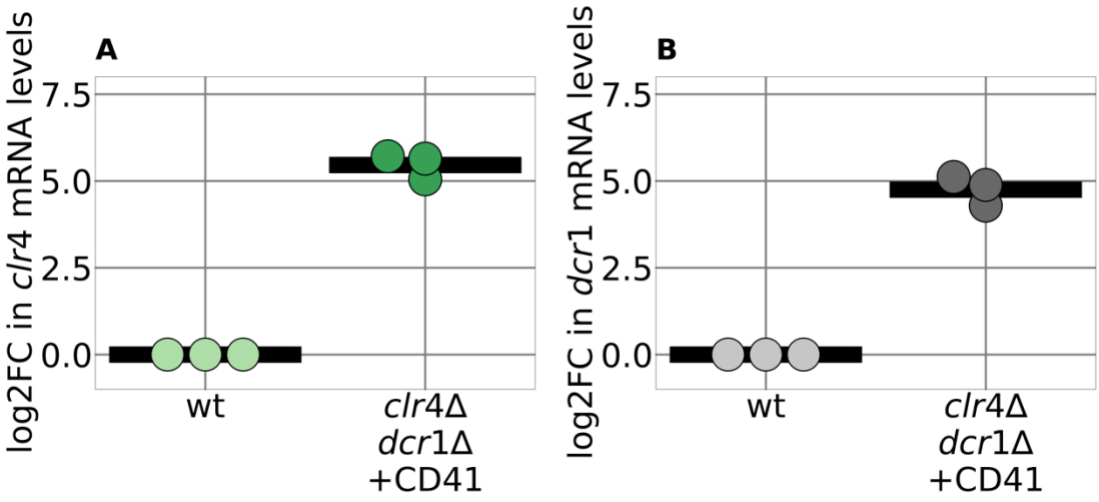

Figure 4-7: Both *clr4*+ and *dcr1*+ genes are overexpressed when the expression is driven from the pREP-CD41 plasmid. RT-qPCR analysis of *clr4*+ **(A)** and *dcr1*+ **(B)** transcript levels relative to *act1*+ in the wild-type and in the *clr4Δ-dcr1Δ* +pREP-CD41 strains (n=3). Black line represents geometric mean.

4.4 Discussion

In this chapter I aimed to identify the molecular characteristics of heterochromatin re-establishment upon the deletions of Tos4, Tfb2, Nse5 and SPBC21C3.12: four proteins identified earlier as candidate establishment factors by the plasmid transformation assay. Clr4+ and Dcr1+ deletions result in loss of H3K9me2 and siRNAs, and an increase in pericentromeric transcript levels. Levels of these markers are expected to be restored to wild-type when the pREP-CD41 plasmid is introduced to the *clr4Δ-dcr1Δ* strain, but not when it is introduced to *goiΔ-clr4Δ-dcr1Δ*, where *goiΔ* is a deletion of a candidate establishment factor.

Introducing the pREP-CD41 plasmid to the *clr4Δ-dcr1Δ* strain led to an increase in pericentromeric H3K9 methylation and siRNA production, suggesting that expression of *clr4+* and *dcr1+* from the pREP-CD41 plasmid can induce *de novo* H3K9 methylation and siRNA production. When the plasmid was introduced to triple mutant cells carrying deletions of the pre-selected candidate establishment factors, only H3K9me and siRNA levels remained low in cells lacking *tos4+* and *tfb2+*. This is consistent with these two factors being required for heterochromatin establishment. However, H3K9me2 and siRNA levels were high in *nse5Δ-clr4Δ-dcr1Δ* and *SPBC21C3.12cΔ-clr4Δ-dcr1Δ* strains upon the pREP-CD41 plasmid

transformation. This is surprising since these triple mutant cells were pale on low adenine media upon pREP-CD41 introduction, suggesting that heterochromatin is perturbed (Fig4-6). Unlike the ChIP and northern blot data, the RT-qPCR data are hard to interpret. It was predicted that transformation with the pREP-CD41 plasmid would reduce the pericentromeric RNA production in the *clr4Δ-dcr1Δ* strain to wild-type levels. However, intermediate RNA levels were observed, higher than the levels present in the wild-type cells and lower than the levels present in the *clr4Δ-dcr1Δ* strain. As a result it makes it difficult to interpret the effect of our four pre-selected candidates on the pericentromeric transcript repression. High RNA expression upon pREP-CD41 introduction to the triple mutant cells might indicate an inability of pREP-CD41 to reduce the expression rather than the deletion of the gene of interest having an effect.

Reintroduction of *clr4+* and *dcr1+* on a plasmid led to the restoration of H3K9me2 and siRNA production, however the transcription remained intermediate. The same pattern was observed by Jih et al, where they showed that H3K9me2 domain is transcription-permissive with siRNA forming over the pericentromeres. However it is not clear why *clr4+* expressed from a plasmid can only lead to H3K9me2. In the paper by Jih et al H3K9me2 was induced by a mutation in *clr4+* (Jih et al., 2017). In our study we introduce a wild-

type copy of *clr4+*, however *clr4+* is overexpressed. Iglesias et al. showed that insertion of an extra copy of *clr4+* leads to stronger silencing at the telomeres as well as to spreading of H3K9me2 beyond their normal domains (Iglesias et al., 2018). Quantification of the mRNA levels of the *clr4+* gene, produced from the pREP-CD41 plasmid, showed that *clr4+* is severely overexpressed compared to the wild-type strain. In the pREP-CD41 plasmid *clr4+* gene is expressed from its endogenous promoter and terminator. However pREP-CD41 is not a low-copy number plasmid, and there might be several plasmid copies present in the cells, resulting in *clr4+* overexpression. The result of *clr4+* overexpression might be spreading of the pre-existing H3K9me domains or formation of new ones, which can lead to silencing of genes required for transitioning from transcription-permissive H3K9me2 to fully silent H3K9me3 domains.

When I repeated the plasmid transformation assay, the results did not replicate the results from the original screen. Strains that appeared pale in the first screen were not as pale the second time around, while other deletion strains displayed a pale/mixed colour that was not seen in the first screen. The only strain that stayed white after both transformation procedures is *nse5Δ-clr4Δ-dcr1Δ.* Even without the reintroduction of *clr4+* and *dcr1+* genes on a

plasmid, *nse5Δ* seems to rescue the heterochromatin defects caused by *clr4Δ-dcr1Δ*. When *clr4+* presence was assessed in *nse5Δ-clr4Δ-dcr1Δ* strain, it had both *clr4+* and *clr4Δ* deletion cassette present. These results indicate that this strain somehow managed to preserve a functional copy of *clr4+* through gene or chromosomal duplication. Pebernard et al. showed that Nse5 is involved in DNA repair during DNA replication, and thus it is potentially important for genome stability (Pebernard et al., 2006). Cells with the deletion of *nse5+* have elongated shape, and they are sensitive to DNA damaging agents, which is suggestive of its role in DNA repair (Pebernard et al., 2006). Moreover, deletion of *clr4+* leads to an elevated rate of chromosome loss (Ekwall et al., 1996). Crossing *nse5Δ* with *clr4Δ-dcr1Δ* strain, where both strains bear genomic instability, can potentially result in genomic rearrangements leading to unpredicted results. Potentially individual colonies with *nse5Δ-clr4Δ-dcr1Δ* background have to be screened and selected for the absence of *clr4+* duplication before conducting any further experiments.

As discussed earlier *clr4+* overexpression can potentially drive the expansion of H3K9me domains or formation of new ones. It can also potentially explain the assay inconsistency. Every pREP-CD41 plasmid transformation can potentially lead to a different copy number of pREP-CD41 plasmid present in the cells. If indeed *clr4+*

overexpression can drive de novo heterochromatin formation, then after each transformation the global H3K9me profile can be different. This, in turn, can lead to contrasting outcomes at every transformation event.

In light of the data presented in chapter 5, assay heterogeneity can also be explained by the stochasticity of heterochromatin establishment. In chapter 5 I describe a cross-based assay, where during a control cross ~60% of colonies do not re-establish heterochromatin immediately, but over time, potentially due to inherent stochasticity of the process. When the impact of previously described establishment factors – *mkt1+* and *tri1+* - was assessed in the cross-based assay, the progeny had a distribution of red and white colonies. When followed over time, some white colonies re-establish heterochromatin, and some do not. This might suggest that the results from the plasmid-based assay are not inconsistent, but stochastic, similar to the results observed in the cross-based assay. Distribution of red and white colonies after each independent plasmid transformation can also point towards randomness (rather than inconsistency), where the proportion of red and white colonies has be to be calculated after each transformation. Then white colonies have to be followed over time to establish an effect of a potential establishment factor.

Since at the time the results obtained from the plasmid-based assay were considered inconsistent, I proceeded to develop a more reliable assay that can subsequently be used for a high-throughput screen. Ultimately we aimed to test all the non-essential gene deletions in *S. pombe* for their effect on heterochromatin establishment. In order to conduct such genome-wide screen, I need a robust assay that can yield consistent results. The plasmid-based assay that I developed and tested, failed to withstand replication, potentially due to the *clr4*+ and/or *dcr1*+ overexpression. Thus we need to use an assay where heterochromatin re-establishment is induced with the endogenous levels of the genes from the RNAi and CLRC pathways. This will allow us to test if the plasmid-based screen inconsistency is indeed due to the *clr4*+ and *dcr1*+ genes overexpression. Moreover using a more endogenous assay will allow us to evaluate if *tos4*+ and *tfb2*+ deletions indeed have any effect on the establishment. Both Tos4 and Tfb2 are transcription factors (Lock et al., 2019). One well-known example of transcription factors contributing to the heterochromatin establishment occurs at the mating type locus in *S. pombe.* In *S. pombe* Atf1/Pcr1 transcription factors bind to a specific DNA sequence at the mating type locus, recruiting histone deacetylase Clr3 and histone methyltransferase Clr4 to establish heterochromatin together with RNAi-machinery (Jia, Noma, & Grewal, 2004; Yamada et al., 2005). Potentially Tos4 and Tfb2 can

have similar to Atf1/Pcr1 roles in heterochromatin establishment at the centromeres. In the next chapter I will discuss a cross-based assay that we developed to further investigate heterochromatin establishment.

Chapter 5 — Crossed-based establishment assay

5.1 Introduction

Thus far I described a plasmid-based establishment assay that identified four potential establishment candidates: Tos4, Tfb2, Nse5 and SPBC21C3.12. Further characterization showed that, upon reintroduction of Clr4, H3K9 methylation and siRNA production cannot be rescued to the wild-type levels without Tos4 and Tfb2, a phenotype consistent with these two factors having a role in heterochromatin establishment. However further characterizations showed that the plasmid-based establishment assay provides inconsistent results potentially due to the pREP-CD41 plasmid overexpression. Thus I developed an assay where the key CLRC/RNAi proteins required to re-establish heterochromatin are expressed endogenously.

5.2 Cross-based establishment assay principle

The new assay relies on a strategy of crossing and selecting against gene deletions via negative selection of cells expressing the *ura4+* gene on media containing 5-Fluoroorotic acid (FOA). When *ura4+*-positive cells are grown on FOA-supplemented media, FOA is incorporated into a toxic product causing cells to die (Allshire et al., 1994). Thus media supplemented with FOA selects for cells that do not express a functional *ura4+* gene.

As in the plasmid-based assay, I deleted genes from both CLRC and RNAi pathways to ensure maximal pericentromeric heterochromatin perturbation, and then re-introduced them to drive heterochromatin re-establishment. However instead of using the plasmid, I used the FOA selection to introduce the wild-type CLRC/RNAi genes via genetic crossing.

I first generate two tester strains: one strain has the *clr4*+ and *ago1*+ genes deleted and another strain has the *rik1*+ and *dcr1*+ genes deleted (Figure 5-1). Then each tester strain is crossed to the strain with the gene of interest deletion to be tested, generating two triple mutant strains (*goiΔ-clr4Δ-ago1Δ* and *goiΔ-rik1Δ-dcr1Δ*). Each CLRC/RNAi gene (but not the gene of interest) is deleted with an antibiotic-resistance cassette genetically linked to the *ura4*+ gene, meaning that selection for/against *ura4*+ will select for/against a respective CLRC/RNAi gene deletion. Importantly the strain with *clr4Δ-ago1Δ* background has wild-type genes of *rik1*+ and *dcr1*+ and vice versa. It is expected that crossing the two tester strains together and plating the resulting F1 generation on media containing FOA would select against all the *ura4*+-linked gene deletions and therefore for the presence of the respective wild-type CLRC/RNAi genes. Introducing the wild-type CLRC/RNAi genes and leaving the gene of interest deleted allows us to test the role that the gene of

interest has in heterochromatin establishment. As in the plasmid-based assay, the state of the pericentromeric heterochromatin is assessed using the pericentromeric *ade6+* reporter assay described in chapter 3.

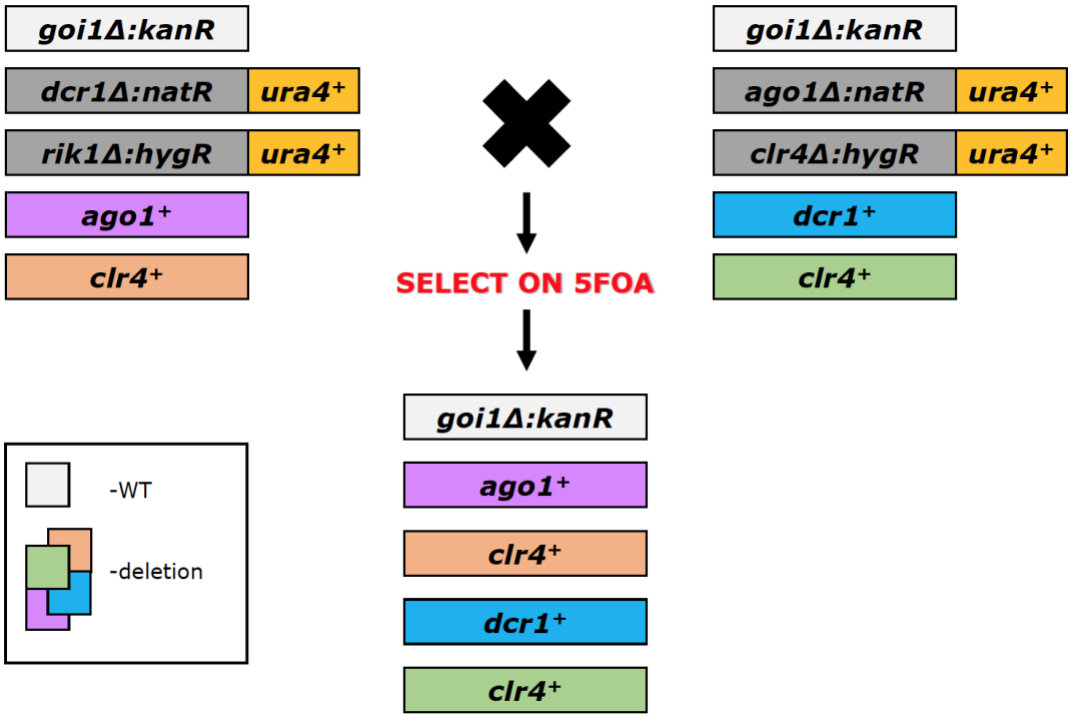

Figure 5-1. Cross-based establishment assay principle. In the cross-based approach two triple mutant strains are generated. One triple mutant strain bears gene of interest, *clr4+* and *ago1+* deletions. Another triple mutant strain bears gene of interest, *dcr1+* and *rik1+* deletions. All the CLRC/RNAi genes are deleted with antibiotic resistance cassettes genetically linked to the *ura4+* gene, so that crossing the two strains together and plating the F1 generation on media supplemented with FOA is predicted to select against the CLRC/RNAi gene deletions linked to *ura4+* gene, and thus for the wild-type CLRC/RNAi genes. The effect of the gene of interest deletion on re-establishment of centromeric heterochromatin is evaluated using the *ade6+* reporter assay.

5.3 Pericentromeric heterochromatin cannot be re-established immediately in ~60% of colonies despite CLRC/RNAi machinery present.

To test the system, first I crossed together the two tester strains, and plated the F1 generation on FOA-supplemented media. I hypothesised that FOA will select for progeny where the *ura4*+-linked CLRC/RNAi gene deletions have been recombined out, thus bringing together the wild-type *clr4*+, *ago1*+, *dcr1*+ and *rik1*+genes. I expect the newly-introduced wild-type copies of CLRC/RNAi genes to drive heterochromatin re-establishment, leading to red colour of F1 colonies on media with limiting adenine.

Interestingly the control cross yielded a distribution of red and white colonies, suggesting that pericentromeric heterochromatin was not re-established in all colonies (Fig 5-2A). I then decided to verify that the wild-type *clr4*+, *ago1*+, *dcr1*+ and *rik1*+ genes are present in six randomly picked white colonies. Interestingly all of the white colonies tested had the aforementioned wild-type CLRC/RNAi genes present. This result suggests that the white colonies have the genes required to re-establish pericentromeric heterochromatin, but this process is somehow prevented.

A

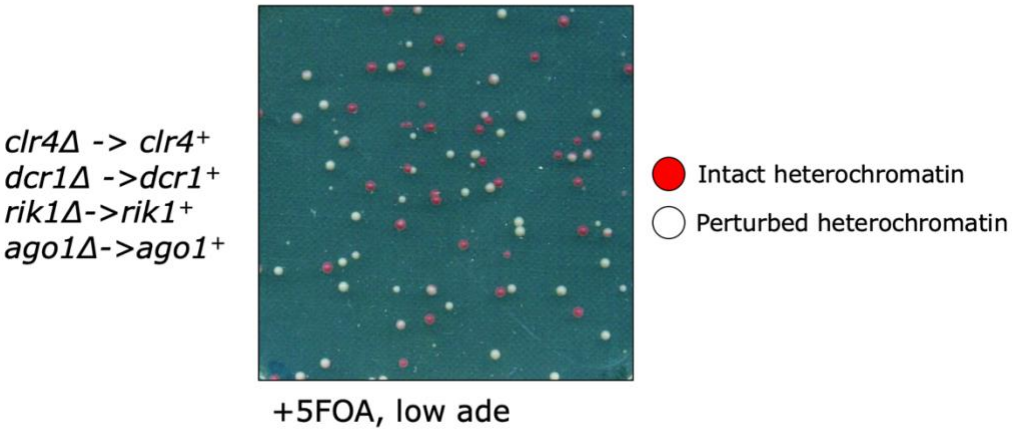
clr4Δ -> clr4+
dcr1Δ ->dcr1+
rik1Δ->rik1+
ago1Δ->ago1+
Intact heterochromatin
Perturbed heterochromatin
+5FOA, low ade

B

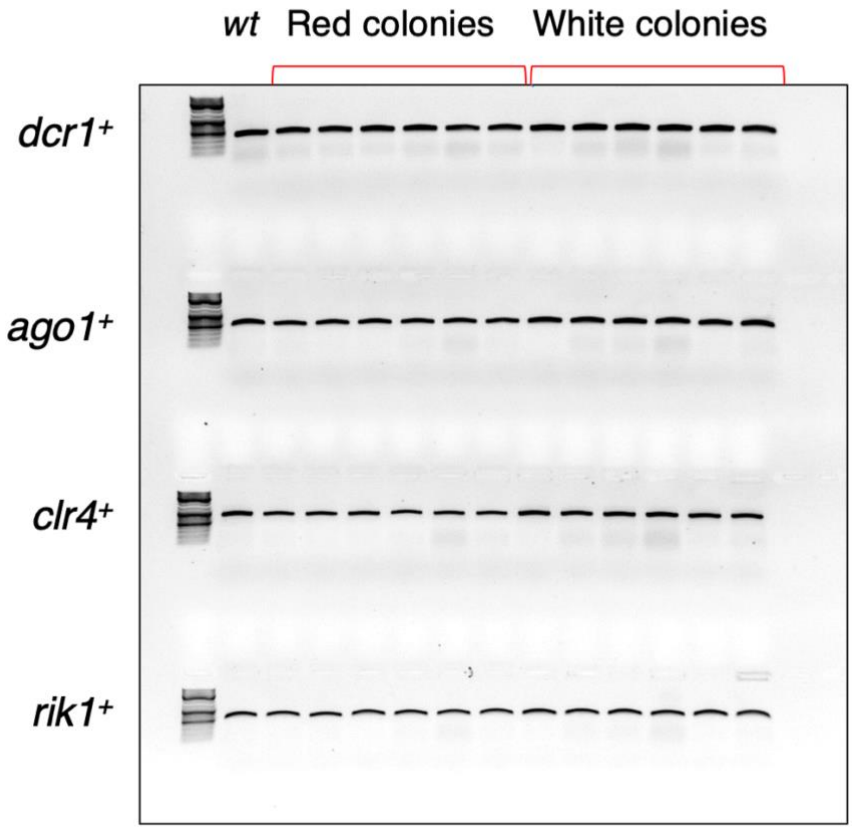
wt
Red colonies
White colonies
dcr1+
ago1+
clr4+
rik1+

Figure 5-2. The cross-based establishment assay revealed that pericentromeric heterochromatin is not re-established immediately in all of the F1 progeny. (A) A cross between the two tester strains yielded red and white F1 progeny on FOA-supplemented media with limiting adenine. Red colonies indicate intact heterochromatin state, white colonies indicate perturbed heterochromatin state.**(B)** PCR analysis of the presence of *clr4*$_+$, *ago1*$_+$, *dcr1*$_+$ and *rik1*$_+$ genes in the red and white F1 colonies.

I then decided to test the colour distribution of F1 colonies in the *dos2Δ* background. Dos2 is a CLRC component, that interacts with Stc1, thus connecting CLRC with RNAi machinery (Kuscu et al., 2014). Pericentromeric heterochromatin cannot be maintained or established without Dos2. As expected, an establishment cross with *dos2Δ* resulted in all of the F1 colonies turning white on FOA-supplemented media with limiting adenine (Fig5-3).

Tri1 and Mkt1 are two factors described to be involved specifically in establishment of heterochromatin(Marasovic et al., 2013; Bayne lab, unpublished data). As with the *dos2+* deletion, I performed an establishment cross with *tri1Δ* and *mkt1Δ strains* and tested the colour of F1 colonies on media with limiting adenine. Similar to the F1 progeny resulting from the wild-type control cross, both the *tri1Δ* and *mkt1Δ* strains generated a mix of red and white colonies (Fig5-3). On average the control cross yielded 34.6% ± 8.4% (STD) red colonies in the F1 generation (Fig5-4). For the *tri1Δ* and *mkt1Δ* strains the average proportions of red colonies were 41.4% ± 16.2% (STD) and 26.9% ± 3.3% (STD) respectively, similar to the control (Cohen's d=0.31 95%CI [-1.08, 1.70] and Cohen's d=0.98 95%CI [-0.60, 2.56] respectively).

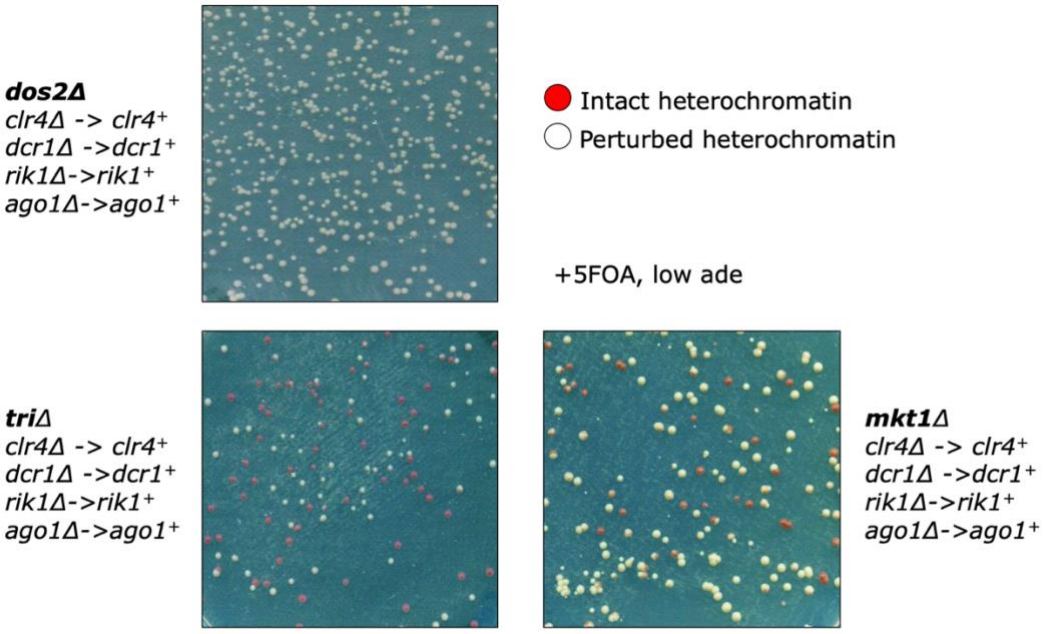

Figure 5-3. Establishment factor deletion leads to a distribution of red and white colonies in the F1. The F1 generation resulting from the cross-based establishment assay with *dos2Δ , triΔ* and *mkt1Δ* strains was plated on FOA-supplemented media, with limiting adenine.

(A)

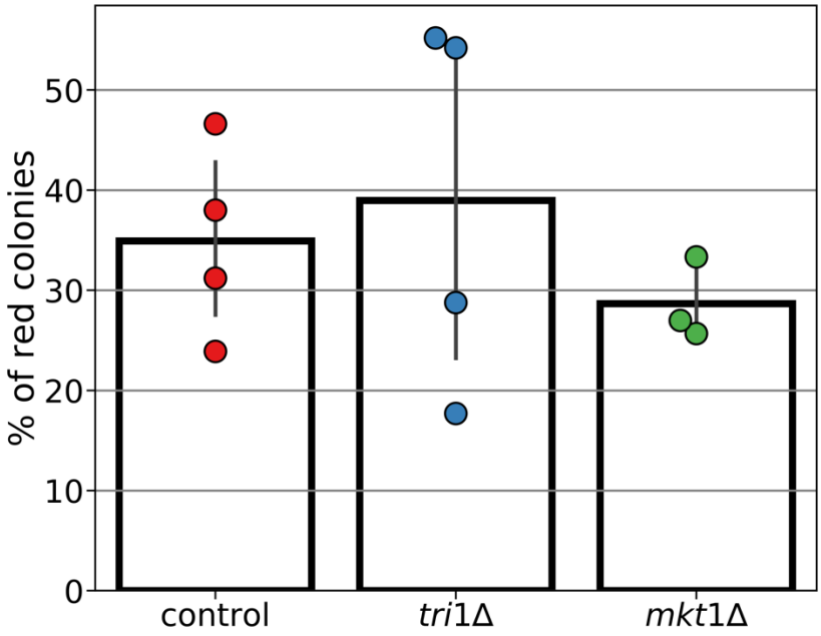

(B)

		Red	White	Total	%red	%white
control	**1**	62	71	133	47.0	53.0
	2	54	89	143	38.0	62.0
	3	93	205	298	31.0	69.0
	4	27	86	113	24.0	76.0
tri1Δ	**0**	43	200	243	18.0	82.0
	1	85	69	154	55.0	45.0
	2	116	98	214	54.0	46.0
	3	21	52	73	29.0	71.0
mkt1Δ	**0**	19	55	74	26.0	74.0
	1	9	18	27	33.0	67.0
	2	51	138	189	27.0	73.0

Figure 5-4. Cross-based establishment assay in *triΔ* and *mkt1Δ* backgrounds yields similar proportion of red colonies compared to wild-type background. (A) F1 colonies were counted on FOA-supplemented media with limiting adenine (n=5). Measure of central tendency : mean, error bars: 95% CI. **(B)** Quantification of red and white colonies presented in (A).

5.4. Sampled white F1 colonies from the control cross re-establish heterochromatin over time

I then evaluated the colour dynamics of F1 colonies over time. I picked six white and six red F1 colonies resulting from the control establishment cross, and six white colonies from the establishment cross in the *dos2Δ* background. As expected the white *dos2Δ* colonies stayed white after being passaged three times (Fig5-5A). There was no growth on thiabendazole (TBZ)-supplemented media (assay described in the discussion of chapter 3), further confirming that pericentromeric heterochromatin was not re-established. The red F1 colonies from the control cross also stayed red, and grew on TBZ-supplemented media (Fig5-5B). Interestingly, the white F1 colonies from the control cross gradually turned red and gained TBZ-resistance over time (Fig5-5C).

A

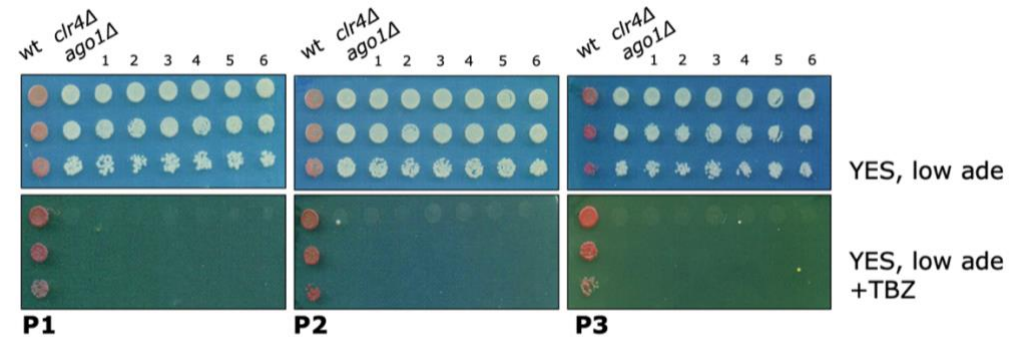

B

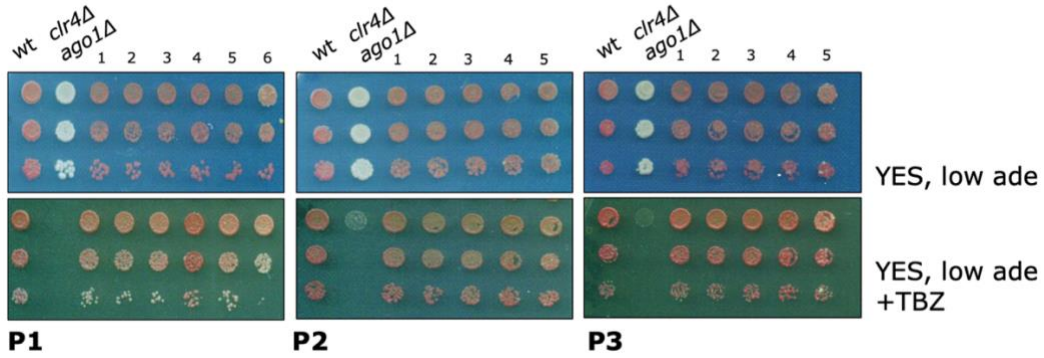

C

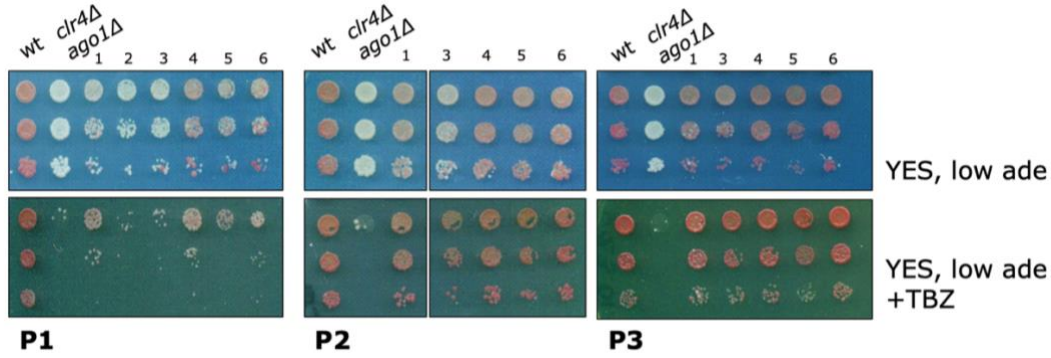

Figure 5-5. White progeny from the control cross re-establish heterochromatin over time. Selected F1 colonies resulting from the control cross (red **(B)** and white **(C)** colonies) , and from the cross in the *dos2Δ* background **(A)** (white colonies), were passaged three times (P1-3) on media with limiting adenine and on TBZ-supplemented media

5.5 Deletions of *tri1*+ and *mkt1*+ lead to heterogenous colours in F1 progeny followed over time.

I then followed selected white F1 colonies from the establishment crosses in *tri*Δ and *mkt1*Δ backgrounds. The F1 colonies from both the *tri*+ and *mkt1*+ deletion strains produced a range of colony colours after three passages, which is indicative of different heterochromatin states (Fig5-6). Two out of three F1 *mkt1*Δ colonies turned red and one stayed pink. Of the *tri*Δ colonies, one F1 colony was red, one was pink and one was white at the end of the third passage. The white *tri*Δ colony did not grow well on TBZ-supplemented media, whereas the pink and red colonies grew well in the presence of TBZ (as did the pink and red colonies from the *mkt1*Δ strain).

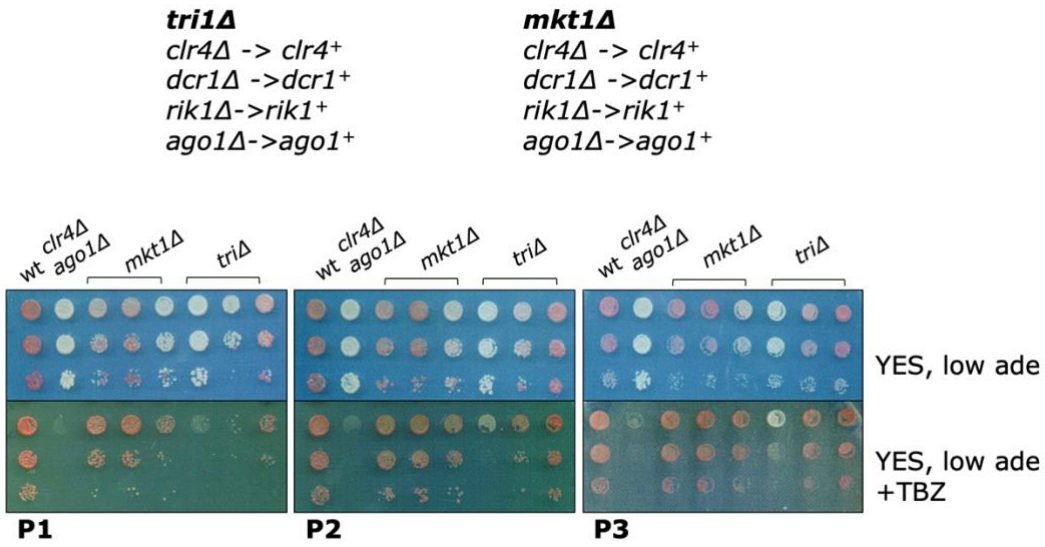

Figure 5-6. Deletion of *mkt1*+ or *tri1*+ leads to heterogeneous patterns of heterochromatin establishment. Cross-based establishment assays were performed in *mkt1Δ* and *tri1Δ* backgrounds, and F1 colonies were passaged three times on both low adenine media and TBZ-supplemented media to check for heterochromatin re-establishment over time.

5.6 Establishment assays with the pre-selected sixteen candidates yielded a distribution of colony colours

I then decided to check the effect that deletion of each of the pre-selected candidates, described in chapters 3 and 4, has on pericentromeric heterochromatin after the cross-based establishment assay. As with the *dos2+* deletion strain, I expect all (or most) of the F1 colonies to be white or pale if the candidate is a 'strong' establishment factor. However none of the sixteen candidate deletions yielded the same result as the *dos2Δ* strain after the cross-based assay: each candidate deletion led to a distribution of red, pink and white F1 colonies. For example, tos4*Δ*, *tfb2Δ*, *SPBC21C3.12Δ* and *nse5Δ* cells that were white on media with limiting adenine in the original plasmid-based screen, led to a mix of red and white F1 colonies in the establishment assay. Other deletion strains, like *urm1Δ,* led to a distribution of pink and red F1 colonies with virtually no white colonies.

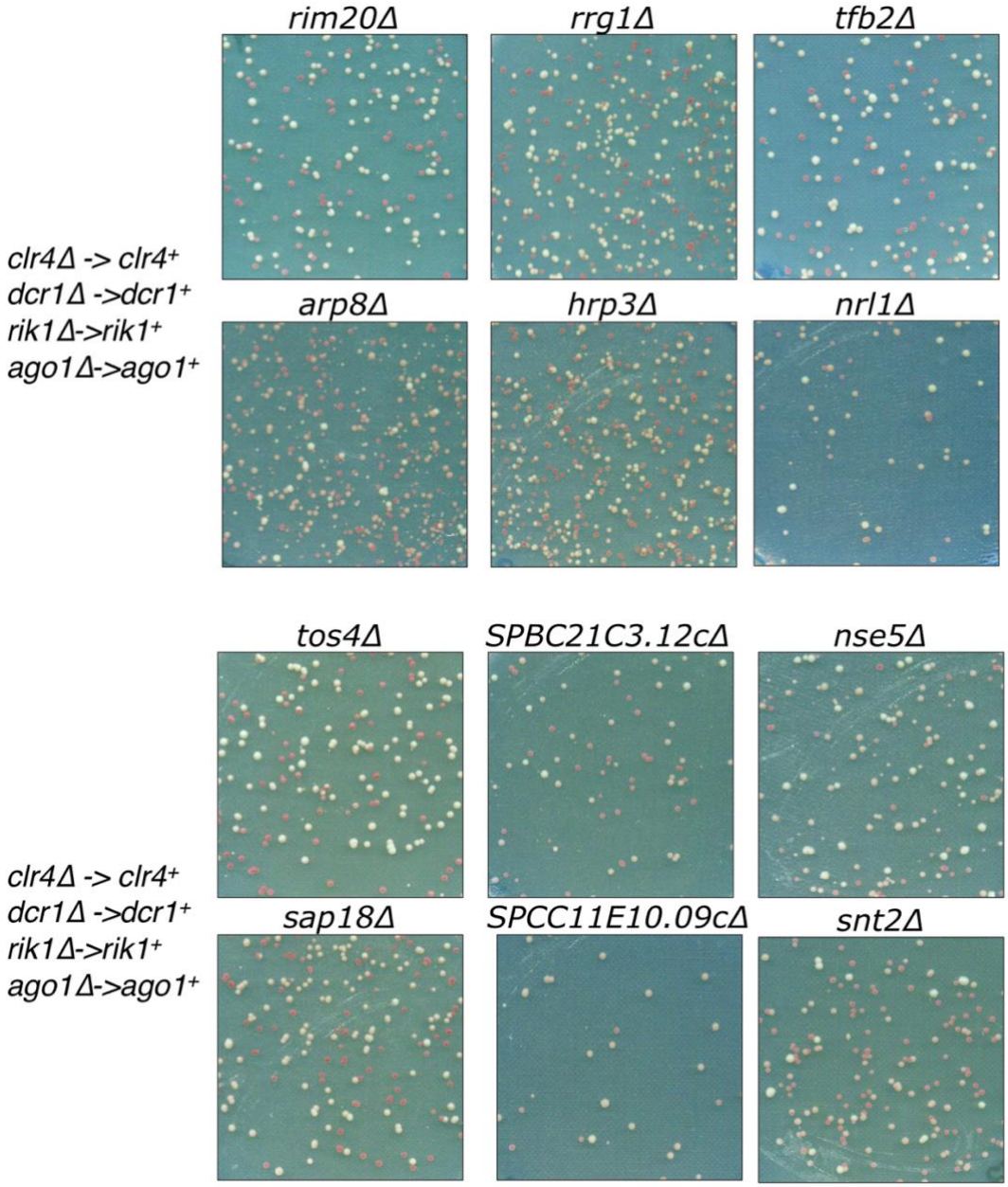
rim20Δ
rrg1Δ
tfb2Δ
clr4Δ -> clr4+
dcr1Δ ->dcr1+
rik1Δ->rik1+
ago1Δ->ago1+
arp8Δ
hrp3Δ
nrl1Δ
tos4Δ
SPBC21C3.12cΔ
nse5Δ
clr4Δ -> clr4+
dcr1Δ ->dcr1+
rik1Δ->rik1+
ago1Δ->ago1+
sap18Δ
SPCC11E10.09cΔ
snt2Δ

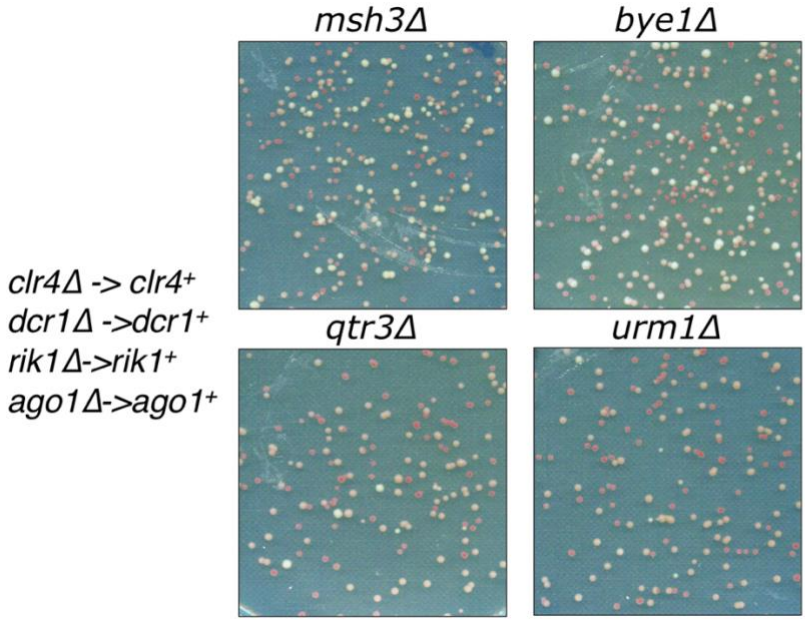

Fig 5-7. Deletion of sixteen establishment candidates yielded a distribution of white, pink and red F1 colonies after the cross-based establishment assay. Sixteen establishment candidates from chapter 3 were subjected to cross based establishment assay, and F1 colonies were plated on 5FOA-supplemented media with limiting adenine.

Genotype	Red	Red (%)	White	White (%)	Pink	Pink (%)	Total
rim20Δ	50	36	89	64	0	0	139
rrg1Δ	77	29	186	71	0	0	263
tfb2Δ	39	31	85	69	0	0	124
arp8Δ	94	30	26	8	197	62	317
hrp3Δ	130	41	189	59	0	0	319
nrl1Δ	13	27	10	20	26	53	49
tos4Δ	49	36	89	64	0	0	138
SPBC21C3.12cΔ	33	50	6	9	27	41	66
nse5Δ	27	22	27	22	68	56	122
sap18Δ	61	39	94	61	0	0	155
SPCC11E10.09cΔ	6	24	2	8	17	68	25
snt2Δ	71	54	15	11	45	34	131
msh3Δ	63	27	69	29	105	44	237
bye1Δ	45	19	36	15	157	66	238
qtr3Δ	61	45	4	3	71	52	136
urm1Δ	65	49	2	2	65	49	132

Table 5-1. Quantification of colonies presented in figure 5-7.

5.7 Heterochromatin establishment is not influenced by the parental source of the *ade6+* reporter.

Red to white distribution of F1 colonies from the control cross was close to 50:50 ratio (~40:60), which might suggest parent-specific *ade6+* reporter inheritance. Thus I wanted to check if red (or white) colony colour is determined by the parental strain which passed the *ade6+* reporter onto the F1 generation. To do this, I modified the *ade6+* reporter in the tester strains. I linked an auxotrophic *leu1+* marker to the pericentromeric *ade6+* (cen1:*ade6+*:*leu1+*) (Fig 5-8A). I then performed two crosses, where each 'tracked' strain is crossed to its untracked counterpart. If the state of cen1:*ade6+* silencing is affected by the parental strain it is inherited from, then on media lacking leucine I would expect 100% red or white F1 colonies depending on the parental strain being tracked. In contrast, I would expect a mix of red and white F1 colonies if the parental source of the *ade6+* reporter has no effect. Reciprocal crosses both gave a distribution of red and white colonies, suggesting that the *ade6+* reporter silencing in F1 does not depend on the parental strain it is inherited from (5-8B).

A

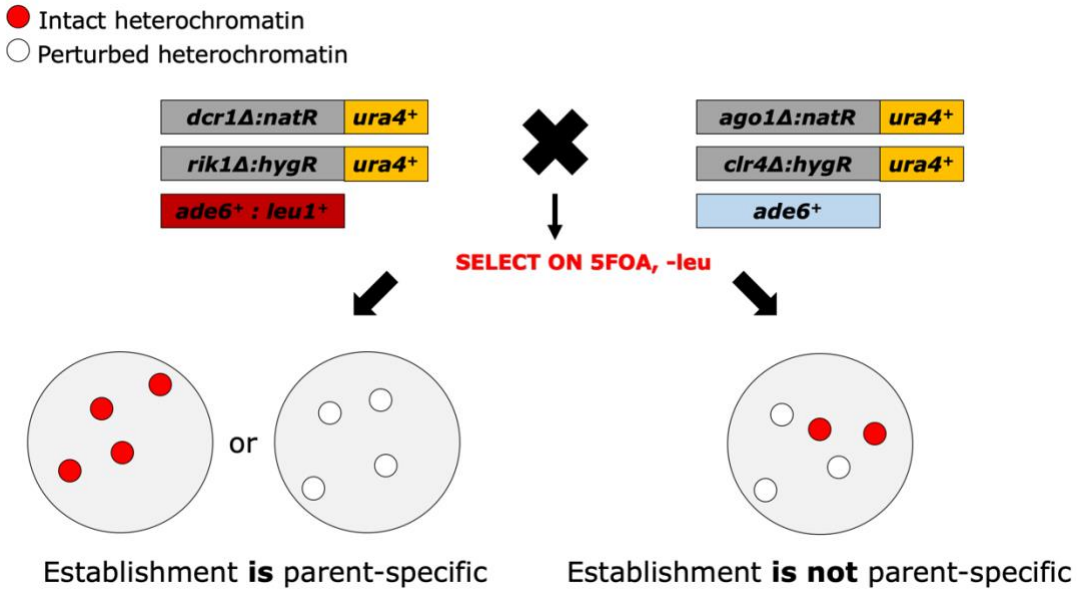

B

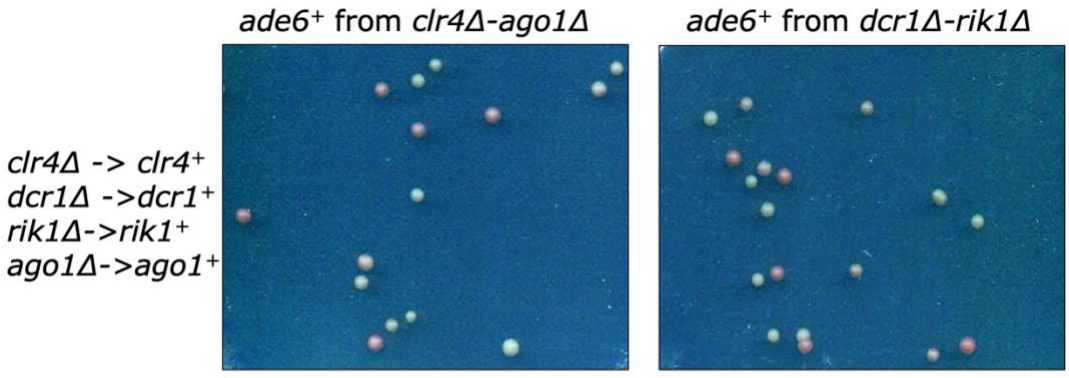

+5FOA,-leu, low ade

Colony counts	Colony counts
White: 8	White: 10
Red: 5	Red: 5
Sectored: 2	Sectored: 3
Total: 15	Total: 18

Figure 5-8. *ade6*$_+$ reporter silencing is not affected by the parent of origin. (A) A schematic diagram of *ade6*$_+$ reporter tracking. In both parental strains the *ade6*$_+$ reporter was marked by adjacent integration of the *leu1*$_+$ gene. Then each 'marked' strain was crossed to its unmarked counterpart and the progeny were plated on media supplemented with FOA (to select for the progeny with re-established heterochromatin limiting adenine (to assess *ade6*$_+$ expression) and limiting leucine (to select for the marked *ade6*$_+$ reporter). **(B)** Progeny from reciprocal crosses each of the tracked crosses plated on the aforementioned selection appears as a mixture of red and white colonies.

5.8 The parental CLRC/RNAi deletion combination affects the colour distribution of F1 colonies

I wanted to further check for any potential effect the parental strain might have on the cen1:*ade6+* silencing in F1. To do so, I created two new tester strains. Originally I used *clr4Δ-ago1Δ* and *rik1Δ-dcr1Δ* tester strains. I then changed the combination of CLRC/RNAi gene deletions, generating *clr4Δ-dcr1Δ* and *rik1Δ-ago1Δ* tester strains. Interestingly, when the new parental strains were crossed together and the F1 generation was plated on FOA-supplemented media with limiting adenine, 100% of the colonies were red (Fig 5-9). When the new establishment cross was performed in a *dos2Δ* background, all of the colonies turned white (Fig5-9).

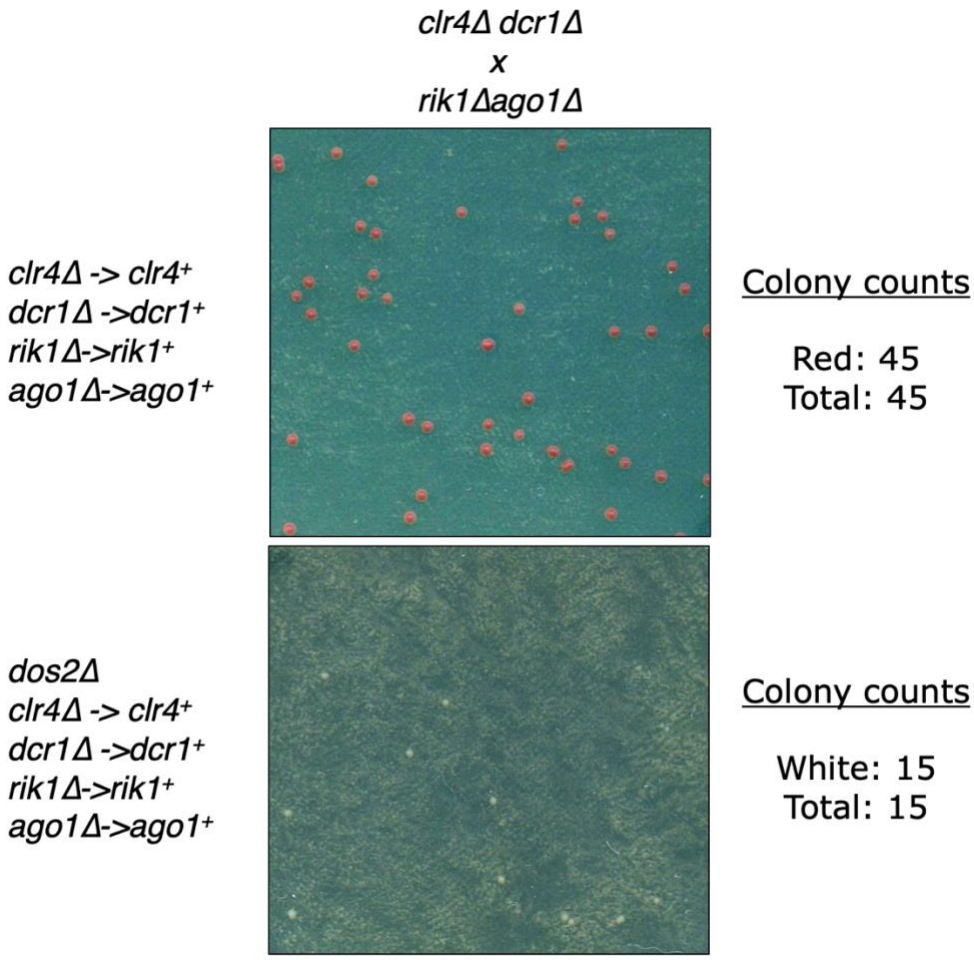

Figure 5-9. Cross between *clr4Δ-dcr1Δ* and *rik1Δ-ago1Δ strains* leads to 100% red F1 progeny. F1 progeny from the crosses between the new tester strains without and with *dos2+* deletion were plated on FOA-supplemented media with limiting adenine. Red colony colour indicates heterochromatin re-establishment.

5.9 The level of *clr4+* mRNA is upregulated in the *dcr1Δ-rik1Δ* strain

Since crossing the new tester strains generated 100% red colonies as expected, it suggested that something specific to the deletion combinations in the original tester strains impaired heterochromatin establishment. The cross between the original tester strains (*clr4Δ-ago1Δ* and *rik1Δ-dcr1Δ*) yields around 60% white colonies in the F1 that turn red over time. I hypothesised that one or more CLRC/RNAi genes might be not properly expressed in the original tester strains, thus preventing pericentromeric heterochromatin from re-establishing in ~60% white F1 colonies. I therefore decided to check the *rik1+*, *dcr1+*, *clr4+* and *ago1+* mRNA levels in both the original and new parental strains. I predicted that the mRNA levels of some of these genes may be deregulated in the original tester strains, which might potentially explain why the majority of F1 colonies appears white on low adenine media. The delay in heterochromatin re-establishment (white colonies turning red) could relate to time taken for normal expression to be restored.

The levels of the majority of the aforementioned mRNAs in each of the tester strains were similar to the levels present in the wild-type (Figure 5-10A ,log2FC is in the range of 0 to 1).

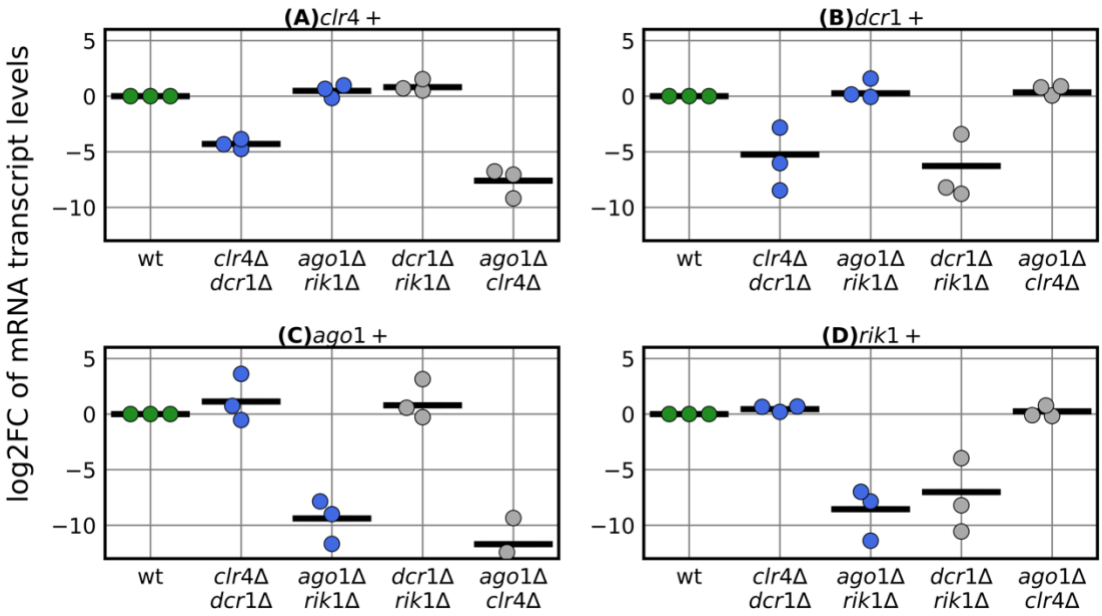

Figure 5-10. mRNA levels in the tester strain are similar to the levels present in the wild - type. RT-qPCR analysis of *clr4*+(A), *dcr1*+(B), *ago1*+(C) and *rik1*+ (D) transcript levels compared to *act1*+, n=3). Horizontal black line represents geometric mean.

5.10 Discussion

After showing that the plasmid-based establishment assay provides inconsistent result, I developed a new cross-based assay. The cross-based assay relies on deleting CLRC and RNAi genes, thus perturbing pericentromeric heterochromatin, and then reintroducing the endogenous copies via meiotic recombination.

I first developed two tester strains: *clr4Δ:ura4+-ago1Δ:ura4+* and *rik1Δ:ura4+-dcr1Δ:ura4+*. I predicted that crossing these two strains together and plating the progeny on FOA-supplemented media would select against the *ura4+*-linked deletions and thus for introduction of the respective wild-type genes. Introduction of the wild-type genes is expected to drive heterochromatin re-establishment, which in the presence of *cen1:ade6+* reporter manifests in red colonies growing on media with limiting adenine. However the control cross between the two tester strains led to a distribution of red and white colonies, where white colonies were the majority (63% ± 8.4% STD). This indicates that heterochromatin is not re-established in the majority of F1 progeny. I first hypothesised that the inefficient heterochromatin re-establishment was due to the absence of wild-type copies of *dcr1+*, *clr4+*, *ago1+* or *rik1+* genes in the white colonies. However PCR analysis showed that these genes were present. It means that the cross-based establishment assay

successfully introduced the wild-type copies of CLRC/RNAi genes, however heterochromatin was not immediately re-established. I then performed series of experiments to try to understand heterochromatin establishment dynamics.

First I hypothesised that the colony colour may depend on the parental strain the reporter is inherited from. However regardless of the parental source of cen1:*ade6+*, the F1 colonies were a mix of red and white colour. It means that the inheritance pattern of the cen1:*ade6+* reporter also does not seem to play a role.

I then performed the cross-based establishment assay in a *dos2+* deletion background. Without Dos2 heterochromatin cannot be maintained or established, and *dos2Δ* strains with cen1:*ade6+* reporter appear white on media with limiting adenine. Thus the cross-based establishment assay in the presence of *dos2+* deletion acts as a negative control. As expected all F1 colonies with *dos2+* deletion are white on FOA-supplemented media with limiting adenine. Thus regardless of the causes behind the red and white F1 colonies resulting from the control cross, this assay has the capacity to detect a 'strong' establishment factor. Like with *dos2Δ,* deletion of a 'strong' establishment factor should result in all the F1 colonies being white in the cross-based establishment assay. Moreover,

because this assay generates ~60% white F1 colonies in the control background, this assay also has the potential to detect a factor that can potentially accelerate heterochromatin re-establishment: in this case all/the majority the F1 colonies should appear red.

I then wanted to follow heterochromatin dynamics in the F1 colonies over time. To do this, I picked six white and six red colonies resulting from the cross between the tester strains and passaged them over time. Interestingly, white colonies started to turn red, and this transition occurred at slightly different rates amongst different colonies. The originally red colonies stayed red. This suggests that in the majority of colonies heterochromatin re-establishment is delayed, but not completely blocked. Once heterochromatin was established in F1, then it is stably inherited.

Inheritance pattern of *ade6*+ reporter and gradual white-to-red transition might suggest that heterochromatin re-establishment, similar to gene expression, is stochastic. (Elowitz et al.,2002). Randomness might determine in which colonies heterochromatin is established first, thus giving rise to a distribution of red and white colonies in F1. During heterochromatin re-establishment over time, individual white colonies turn red at slightly different rates, which can also be due to stochasticity.

What are the heterochromatin state dynamics, when known establishment factors are deleted? Absence of a factor absolutely required for establishment is expected to result in ~100% white colonies in the F1 generation, with no subsequent heterochromatin re-establishment over time. However the phenotype is more subtle in the absence of *mkt1+* and *tri1+.* Unlike the cross in the *dos2Δ* background, crosses in the *mkt1Δ* and *tri1Δ* lead to a distribution of red and white F1 colonies, similar to the control cross. However the effects of *mkt1Δ* and *tri1Δ* become apparent when the white F1 colonies are followed over time. Not all of the white colonies turn red: in the *mkt1Δ* strain some colonies turned red and some pink. In the *tri1Δ* strain one colony turned red, one turned pink and one stayed white. In the future more colonies have to be followed, however these data already suggest that the effect of the establishment factor deletion becomes visible over time.

I also subjected the sixteen pre-selected candidates discussed in chapters 3 and 4 to the cross-based establishment assay. All of the crosses yielded a mix of red, pink and white colonies. This suggests that deletions of these factors do not have an immediate effect on heterochromatin establishment. However some of these deletions might still affect the rate of heterochromatin reestablishment, as

mkt1Δ and *tri1Δ.* Thus the individual colonies have to be followed over time.

I then tested if the combination of CLRC/RNAi protein deletions the parental strains play a role in the rate of heterochromatin re-establishment in the progeny. To do so, I designed new tester strains. Originally I developed *clr4Δ:ura4+-ago1Δ :ura4+*and *rik1Δ:ura4+-dcr1Δ:ura4+* tester strains. I then used the same ura4+-marked individual deletion strains to create *clr4Δ-dcr1Δ* and *ago1Δ-rik1Δ* strains*.* Surprisingly all the colonies were red after crossing the new tester strains and selecting for the presence of the wild-type genes in the progeny (plating the spores on media with FOA). When *dos2+* deletion was included in the cross, all of the F1 colonies turned white, however not many colonies grew on FOA-supplemented media. I could not recover any F1 colonies in both *mkt1Δ* and *tri1Δ* backgrounds. This suggests that combining new tester strains with either *mkt1+, tri1+* or *dos2+* somehow impairs either mating or recombination. In the future it would be interesting to assess the difference in transcriptome and proteome in original and new tester strains to potentially understand the difference between the rate of heterochromatin establishment after the respective crosses, and to understand the lack of F1 colonies growing on 5FOA supplemented media in *mkt1Δ, tri1Δ* or *dos2Δ* background.

In the case of the cross with the original tester strains, despite the fact that the CLRC/RNAi genes that were deleted in the parental strains are present in the F1 progeny, they might not be properly expressed. Previously *clr4+* was shown to have a global regulatory effect on multiple genes across the genome (Hansen et al., 2005). Since our parental strains are double mutants for CLRC and RNAi components, they might similarly have transcription deregulation, thus providing an explanation for the delay in heterochromatin re-establishment in the majority of the F1 colonies. To test this, I assessed the mRNA levels of *dcr1+*, *clr4+*, *ago1+*and *rik1+* genes in both the original and new tester strains by RT-qPCR. However there was no apparent upregulation of the aforementioned genes. Despite this result, we cannot rule out the possibility of transcriptome deregulation since mRNA levels were only assessed for a subset of genes. Other factors, required for immediate heterochromatin establishment, might not be properly expressed in the F1 progeny. Passaging F1 cells several times might lead to the re-establishment of normal gene expression with subsequent heterochromatin formation.

Potential stochasticity of heterochromatin establishment requires thorough quantifications after each independent cross. Namely, the

proportion of red, white and pink F1 colonies has to be recorded. Since control white colonies turn red at slightly different rates, these differences also have to be measured. After following white colonies in *mkt1Δ* and *tri1Δ* backgrounds, the proportion of colonies that turn either red, pink or white also has to be evaluated.

Thus the results of the cross-based assay leave a lot of questions to be answered. Mainly we need to explain the differences between the original tester strains and the new tester strains, and understand patterns of heterochromatin establishment that originate in the cross-based establishment assay described here. Potentially a set of global experiments, such as ChIP-seq, transcriptome and proteome analyses can be performed to investigate the process of heterochromatin establishment.

Chapter 6 — Concluding remarks

Heterochromatin is an important configuration of eukaryotic chromosomes that functionally defines certain genomic regions (Allshire & Madhani, 2018; Grewal & Jia, 2007). The main heterochromatic locations are repetitive DNA sequences like centromeres, transposon-rich regions or telomeres, and heterochromatin formation over these regions is crucial to prevent genome instability. Heterochromatin formation driven by non-coding RNAs has been shown to be a conserved mechanism of gene silencing across multiple eukaryotes (Bernstein & Allis, 2005). One of the model organisms where RNAi-dependent heterochromatin formation has been extensively studied is *S. pombe* (Allshire & Ekwall, 2015). Heterochromatin formation in *S. pombe* is understood fairly well, however there are still some unanswered questions. One such question is how exactly heterochromatin establishment is initiated. Specifically, it is not yet clear in what order the known pathways (RNAi and CLRC-driven histone methylation) act, as well as what additional factors are required specifically for heterochromatin establishment. In this study I aimed to develop a reliable assay to investigate *de novo* heterochromatin formation.

One approach to study heterochromatin establishment (other methods are discussed in the introduction of chapter 3) involves removing pre-existing heterochromatin and then inducing

heterochromatin re-establishment. In *S. pombe* deletion of either RNAi or CLRC components significantly reduces the levels of siRNAs and H3K9 methylation, thus perturbing heterochromatin maintenance (Volpe et al., 2002). However I aimed to develop an assay where components from both pathways are deleted simultaneously to ensure that no residual signal accelerating re-establishment is left.

I developed two assays — plasmid-based and cross-based assays — both of which involved deletion of core RNAi and CLRC components, thus erasing pre-existing heterochromatin. In the plasmid-based assay, the deleted genes were re-introduced on a plasmid (*clr4*Δ *dcr1*$\Delta \rightarrow$ *clr4*$^+$ *dcr1*$^+$). However, as extensively discussed in chapter 4, the plasmid-based assay was initially considered unreliable. First I attributed the lack of reproducibility to *clr4*$^+$ overexpression. Using ChIP sequencing Iglesias et al showed that introducing two copies of the *clr4*$^+$ gene induces sporadic heterochromatin formation in the genome (Iglesias et al., 2018). In the future it would be interesting to investigate if *clr4*$^+$ overexpression from the plasmid causes sporadic heterochromatin formation and then to investigate if it makes *de novo* heterochromatin formation unstable. Moreover in our study not only is the *clr4*$^+$ gene overexpressed, but also *dcr1*$^+$. Thus it would be interesting to investigate the effect of *dcr1*$^+$

overexpression as well. However results obtained in the cross-based assay might suggest that heterochromatin re-establishment is stochastic, which, in turn, can also explain heterogeneity of the plasmid-based assay.

In the cross-based assay the deleted RNAi and CLRC genes were re-introduced via crossing, and, depending on the deletions present in the parental strains, either heterochromatin was fully re-established immediately, or re-establishment occurred over time. It is interesting that in both parental strains tested both CLRC and RNAi pathways are perturbed, however the outcome is different depending on which genes from each pathway are deleted. Therefore the main question that stems from these results is what causes this difference. In the future it would be interesting to construct more strains, where different RNAi/CLRC deletions are combined together. This potentially could pinpoint which deletion combination prevents an immediate heterochromatin formation in the F1. It would also be interesting to assess the difference between the parental strains globally using mass spectrometry or RNA sequencing. The global analysis could potentially detect upregulation or downregulation of factors that are responsible for heterochromatin establishment dynamics. As discussed in chapter 5, thorough quantification and

replication are also essential to evaluate the importance of stochasticity in heterochromatin formation.

Subjecting the sixteen pre-selected candidates to the cross-based establishment assay did not identify any factor that entirely prevented heterochromatin establishment: in all cases the cross progeny exhibited a mix of heterochromatin states as inferred from the colony colour. As described before, red colony colour indicates intact heterochromatin, whereas white colony colour indicates perturbed heterochromatin. Introducing some candidate deletions also resulted in uniformly pink F1 colonies, absent from the control F1 colonies. It can be argued that pink colonies could result from a combination of red and white cells. However pink F1 colonies were absent from the control cross, suggesting that candidate deletions might influence the formation of intermediate heterochromatin states. Thus in the future these pink colonies should be further investigated. Pink colonies might potentially indicate unstable heterochromatin formation, where heterochromatin state can fluctuate between perturbed (white colony colours) and semi-formed (pink) or fully-formed (red). This can be tested by following the colour dynamics of pink colonies over time. The pink colour also might indicate that fully silenced heterochromatin, marked by H3K9me3, cannot form. Instead pink colonies might be indicative of

establishment of only H3K9me2, which is a transcriptionally permissive predecessor of H3K9me3 (Jih et al., 2017). Inserting a GFP tag at the end of the *ade6*$_+$ gene at the pericentromeres can help us to investigate if pink colony colour is indicative of H3K9me2 domain formation, or if it corresponds to the combination of red and white colonies. It can be hypothesised that pink colonies might have an intermediate fluorescence intensity due to transcriptionally permissive H3K9me2 mark compared to the low fluorescence intensity in red colonies (due to the fully silent H3K9me3 domains) and high fluorescence intensity in white colonies (due to the absence of H3K9me2/3). However intermediate fluorescence intensity in pink colonies might also be indicative of combination of white and red cells. To differentiate between these two possibilities, fluorescence can be measured in individual cells from a single pink colony. If fluorescence intensity is low in some cells and high in other, it potentially indicates that cells originate from a mixed population. If, however, fluorescence is uniform in all cells, then it might be concluded that cells are coming from a homogenous population, and pink colony colour is not caused by the mixed population. Alternatively, instead of introducing a wild-type *clr4*$_+$ gene, *clr4* with a F499 to Y substitution (*clr4*$_{F449Y}$) can be introduced (Jih et al., 2017). The *clr4*$_{F449}$ mutant can only drive H3K9me2

formation, thus allowing us to investigate the difference between H3K9 methylation states.

Since Tos4 and Tfb2 were the most promising candidates revealed in the plasmid-based assay, I would be curious to evaluate the effect of Tos4 and Tfb2 deletions on heterochromatin establishment by following individual colonies, derived from the cross-based assay, over time. As mentioned before, both Tos4 and Tfb2 are transcription factors (Horak et al., 2002; Warfield et al., 2016). Tos4 has multiple positive genetic interactions with RNAi genes, consistent with them functioning in the same pathway. The Tos4 protein has a conserved forkhead domain that can bind to two different DNA motifs (Nakagawa et al., 2013). If Tos4 deletion impairs heterochromatin establishment over time, it would be interesting to see if these DNA motifs are present at the centromeres. Previously transcription factors Atf1/Pcr1 were shown to interact with Clr4 and Swi6 and have a specific binding site at the *mat* locus, where they act in parallel with RNAi to nucleate heterochromatin (Jia et al., 2004). Thus it would be interesting to investigate if Tos4, similarly to Atf1/Pcr1, can bind to the motif at the centromeres and help drive heterochromatin re-establishment. Tfb2 is a core subunit of the TFIIH complex, essential for Pol II-mediated transcription (Warfield et al., 2016). In *Drosophila,*

Moonshiner, which is a transcription factor IIA (TFIIA) subunit paralogue, was shown to localize to piRNA clusters by interacting with Rhino (HP1 homologue), where it is required for the Pol II-driven transcription of piRNAs (Andersen et al., 2017). It would be interesting to see if Tfb2 can function similarly, localizing to the centromeric repeats and influencing RNA pol II transcription during heterochromatin establishment.

Following F1 colonies from other candidate deletion backgrounds might still reveal heterochromatin establishment defects at the centromeres similar to *mkt1Δ* and *tri1Δ*. For example, Nrl1 together with splicing machinery was shown to recruit RNAi and induce heterochromatin assembly at sites called *h*eter*o*chr*o*matin *d*omains (HOODs) associated with the sexual differentiation genes and transposons (Lee et al., 2013). Moreover Nrl1 was show to interact with Mtl1, which, in turn, interacts with Mkt1 — an establishment factor identified in our group (Egan et al.,2014; Lee et al., 2013; Bayne lab, unpublished data). Thus it would be interesting to follow the white F1 colonies in *nrl1Δ* background and investigate if Nrl1 and Mkt1 can act together to establish heterochromatin. Sap18 (predicted HDAC complex component) can also have interesting links to heterochromatin establishment. Previously nuclear actin was shown to interact with HDACs in HeLa cells, where monomeric actin

was shown to supress deacetylase activity and polymerised actin was shown to increase HDAC function (Serebryannyy, Cruz, & De Lanerolle, 2016). Since deacetylation was shown to be crucial for centromeric heterochromatin establishment in *S. pombe* (Martienssen & Moazed, 2015), it would be interesting to investigate if Sap18 has any effect on establishment through its potential interaction with actin.

The ultimate goal of this project was to develop an assay that would be applicable for genome-wide screening. The cross-based establishment assay was shown to have the potential to detect factors perturbing heterochromatin establishment (like *tri1*+ and *mkt1*+), however individual colonies have to be followed over time for the effect to be visible. This is problematic, since we aimed to conduct the screen in a high-throughput manner. However it cannot be excluded that in the high-throughput screen, a strong establishment factor would prevent any immediate heterochromatin re-establishment, thus leading to 100% white F1 colonies.

Overall this study has furthered investigation of the process of heterochromatin establishment. The findings pose new questions about heterochromatin establishment dynamics and the role of

additional establishment factors that hopefully can be addressed in the near future.

References

Allfrey, G., Faulkner, R., & Mirsky, A. E. (1964). Acetylation and methylation of hisones and their possible role in the regulation of RNA synethesis, *315*(1938), 786–794.

Allis, C. D., & Jenuwein, T. (2016). The molecular hallmarks of epigenetic control. *Nature Reviews Genetics*, *17*(8), 487–500. https://doi.org/10.1038/nrg.2016.59

Allshire, R., & Ekwall, K. (2015). Epigenetics regulation of chromatin states in Schizosaccharomyces pombe. *Cold Spring Harb Perspectives in Biology*, *7*, 1–25. https://doi.org/10.1101/cshperspect.a018770

Allshire, R C, Nimmo, E. R., Ekwall, K., & Cranston., G. (1995). Mutations derepressing silent domains within fission yeast centromeres disrupt chromosome segregation. *Genes Dev.*, *9*, 218–233. https://doi.org/10.1101/gad.9.2.218

Allshire, Robin C., Javerzat, J. P., Redhead, N. J., & Cranston, G. (1994). Position effect variegation at fission yeast centromeres. *Cell*, *76*(1), 157–169. https://doi.org/10.1016/0092-8674(94)90180-5

Allshire, Robin C., & Madhani, H. D. (2018). Ten principles of heterochromatin formation and function. *Nature Reviews Molecular Cell Biology*, *19*(4), 229–244. https://doi.org/10.1038/nrm.2017.119

Amor, D. J., Kalitsis, P., Sumer, H., & Choo, K. H. A. (2004). Building the centromere: From foundation proteins to 3D organization. *Trends in Cell Biology*, *14*(7), 359–368. https://doi.org/10.1016/j.tcb.2004.05.009

Andersen, P. R., Tirian, L., Vunjak, M., & Brennecke, J. (2017). A heterochromatin-dependent transcription machinery drives piRNA expression. *Nature*, *549*(7670), 54–59. https://doi.org/10.1038/nature23482

Bannister, A. J., & Kouzarides, T. (2011). Regulation of chromatin by histone modifications. *Cell Research*, *21*(3), 381–395. https://doi.org/10.1038/cr.2011.22

Bartel, D. (2004). MicroRNAs：Genomics, Biogenesis, Mechanism, and

Function.pdf. *Cell*, *116*(2), 281–297. Retrieved from http://www.ncbi.nlm.nih.gov/pubmed/14744438

Bayne, E H, Bijos, D. A., White, S. A., de Lima Alves, F., Rappsilber, J., & Allshire, R. C. (2014). A systematic genetic screen identifies new factors influencing centromeric heterochromatin integrity in fission yeast. *Genome Biol*, *15*(10). https://doi.org/10.1186/s13059-014-0481-4

Bayne, Elizabeth H., White, S. A., Kagansky, A., Bijos, D. A., Sanchez-Pulido, L., Hoe, K. L., … Allshire, R. C. (2010). Stc1: A Critical Link between RNAi and Chromatin Modification Required for Heterochromatin Integrity. *Cell*, *140*, 666–677. https://doi.org/10.1016/j.cell.2010.01.038

Beach, D. H., & Klar, A. J. (1984). Rearrangements of the transposable mating-type cassettes of fission yeast. *The EMBO Journal*, *3*(3), 603–610. https://doi.org/10.1002/j.1460-2075.1984.tb01855.x

Bernstein, E, Caudy, A., Hammond, S. M., & Hannon, G. J. (2001). Role for a bidentate ribonuclease in the initiation step of RNA interference. *Nature*, *409*(6818), 363–366. https://doi.org/10.1038/35053110

Bernstein, Emily, & Allis, C. D. (2005). RNA meets chromatin review.pdf. *Genes & Development*, (212), 1635–1655. https://doi.org/10.1101/gad.1324305.GENES

Bird, A. (2007). Perceptions of epigenetics. *Nature*, *447*(7143), 396–398. https://doi.org/10.1038/nature05913

Borges, F., & Martienssen, R. (2015). The expanding world of small RNAs in plants. *Physiology & Behavior*, *16*(12), 727–741. https://doi.org/10.1016/j.physbeh.2017.03.040

Braun, S., Garcia, J. F., Rowley, M., Rougemaille, M., Shankar, S., & Madhani, H. (2011). The Cul4-Ddb1Cdt2 Ubiquitin Ligase Inhibits Invasion of a Boundary-Associated Antisilencing Factor into Heterochromatin. *Cell*, *144*(1), 41–54. https://doi.org/10.1038/jid.2014.371

Brennecke, J., Aravin, A. A., Stark, A., Dus, M., Kellis, M., Sachidanandam, R., & Hannon, G. J. (2007). Discrete Small RNA-

Generating Loci as Master Regulators of Transposon Activity in Drosophila. *Cell*, *128*(6), 1089–1103. https://doi.org/10.1016/j.cell.2007.01.043

Brower-Toland, B., Findley, S. D., Jiang, L., Liu, L., Yin, H., Dus, M., … Lin, H. (2007). Drosophila PIWI associates with chromatin and interacts directly with HP1a. *Genes and Development*, *21*(18), 2300–2311. https://doi.org/10.1101/gad.1564307

Bühler, M., Haas, W., Gygi, S. P., & Moazed, D. (2007). RNAi-Dependent and -Independent RNA Turnover Mechanisms Contribute to Heterochromatic Gene Silencing. *Cell*, *129*(4), 707–721. https://doi.org/10.1016/j.cell.2007.03.038

Bühler, M., Verdel, A., & Moazed, D. (2006). Tethering RITS to a Nascent Transcript Initiates RNAi- and Heterochromatin-Dependent Gene Silencing. *Cell*, *125*(5), 873–886. https://doi.org/10.1016/j.cell.2006.04.025

Buker, S. M., Iida, T., Bühler, M., Villén, J., Gygi, S. P., Nakayama, J.-I., & Moazed, D. (2007). Two different Argonaute complexes are required for siRNA generation and heterochromatin assembly in fission yeast. *Nature Structural & Molecular Biology*, *14*(3), 200–207. https://doi.org/10.1038/nsmb1211

Burkhart, K. B., Guang, S., Buckley, B. A., Wong, L., Bochner, A. F., & Kennedy, S. (2011). A pre-mrna-associating factor links endogenous sirnas to chromatin regulation. *PLoS Genetics*, *7*(8). https://doi.org/10.1371/journal.pgen.1002249

Buscaino, A., Lejeune, E., Audergon, P., Hamilton, G., Pidoux, A., & Allshire, R. C. (2013). Distinct roles for Sir2 and RNAi in centromeric heterochromatin nucleation, spreading and maintenance. *EMBO Journal*, *32*(9), 1250–1264. https://doi.org/10.1038/emboj.2013.72

Bustard, D. E., Ball, L. G., & Cobb, J. A. (2016). Non-Smc element 5 (Nse5) of the Smc5/6 complex interacts with SUMO pathway components. *Biology Open*, *5*(6), 777–785. https://doi.org/10.1242/bio.018440

Byvoet, P., Shepherd, G. R., Hardin, J. M., & Noland, B. J. (1972). The

distrubution and Turnover of Labeled Methyl Groups in Histone Fractions of CUlturesMammalian Cells, (13), 558–567.

Cam, H. P., Sugiyama, T., Chen, E. S., Chen, X., FitzGerald, P. C., & Grewal, S. I. S. (2005). Comprehensive analysis of heterochromatin- and RNAi-mediated epigenetic control of the fission yeast genome. *Nature Genetics*, *37*(8), 809–819. https://doi.org/10.1038/ng1602

Cao, R., Wang, L., Wang, H., Xia, L., Erdjument-Bromage, H., Tempst, P., … Zhang, Y. (2002). Role of histone H3 lysine 27 methylation in polycomb-group silencing. *Science*, *298*(5595), 1039–1043. https://doi.org/10.1126/science.1076997

Castel, S. E., & Martienssen, R. (2013). RNA interference (RNAi) in the Nucleus: roles for small RNA in transcription, epigenetics and beyon. *Nature Reviews Genetics*, *14*(2), 100–112. https://doi.org/10.1038/jid.2014.371

Chaudhuri, B., Ingavale, S., & Bachhawat, A. K. (1997). apd1+, a gene required for red pigment formation in ade6 mutants of Schizosaccharomyces pombe, encodes an enzyme required for glutathione biosynthesis: A role for glutathione and a glutathione-conjugate pump. *Genetics*, *145*(1), 75–83.

Chen, E. S., Zhang, K., Nicolas, E., Cam, H. P., Zofall, M., & Grewal, S. I. S. (2008). Cell cycle control of centromeric repeat transcription and heterochromatin assembly. *Nature*, *451*(7179), 734–737. https://doi.org/10.1038/nature06561

Creyghton, M. P., Cheng, A. W., Welstead, G. G., Kooistra, T., Carey, B. W., Steine, E. J., … Jaenisch, R. (2010). Histone H3K27ac separates active from poised enhancers and predicts developmental state. *Proceedings of the National Academy of Sciences of the United States of America*, *107*(50), 21931–21936. https://doi.org/10.1073/pnas.1016071107

Dehé, P. M., & Cooper, J. P. (2010). Fission yeast telomeres forecast the end of the crisis. *FEBS Letters*, *584*(17), 3725–3733. https://doi.org/10.1016/j.febslet.2010.07.045

Dehennaut, V., Leprince, D., & Lefebvre, T. (2014). O-GlcNAcylation, an

epigenetic mark. Focus on the histone code, TET family proteins, and polycomb group proteins. *Frontiers in Endocrinology*, *5*(SEP), 1–7. https://doi.org/10.3389/fendo.2014.00155

Dhalluin, C., Carlson, J. E., Zeng, L., He, C., Aggarwal, A. K., & Zhou, M. M. (1999). Structure and ligand of a histone acetyltransferase bromodomain. *Nature*, *399*(6735), 491–496. https://doi.org/10.1038/20974

Djupedal, I., Kos-Braun, I. C., Mosher, R. A., Söderholm, N., Simmer, F., Hardcastle, T. J., … Ekwall, K. (2009). Analysis of small RNA in fission yeast; centromeric siRNAs are potentially generated through a structured RNA. *The EMBO Journal*, *28*(24), 3832–3844. https://doi.org/10.1038/emboj.2009.351

Djupedal, I., Portoso, M., Spåhr, H., Bonilla, C., Gustafsson, C. M., Allshire, R. C., & Ekwall, K. (2005). RNA Pol II subunit Rpb7 promotes centromeric transcription and RNAi-directed chromatin silencing. *Genes and Development*, *19*(19), 2301–2306. https://doi.org/10.1101/gad.344205

Egan, E. D., Braun, C. R., Gygi, S. P., & Moazed, D. (2014). Post-transcriptional regulation of meiotic genes by a nuclear RNA silencing complex. *Rna*, *20*(6), 867–881. https://doi.org/10.1261/rna.044479.114

Ekwall, K, Nimmo, E. R., Javerzat, J. P., Borgstrøm, B., Egel, R., Cranston, G., & Allshire, R. (1996). Mutations in the fission yeast silencing factors clr4+ and rik1+ disrupt the localisation of the chromo domain protein Swi6p and impair centromere function. *Journal of Cell Science*, *109*, 2637–2648.

Ekwall, Karl, Olsson, T., Turner, B. M., Cranston, G., & Allshire, R. C. (1997). Transient inhibition of histone deacetylation alters the structural and functional imprint at fission yeast centromeres. *Cell*, *91*(7), 1021–1032. https://doi.org/10.1016/S0092-8674(00)80492-4

Elgin, S. C. R., & Reuter, G. (2013). Position-effect variegation, heterochromatin formation, and gene silencing in Drosophila. *Cold*

Spring Harbor Perspectives in Biology, *5*(8), 1–26. https://doi.org/10.1101/cshperspect.a017780

Elowitz, M. B., Levine, A. J., Siggia, E. D., & Swain, P. S. (2002). Stochastic gene expression in a single cell. *Science*, *297*(5584), 1183–1186. https://doi.org/10.1126/science.1070919

Fagegaltier, D., Bougé, A.-L., Berry, B., Poisot, E., Sismeiro, O., Coppée, J.-Y., … Antoniewski, C. (2009). The endogenous siRNA pathway is involved in heterochromatin formation in Drosophila. *Proceedings of the National Academy of Sciences of the United States of America*, *106*(50), 21258–21263. https://doi.org/10.1073/pnas.0809208105

Fairhead, C., Llorente, B., Denis, F., Soler, M., & Dujon, B. (1996). New vectors for combinatorial deletions in yeast chromosomes and for gap-repair cloning using "split-marker" recombination. *Yeast*, *12*(14), 1439–1457. https://doi.org/10.1002/(SICI)1097-0061(199611)12:14<1439::AID-YEA37>3.0.CO;2-O

Felsenfeld, G., & Groudine, M. (2003). Controling the double helix. *Nature*, *421*(6921), 444–448. https://doi.org/10.1038/nature01410

Feng, Q., Wang, H., Ng, H. H., Erdjument-bromage, H., Tempst, P., Struhl, K., … Carolina, N. (2002). Methylation of H3-Lysine 79 Is Mediated by a New Family of HMTases without a SET Domain University of North Carolina at Chapel Hill. *Current Opinion in Cell Biology*, *12*(12), 1052–1058.

Fire, A., Xu, S., Montgomery, M., Kostas, S., Driver, S., & Mello, C. (1998). Potent and specific genetic interference by double-stranded RNA in Caenorhabditiselegans. *Nature*, *391*, 806–811.

Fischle, W., Boo, S. T., Dormann, H. L., Ueberheide, B. M., Garcia, B. A., Shabanowitz, J., … Allis, C. D. (2005). Regulation of HP1-chromatin binding by histone H3 methylation and phosphorylation. *Nature*, *438*(7071), 1116–1122. https://doi.org/10.1038/nature04219

Forsburg, S. L., & Rhind, N. (2006). Basic methods for fission yeast. *Yeast (Chichester, England)*, *23*(3), 173–183. https://doi.org/10.1002/yea.1347

Foster, E. R., & Downs, J. A. (2005). Histone H2A phosphorylation in DNA

double-strand break repair. *FEBS Journal*, *272*(13), 3231–3240. https://doi.org/10.1111/j.1742-4658.2005.04741.x

Garcia, J. F., Dumesic, P. A., Hartley, P. D., El-samad, H., & Madhani, H. D. (2010). for Heterochromatic Silencing Factors in the Elimination of Nucleosome-Free Regions. *Genes & Development*, 1758–1771. https://doi.org/10.1101/gad.1946410.derstood.

Ghildiyal, M., & Zamore, P. (2009). Small silencing RNAs: an expanding universe. *Nature Reviews Genetics*, *10*(2), 94–108. https://doi.org/10.1038/nrg2504.Small

Gietz, R. D., & Schiestl, R. H. (2007). Microtiter plate transformation using the LiAc/SS carrier DNA/PEG method. *Nature Protocols*, *2*(1), 5–8. https://doi.org/10.1038/nprot.2007.16

Gill, G. (2004). SUMO and ubiquitin in the nucleus: Different functions, similar mechanisms? *Genes and Development*, *18*(17), 2046–2059. https://doi.org/10.1101/gad.1214604

Greer, E., & Shi, Y. (2014). Histone methylation: a dynamic mark in health, disease and inheritance. *Nature Reviews Genetics*, *13*(5), 343–357. https://doi.org/10.1038/nrg3173.Histone

Grewal, S. I. S. (2000). Transcriptional silencing in fission yeast. *Journal of Cellular Physiology*, *184*(3), 311–318. https://doi.org/10.1002/1097-4652(200009)184:3<311::AID-JCP4>3.0.CO;2-D

Grewal, S. I. S., & Jia, S. (2007). Heterochromatin revisited. *Nature Reviews. Genetics*, *8*(1), 35–46. https://doi.org/10.1038/nrg2008

Grewal, S. I. S., & Klar, A. J. S. (1997). A recombinationally repressed region between mat2 and mat3 loci shares homology to centromeric repeats and regulates directionality of mating-type switching in fission yeast. *Genetics*, *146*(4), 1221–1238.

Haldar, S., Saini, A., Nanda, J. S., Saini, S., & Singh, J. (2011). Role of Swi6/HP1 self-association-mediated recruitment of Clr4/Suv39 in establishment and maintenance of heterochromatin in fission yeast. *Journal of Biological Chemistry*, *286*(11), 9308–9320. https://doi.org/10.1074/jbc.M110.143198

Halic, M., & Moazed, D. (2010). Dicer-Independent Primal RNAs Trigger RNAi and Heterochromatin Formation. *Cell*. https://doi.org/10.1016/j.cell.2010.01.019

Hall, I. M., Noma, K. -i., & Grewal, S. I. S. (2003). RNA interference machinery regulates chromosome dynamics during mitosis and meiosis in fission yeast. *Proceedings of the National Academy of Sciences*, *100*(1), 193–198. https://doi.org/10.1073/pnas.232688099

Hamilton, A., & Baulcombe, D. C. (1999). A species of small antisense RNA in posttranscriptional gene silencing in plants. *Science*, *286*(5441), 950–952.

Hansen, K. R., Burns, G., Mata, J., Volpe, T. A., Martienssen, R. A., Bahler, J., & Thon, G. (2005). Global Effects on Gene Expression in Fission Yeast by Silencing and RNA Interference Machineries. *Molecular and Cellular Biology*, *25*(2), 590–601. https://doi.org/10.1128/mcb.25.2.590-601.2005

Hansen, Klavs R., Ibarra, P. T., & Thon, G. (2006). Evolutionary-conserved telomere-linked helicase genes of fission yeast are repressed by silencing factors, RNAi components and the telomere-binding protein Taz1. *Nucleic Acids Research*, *34*(1), 78–88. https://doi.org/10.1093/nar/gkj415

Henikoff, S., & Smith, M. M. (2015). Histone variants and epigenetics. *Cold Spring Harbor Perspectives in Biology*, *7*(1), 1–25. https://doi.org/10.1101/cshperspect.a019364

Hirota, T., Lipp, J. J., Toh, B. H., & Peters, J. M. (2005). Histone H3 serine 10 phosphorylation by Aurora B causes HP1 dissociation from heterochromatin. *Nature*, *438*(7071), 1176–1180. https://doi.org/10.1038/nature04254

Hoffman, C. S., Wood, V., & Fantes, P. A. (2015). An ancient yeast for young geneticists: A primer on the Schizosaccharomyces pombe model system. *Genetics*, *201*(2), 403–423. https://doi.org/10.1534/genetics.115.181503

Hong, E. J. E., Villén, J., Gerace, E. L., Gygi, S. P., & Moazed, D. (2005).

A cullin E3 ubiquitin ligase complex associates with Rik1 and the Clr4 histone H3-K9 methyltransferase and is required for RNAi-mediated heterochromatin formation. *RNA Biology*, *2*(3), 106–111. https://doi.org/10.4161/rna.2.3.2131

Horak, C. E., Luscombe, N. M., Qian, J., Bertone, P., Piccirrillo, S., Gerstein, M., & Snyder, M. (2002). Complex transcriptional circuitry at the G1/S transition in. *Genes & Development*, 3017–3033. https://doi.org/10.1101/gad.1039602.elucidating

Horn, P. J., Bastie, J., & Peterson, C. L. (2005). E3 ubiquitin ligase is essential for heterochromatin formation. *Genes & Development*, 1705–1714. https://doi.org/10.1101/gad.1328005.(HMT)

Houseley, J., LaCava, J., & Tollervey, D. (2006). RNA-quality control by the exosome. *Nature Reviews* , *7*, 529–539.

Iglesias, N., Currie, M. A., Jih, G., Paulo, J. A., Siuti, N., Kalocsay, M., … Moazed, D. (2018). Automethylation-induced conformational switch in Clr4 (Suv39h) maintains epigenetic stability. *Nature*, *4*(July). https://doi.org/10.1038/s41586-018-0398-2

Ishizu, H., Kinoshita, T., Hirakata, S., Komatsuzaki, C., & Siomi, M. C. (2019). Distinct and Collaborative Functions of Yb and Armitage in Transposon-Targeting piRNA Biogenesis. *Cell Reports*, *27*(6), 1822-1835.e8. https://doi.org/10.1016/j.celrep.2019.04.029

Ivanova, A. V., Bonaduce, M. J., Ivanov, S. V., & Klar, A. J. S. (1998). The chromo and SET domains of the Clr4 protein are essential for silencing in fission yeast. *Nature Genetics*, *19*(2), 192–195. https://doi.org/10.1038/566

Izumi, N., Shoji, K., Sakaguchi, Y., Honda, S., Kirini, Y., Suzuki, T., … Tomari, Y. (2016). Identification and functional analysis of the pre-piRNA 3′ Trimmer in silkworms. *Cell*, *164*(5), 962–973. https://doi.org/10.1016/j.physbeh.2017.03.040

Jacobson, R. H., Ladurner, A. G., King, D. S., & Tjian, R. (2000). Structure and function of a human TAF(II)250 double bromodomain module. *Science*, *288*(5470), 1422–1425. https://doi.org/10.1126/science.288.5470.1422

Jenuwein, T., & Allis, C. D. (2001). Translating the histone code. *Science (New York, N.Y.)*. https://doi.org/10.1126/science.1063127

Jia, S., Kobayashi, R., & Grewal, S. I. S. (2005). Ubiquitin ligase component Cul4 associates with Clr4 histone methyltransferase to assemble heterochromatin. *Nature Cell Biology*, *7*(10), 1007–1013. https://doi.org/10.1038/ncb1300

Jia, S., Noma, K. I., & Grewal, S. I. S. (2004). RNAi-independent heterochromatin nucleation by the stress-activated ATF/CREB family proteins. *Science*, *304*(5679), 1971–1976. https://doi.org/10.1126/science.1099035

Jih, G., Iglesias, N., Currie, M. A., Bhanu, N. V., Paulo, J. A., Gygi, S. P., … Moazed, D. (2017). Unique roles for histone H3K9me states in RNAi and heritable silencing of transcription. *Nature*, 1–26. https://doi.org/10.1038/nature23267

Jih, G., Iglesias, N., Currie, M. A., Natarajan, B., Paulo, J. A., Gygi, S., … Moazed, D. (2017). Unique roles for histone H3K9me states in RNAi and heritable silencing of transcription. *Nature Publishing Group*, *547*(7664), 463–467. https://doi.org/10.1038/nature23267

Jones, P. A., & Liang, G. (2009). Rethinking how DNA methylation patterns are maintained. *Nature Reviews Genetics*, *10*(11), 805–811. https://doi.org/10.1038/nrg2651

Kawai, S., Hashimoto, W., & Murata, K. (2010). Transformation of Saccharomyces cerevisiae and other fungi: methods and possible underlying mechanism. *Bioengineered Bugs*, *1*(6), 395–403. https://doi.org/10.4161/bbug.1.6.13257

Kawaoka, S., Izumi, N., Katsuma, S., & Tomari, Y. (2011). 3′ End Formation of PIWI-Interacting RNAs In Vitro. *Molecular Cell*, *43*(6), 1015–1022. https://doi.org/10.1016/j.molcel.2011.07.029

Keller, C., Woolcock, K., Hess, D., & Bühler, M. (2010). Proteomic and functional analysis of the noncanonical poly(A) polymerase Cid14. *Rna*, *16*(6), 1124–1129. https://doi.org/10.1261/rna.2053710

Keohane, A. M., O'Neill, L. P., Belyaev, N. D., Lavender, J. S., & Turner, B. M. (1996). X-inactivation and histone H4 acetylation in embryonic

stem cells. *Developmental Biology*, *180*(2), 618–630. https://doi.org/10.1006/dbio.1996.0333

Ketting, R. F., Fischer, S. E. J., Bernstein, E., Sijen, T., Hannon, G. J., & Plasterk, R. H. A. (2001). Dicer functions in RNA interference and in synthesis of small RNA involved in developmental timing in C. elegans. *Genes and Development*, *15*(20), 2654–2659. https://doi.org/10.1101/gad.927801

Kim, D. H., Villeneuve, L. M., Morris, K. V., & Rossi, J. J. (2006). Argonaute-1 directs siRNA-mediated transcriptional gene silencing in human cells. *Nature Structural and Molecular Biology*, *13*(9), 793–797. https://doi.org/10.1038/nsmb1142

Klattenhoff, C., Xi, H., Li, C., Lee, S., Xu, J., Khurana, J. S., … Theurkauf, W. E. (2009). The Drosophila HP1 Homolog Rhino Is Required for Transposon Silencing and piRNA Production by Dual-Strand Clusters. *Cell*, *138*(6), 1137–1149. https://doi.org/10.1016/j.cell.2009.07.014

Kloc, A., Zaratiegui, M., Nora, E., & Martienssen, R. (2008). RNA interference guides histone modification during the S phase of chromosomal replication Anna. *Current Biology*, *18*(7), 490–495. https://doi.org/10.1038/jid.2014.371

Kniola, B., Mellone, B., O'Toole, E., McIntosh, J. R., Ekwall, K., Hultenby, K., … Mengarelli, S. (2001). The domain structure of centromeres is conserved from fission yeast to humans. *Molecular Biology of the Cell*, *12*(9), 2767–2775. Retrieved from http://www.ncbi.nlm.nih.gov/pubmed/11553715%5Cnhttp://www.ncbi.nlm.nih.gov/pubmed/11553715?dopt=AbstractPlus%5Cnhttp://www.pubmedcentral.nih.gov/picrender.fcgi?artid=59711&blobtype=pdf

Kouzarides, T. (2007). Chromatin Modifications and Their Function. *Cell*, *128*(4), 693–705. https://doi.org/10.1016/j.cell.2007.02.005

Kuscu, C., Zaratiegui, M., Kim, H. S., Wah, D. A., Martienssen, R. A., Schalch, T., & Joshua-Tor, L. (2014). CRL4-like Clr4 complex in Schizosaccharomyces pombe depends on an exposed surface of Dos1 for heterochromatin silencing. *Proceedings of the National Academy*

of Sciences of the United States of America, *111*(5), 1795–1800. https://doi.org/10.1073/pnas.1313096111

Lachner, M., O'Carroll, D., Rea, S., Mechtler, K., & Jenuwein, T. (2001). Methylation of histone H3 lysine 9 creates a binding site for HP1 proteins. *Nature*, *410*(6824), 116–120. https://doi.org/10.1038/35065132

Lakens, D. (2013). Calculating and reporting effect sizes to facilitate cumulative science: a practical primer for t-tests and ANOVAs. *Frontiers in Psychology*, *4*(November), 1–12. https://doi.org/10.3389/fpsyg.2013.00863

Lee, D. K. (2016). Alternatives to P value: Confidence interval and effect size. *Korean Journal of Anesthesiology*, *69*(6), 555–562. https://doi.org/10.4097/kjae.2016.69.6.555

Lee, N. N., Chalamcharla, V. R., Reyes-Turcu, F., Mehta, S., Zofall, M., Balachandran, V., … Grewal, S. I. S. (2013). Mtr4-like protein coordinates nuclear RNA processing for heterochromatin assembly and for telomere maintenance. *Cell*, *155*(5), 1061. https://doi.org/10.1016/j.cell.2013.10.027

Lee, Y., Ahn, C., Han, J., Choi, H., Kim, J., Yim, J., … Kim, V. N. (2003). The nuclear RNase III Drosha initiates microRNA processing. *Nature*, *425*(September), 415–418.

Lee, Y., Kim, M., Han, J., Yeom, K. H., Lee, S., Baek, S. H., & Kim, V. N. (2004). MicroRNA genes are transcribed by RNA polymerase II. *EMBO Journal*, *23*(20), 4051–4060. https://doi.org/10.1038/sj.emboj.7600385

Lock, A., Rutherford, K., Harris, M. A., Hayles, J., Oliver, S. G., Bähler, J., & Wood, V. (2019). PomBase 2018: User-driven reimplementation of the fission yeast database provides rapid and intuitive access to diverse, interconnected information. *Nucleic Acids Research*, *47*(D1), D821–D827. https://doi.org/10.1093/nar/gky961

Lorenz, A. (2015). New cassettes for single-step drug resistance and prototrophic marker switching in fi ssion yeast. *Yeast*, *32*, 703–710. https://doi.org/10.1002/yea

Luger, K., Mäder, A. W., Richmond, R. K., Sargent, D. F., & Richmond, T. J. (1997). Crystal structure of the nucleosome core particle at 2.8 Å resolution. *Nature*, *389*(6648), 251–260. https://doi.org/10.1038/38444

Luk, E., Ranjan, A., FitzGerald, P. C., Mizuguchi, G., Huang, Y., Wei, D., & Wu, C. (2010). Stepwise histone replacement by SWR1 requires dual activation with histone H2A.Z and canonical nucleosome. *Cell*, *143*(5), 725–736. https://doi.org/10.1016/j.cell.2010.10.019

Lund, E., Guttinger, S., Calado, An., Dahlberg, J., & Kutay, U. (2004). Nuclear Export of MicroRNA Precursors. *Science*, *303*, 95–98. https://doi.org/10.1016/j.biolcel.2004.04.014

Luteijn, M. J., & Ketting, R. F. (2013). PIWI-interacting RNAs: From generation to transgenerational epigenetics. *Nature Reviews Genetics*, *14*(8), 523–534. https://doi.org/10.1038/nrg3495

Ma, M. K. W., Heath, C., Hair, A., & West, A. G. (2011). Histone crosstalk directed by H2B ubiquitination is required for chromatin boundary integrity. *PLoS Genetics*, *7*(7). https://doi.org/10.1371/journal.pgen.1002175

Marasovic, M., Zocco, M., & Halic, M. (2013). Argonaute and triman generate dicer-independent prirnas and mature siRNAs to initiate heterochromatin formation. *Molecular Cell*, *52*(173–183). https://doi.org/10.1016/j.molcel.2013.08.046

Martienssen, R., & Moazed, D. (2015). RNAi and Heterochromatin Assembly. *Cold Spring Harbor Perspectives in Biology*, *7*(8), a019323. https://doi.org/10.1101/cshperspect.a019323

McHugh, C. A., Chen, C. K., Chow, A., Surka, C. F., Tran, C., McDonel, P., … Guttman, M. (2015). The Xist lncRNA interacts directly with SHARP to silence transcription through HDAC3. *Nature*, *521*(7551), 232–236. https://doi.org/10.1038/nature14443

McKittrick, E., Gafken, P. R., Ahmad, K., & Henikoff, S. (2004). Histone H3.3 is enriched in covalent modifications associated with active chromatin. *Proceedings of the National Academy of Sciences of the United States of America*, *101*(6), 1525–1530.

https://doi.org/10.1073/pnas.0308092100

Motamedi, M. R., Hong, E. E., Li, X., Gerber, S., Gygi, S., & Moazed, D. (2008). HP1 Proteins Form Distinct Complexes and Mediate Heterochromatic Gene Silencing by Non-Overlapping Mechanisms. *Molecular Cell*, *32*(6), 778–790.

Motamedi, M. R., Verdel, A., Colmenares, S. U., Gerber, S. A., Gygi, S. P., & Moazed, D. (2004). Two RNAi complexes, RITS and RDRC, physically interact and localize to noncoding centromeric RNAs. *Cell*, *119*(6), 789–802. https://doi.org/10.1016/j.cell.2004.11.034

Muller, H. J. (1930). Types of visible variations induced by X-rays in Drosophila. *Journal of Genetics*, *22*(3), 299–334. https://doi.org/10.1007/BF02984195

Musselman, C., Avvakumov, N., Watanabe, R., Abraham, C., Lalonde, M.-E., Hong, Z., … Kutateladze, T. (2012). Molecular basis for H3K36me3 recognition by the Tudor domain of PHF1. *Nature Structural & Molecular Biology*, *19*(12), 1266–1272. https://doi.org/10.1038/nsmb.2435

Musselman, C., Lalonde, M.-E., Cote, J., & Kutateladze, T. (2012). Perceiving the epigenetic landscape through histone readers. *Nature Structural and Molecular Biology*, *19*(12), 1218–1227. https://doi.org/10.1038/jid.2014.371

Nakagawa, S., Gisselbrecht, S. S., Rogers, J. M., Hartl, D. L., & Bulyk, M. L. (2013). DNA-binding specificity changes in the evolution of forkhead transcription factors. *Proceedings of the National Academy of Sciences of the United States of America*, *110*(30), 12349–12354. https://doi.org/10.1073/pnas.1310430110

Nakagawachi, T., Soejima, H., Urano, T., Zhao, W., Higashimoto, K., Satoh, Y., … Mukai, T. (2003). Silencing effect of CpG island hypermethylation and histone modifications on O6-methylguanine-DNA methyltransferase (MGMT) gene expression in human cancer. *Oncogene*, *22*(55), 8835–8844. https://doi.org/10.1038/sj.onc.1207183

Nakayama, J. -i., Rice, J. C., Strahl, B. D., Allis, C. D., & Grewal, S. I. S.

(2001). Role of Histone H3 Lysine 9 Methylation in Epigenetic Control of Heterochromatin Assembly. *Science*, *292*(5514), 110–113. https://doi.org/10.1126/science.1060118

Narlikar, G. J., Sundaramoorthy, R., & Owen-Hughes, T. (2013). Mechanisms and functions of ATP-dependent chromatin-remodeling enzymes. *Cell*, *154*(3), 490–503. https://doi.org/10.1016/j.cell.2013.07.011

Nishimasu, H., Ishizu, H., Saito, K., Fukuhara, S., Kamatani, M. K., Bonnefond, L., … Nureki, O. (2012). Structure and function of Zucchini endoribonuclease in piRNA biogenesis. *Nature*, *491*(7423), 284–287. https://doi.org/10.1038/nature11509

Noma, K. I., Sugiyama, T., Cam, H., Verdel, A., Zofall, M., Jia, S., … Grewal, S. I. S. (2004). RITS acts in cis to promote RNA interference-mediated transcriptional and post-transcriptional silencing. *Nature Genetics*, *36*(11), 1174–1180. https://doi.org/10.1038/ng1452

Noma, K. ichi, Cam, H. P., Maraia, R. J., & Grewal, S. I. S. (2006). A Role for TFIIIC Transcription Factor Complex in Genome Organization. *Cell*, *125*(5), 859–872. https://doi.org/10.1016/j.cell.2006.04.028

O'Brien, J., Hayder, H., Zayed, Y., & Peng, C. (2018). Overview of microRNA biogenesis, mechanisms of actions, and circulation. *Frontiers in Endocrinology*, *9*(AUG), 1–12. https://doi.org/10.3389/fendo.2018.00402

Olivieri, D., Sykora, M. M., Sachidanandam, R., Mechtler, K., & Brennecke, J. (2010). An in vivo RNAi assay identifies major genetic and cellular requirements for primary piRNA biogenesis in Drosophila. *EMBO Journal*, *29*(19), 3301–3317. https://doi.org/10.1038/emboj.2010.212

Palazzo, L., Mikolčević, P., Mikoč, A., & Ahel, I. (2019). ADP-ribosylation signalling and human disease. *Open Biology*, *9*(4). https://doi.org/10.1098/rsob.190041

Palmer, D. K., O'Day, K., Trong, H. L. E., Charbonneau, H., & Margolis, R. L. (1991). Purification of the centromere-specific protein CENP-A and

demonstration that it is a distinctive histone. *Proceedings of the National Academy of Sciences of the United States of America*, *88*(9), 3734–3738. https://doi.org/10.1073/pnas.88.9.3734

Pandey, R. R., Homolka, D., Chen, K. M., Sachidanandam, R., Fauvarque, M. O., & Pillai, R. S. (2017). Recruitment of Armitage and Yb to a transcript triggers its phased processing into primary piRNAs in Drosophila ovaries. *PLoS Genetics*, *13*(8), 1–20. https://doi.org/10.1371/journal.pgen.1006956

Parthun, M. R. (2007). Hat1: The emerging cellular roles of a type B histone acetyltransferase. *Oncogene*, *26*(37), 5319–5328. https://doi.org/10.1038/sj.onc.1210602

Pebernard, S., Wohlschlegel, J., McDonald, W. H., Yates, J. R., & Boddy, M. N. (2006). The Nse5-Nse6 Dimer Mediates DNA Repair Roles of the Smc5-Smc6 Complex. *Molecular and Cellular Biology*, *26*(8), 3336–3336. https://doi.org/10.1128/mcb.26.8.3336.2006

Pidoux, A., & Allshire, R. (2004). Kinetochore and heterochromatin domains of the fission yeast centromere. *Chromosome Research*, *12*(6), 521–534. https://doi.org/10.1023/B:CHRO.0000036586.81775.8b

Pidoux, A. L., & Allshire, R. C. (2005). The role of heterochromatin in centromere function. *Philos Trans R Soc Lond B Biol Sci*, *360*(1455), 569–579. https://doi.org/10.1098/rstb.2004.1611

Pikaard, C. S., & Scheid, O. M. (2014). Epigenetic regulation in plants. *Cold Spring Harbor Perspectives in Biology*. https://doi.org/10.1101/cshperspect.a019315

Pombo, A., & Dillon, N. (2015). Three-dimensional genome architecture: players and mechanisms. *Nature Reviews. Molecular Cell Biology*, *16*(4), 245–257. https://doi.org/10.1038/nrm3965

Ptashne, M. (2013). Epigenetics: Core misconcept. *Proceedings of the National Academy of Sciences of the United States of America*, *110*(18), 7101–7103. https://doi.org/10.1073/pnas.1305399110

Rea, S., Eisenhaber, F., O'Carroll, D., Strahl, B. D., Sun, Z. W., Schmid, M., … Jenuwein, T. (2000). Regulation of chromatin structure by site-

specific histone H3 methyltransferases. *Nature*, *406*(6796), 593–599. https://doi.org/10.1038/35020506

Rocha, A. J., Miranda, R. de S., Sousa, A. J. S., & Coelho da Silva, A. L. (2016). Guidelines for Successful Quantitative Gene Expression in Real-Time qPCR Assays. https://doi.org/10.1016/j.colsurfa.2011.12.014

Rougemaille, M., Braun, S., Coyle, S., Dumesic, P. A., Garcia, J. F., Isaac, R. S., … Madhani, H. D. (2012). Ers1 links HP1 to RNAi. *Proceedings of the National Academy of Sciences of the United States of America*, *109*(28), 11258–11263. https://doi.org/10.1073/pnas.1204947109

Rougemaille, M., Shankar, S., Braun, S., Rowley, M., & Madhani, H. D. (2008). Ers1, a rapidly diverging protein essential for RNA interference-dependent heterochromatic silencing in Schizosaccharomyces pombe. *Journal of Biological Chemistry*, *283*(38), 25770–25773. https://doi.org/10.1074/jbc.C800140200

Sadaie, M., Iida, T., Urano, T., & Nakayama, J. I. (2004). A chromodomain protein, Chp1, is required for the establishment of heterochromatin in fission yeast. *EMBO Journal*, *23*(19), 3825–3835. https://doi.org/10.1038/sj.emboj.7600401

Schwartz, B. E., & Ahmad, K. (2005). Transcriptional activation triggers deposition and removal of the histone variant H3.3. *Genes and Development*, *19*(7), 804–814. https://doi.org/10.1101/gad.1259805

Serebryannyy, L. A., Cruz, C. M., & De Lanerolle, P. (2016). A role for nuclear actin in HDAC 1 and 2 regulation. *Scientific Reports*, *6*(May), 1–10. https://doi.org/10.1038/srep28460

Shanker, S., Job, G., George, O. L., Creamer, K. M., Shaban, A., & Partridge, J. F. (2010). Continuous requirement for the Clr4 complex but not RNAi for centromeric heterochromatin assembly in fission yeast harboring a disrupted RITS complex. *PLoS Genetics*, *6*(10), 1–16. https://doi.org/10.1371/journal.pgen.1001174

Shi, X., Hong, T., Walter, K. L., Ewalt, M., Michishita, E., Hung, T., … Gozani, O. (2006). ING2 PHD domain links histone H3 lysine 4

methylation to active gene repression. *Nature*, *442*(7098), 96–99. https://doi.org/10.1038/nature04835

Shi, Y., Lan, F., Matson, C., Mulligan, P., Whetstine, J., Cole, P., … Shi, Y. (2004). Histone Demethylation Mediated by the Nuclear Amine Oxidase Homolog LSD1 Yujiang. *Cell*, *119*, 941–953. https://doi.org/10.1039/FT9949000533

Shin, J. A., Eun, S. C., Hyun, S. K., Ho, J. C. Y., Watts, F. Z., Sang, D. P., & Jang, Y. K. (2005). SUMO modification is involved in the maintenance of heterochromatin stability in fission yeast. *Molecular Cell*, *19*(6), 817–828. https://doi.org/10.1016/j.molcel.2005.08.021

Sijen, T., Fleenor, J., Simmer, F., Thijssen, K., Parrish, S., Timmons, L., … Fire, A. (2001). On the role of RNA in gene amplification. *Cell*, *107*, 465–476.

Siomi, M. C., Sato, K., Pezic, D., & Aravin, A. A. (2011). PIWI-interacting small RNAs: The vanguard of genome defence. *Nature Reviews Molecular Cell Biology*, *12*(4), 246–258. https://doi.org/10.1038/nrm3089

Song, J. J., Smith, S. K., Hannon, G. J., & Joshua-Tor, L. (2004). Crystal structure of argonaute and its implications for RISC slicer activity. *Science*, *305*(5689), 1434–1437. https://doi.org/10.1126/science.1102514

Su, D., Hu, Q., Li, Q., Thompson, J. R., Cui, G., Fazly, A., … Mer, G. (2012). Structural basis for recognition of H3K56-acetylated histone H3-H4 by the chaperone Rtt106. *Nature*, *483*(7387), 104–109. https://doi.org/10.1038/nature10861

Sugioka-Sugiyama, R., & Sugiyama, T. (2011). Sde2: A novel nuclear protein essential for telomeric silencing and genomic stability in Schizosaccharomyces pombe. *Biochemical and Biophysical Research Communications*, *406*(3), 444–448. https://doi.org/10.1016/j.bbrc.2011.02.068

Tie, F., Banerjee, R., Stratton, C. A., Prasad-Sinha, J., Stepanik, V., Zlobin, A., … Harte, P. J. (2009). CBP-mediated acetylation of histone H3 lysine 27 antagonizes Drosophila Polycomb silencing.

Development, *136*(18), 3131–3141. https://doi.org/10.1242/dev.037127

Treiber, T., Treiber, N., & Meister, G. (2019). Regulation of microRNA biogenesis and its crosstalk with other cellular pathways. *Nature Reviews Molecular Cell Biology*, *20*(1), 5–20. https://doi.org/10.1038/s41580-018-0059-1

Verdel, Andre, Jia, S., Gerber, S., Sugiyama, T., Gygi, S., Grewal, S. I. S., & Moazed, D. (2004). RNAi-Mediated Targeting of Heterochromatin by the RITS Complex. *Science*, *303*(5658), 672–676. https://doi.org/10.1126/science.1093686

Verdel, André, Jia, S., Gerber, S., Sugiyama, T., Gygi, S., Grewal, S. I. S., & Moazed, D. (2004). RNAi-Mediated Targeting of Heterochromatin by the RITS Complex. *Science*, *303*(5658), 672–676. https://doi.org/10.1126/science.1093686.RNAi-Mediated

Vermeulen, M., Mulder, K. W., Denissov, S., Pijnappel, W. W. M. P., van Schaik, F. M. A., Varier, R. A., … Timmers, H. T. M. (2007). Selective Anchoring of TFIID to Nucleosomes by Trimethylation of Histone H3 Lysine 4. *Cell*, *131*(1), 58–69. https://doi.org/10.1016/j.cell.2007.08.016

Volpe, T. A., Kidner, C., Hall, I. M., Teng, G., Grewal, S. I. S., & Martienssen, R. A. (2002). Regulation of Heterochromatic Silencing and Histone H3 Lysine-9 Methylation by RNAi. *Science*, *297*, 1833–1837.

Waddington, C. H. (2012). The epigenotype. 1942. *International Journal of Epidemiology*, *41*(1), 10–13. https://doi.org/10.1093/ije/dyr184

Wang, S. H., & Elgin, S. C. R. (2011). Drosophila Piwi functions downstream of piRNA production mediating a chromatin-based transposon silencing mechanism in female germ line. *Proceedings of the National Academy of Sciences of the United States of America*, *108*(52), 21164–21169. https://doi.org/10.1073/pnas.1107892109

Wapenaar, H., & Dekker, F. J. (2016). Histone acetyltransferases: challenges in targeting bi-substrate enzymes. *Clinical Epigenetics*, *8*(1), 1–11. https://doi.org/10.1186/s13148-016-0225-2

Warfield, L., Luo, J., Ranish, J., & Hahn, S. (2016). Function of Conserved Topological Regions within the Saccharomyces cerevisiae Basal Transcription Factor TFIIH. *Molecular and Cellular Biology*, *36*(19), 2464–2475. https://doi.org/10.1128/mcb.00182-16

Weinberg, M. S., & Morris, K. V. (2016). Transcriptional gene silencing in humans. *Nucleic Acids Research*, *44*(14), 6505–6517. https://doi.org/10.1093/nar/gkw139

Wood, V., Gwilliam, R., Rajandream, M. A., Lyne, M., Lyne, R., Stewart, A., … Schäfer, M. (2002). The genome sequence of Schizosaccharomyces pombe. *Nature*, *415*(6918), 94.

Wutz, A. (2011). Gene silencing in X-chromosome inactivation: Advances in understanding facultative heterochromatin formation. *Nature Reviews Genetics*, *12*(8), 542–553. https://doi.org/10.1038/nrg3035

Xu, C., Bian, C., Yang, W., Galka, M., Ouyang, H., Chen, C., … Min, J. (2010). Binding of different histone marks differentially regulates the activity and specificity of polycomb repressive complex 2 (PRC2). *Proceedings of the National Academy of Sciences of the United States of America*, *107*(45), 19266–19271. https://doi.org/10.1073/pnas.1008937107

Yamada, T., Fischle, W., Sugiyama, T., Allis, C. D., & Grewal, S. I. S. (2005). The nucleation and maintenance of heterochromatin by a histone deacetylase in fission yeast. *Molecular Cell*, *20*(2), 173–185. https://doi.org/10.1016/j.molcel.2005.10.002

Yon, J., & Fried, M. (1989). Price gene fusion by PCR. *Nucleic Acids Research*, *17*(12), 4895. https://doi.org/10.1007/978-3-642-04898-2_214

Zeng, L., Zhang, Q., Li, S., Plotnikov, A., Walsh, M., & Zhou, M.-M. (2010). Mechanism and Regulation of Acetylated Histone Binding by the Tandem PHD Finger of DPF3b. *Nature*, *466*(7303), 258–262. https://doi.org/10.1016/j.physbeh.2017.03.040

Zhang, K., Mosch, K., Fischle, W., & Grewal, S. I. S. (2008). Roles of the Clr4 methyltransferase complex in nucleation, spreading and maintenance of heterochromatin. *Nature Structural & Molecular*

Biology, *15*(4), 381–388. https://doi.org/10.1038/nsmb.1406

Zhou, V. W., Goren, A., & Bernstein, B. E. (2011). Charting histone modifications and the functional organization of mammalian genomes. *Nature Reviews. Genetics*, *12*(1), 7–18. https://doi.org/10.1038/nrg2905

Zofall, M., & Grewal, S. I. S. (2006). Swi6/HP1 Recruits a JmjC Domain Protein to Facilitate Transcription of Heterochromatic Repeats. *Molecular Cell*, *22*(5), 681–692. https://doi.org/10.1016/j.molcel.2006.05.010

Appendix

Appendix A: Plasmid maps

I. pREP – clr4

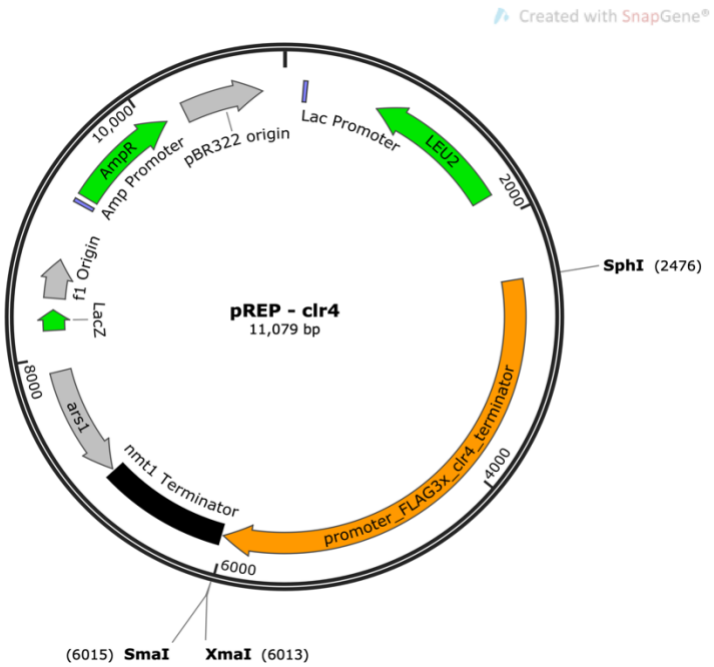

II. pREP – CM1

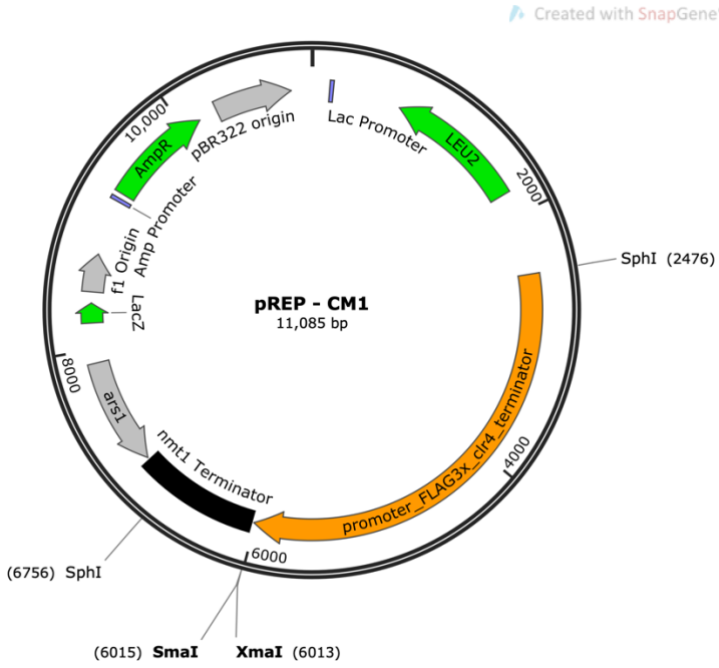

III. pREP – CM2

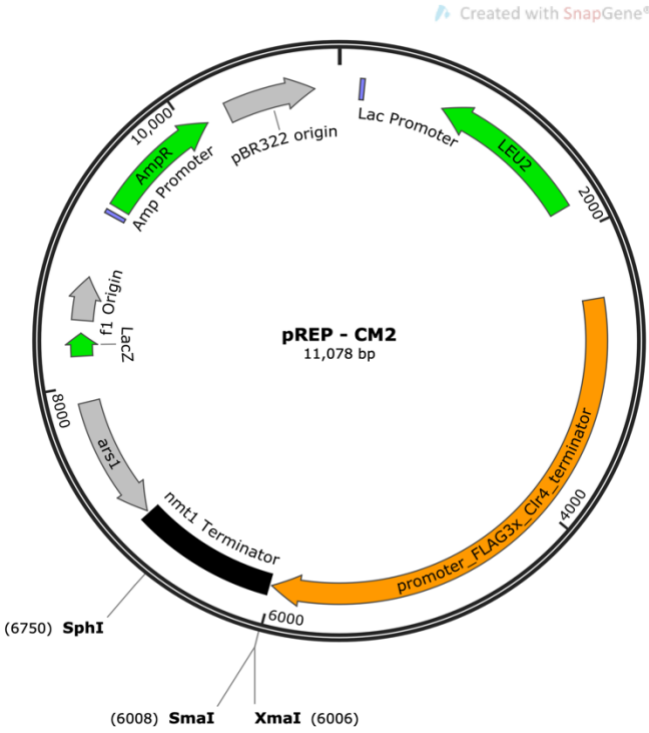

IV. pREP-CD41

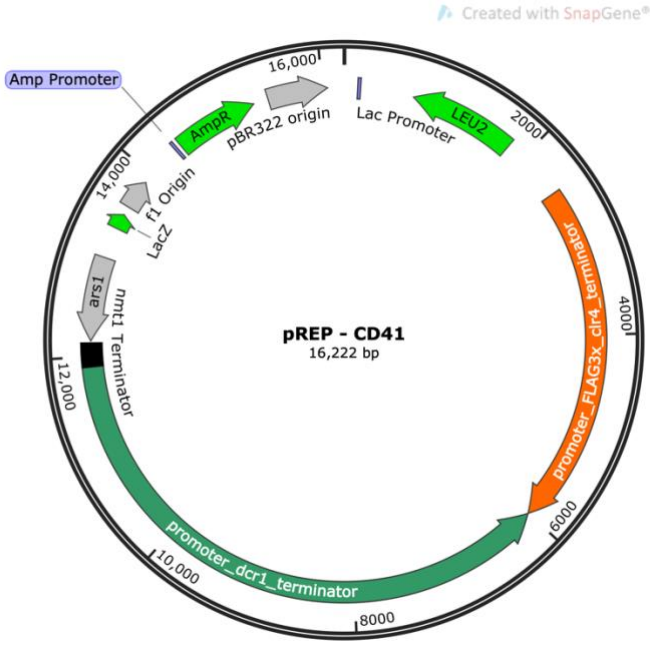

Appendix B: Sample Python code to analyse qPCR data

```
import pandas as pd
import matplotlib.pyplot as plt
from scipy.stats.mstats import gmean
import math
import seaborn as sns
from matplotlib import rcParams

plt.rcParams["patch.force_edgecolor"] = True
get_ipython().run_line_magic('matplotlib', 'inline')

import warnings

warnings.filterwarnings("ignore")


def qpcr_fold(x):
   x_mean = x.groupby('Gt', sort=False).mean()
   GOIeff = 1.855973
   HKeff = 1.99
   pwr_goi = GOIeff ** x_mean['GOI']
   pwr_hk = HKeff ** x_mean['HK']
   pgi = 1 / pwr_goi
   phi = 1 / pwr_hk
   abs_change = pd.DataFrame(pgi / phi)
   control = abs_change.iloc[0][0]
   fold_change = abs_change / control
   return fold_change


# to calculate log2FC
def log_df(df, base):
   logs = [1]
   for i in df[1:len(df)][0]:
      logs.append(math.log(i, base))
   return logs


# Repeat this for all the three replicas
t1 = pd.read_excel('rt_tos1.xlsx')
t1d = pd.DataFrame(qpcr_fold(t1))
t1d.reset_index(inplace=True)
t1d['Gt'][1] = '$\it{clr4Δdcr1Δ}$'
t1d['Gt'][2] = '$\it{clr4Δdcr1Δ+CD41}$'
t1d['Gt'][3] = '$\it{tos4Δclr4Δdcr1Δ}$'
t1d['Gt'][4] = '$\it{tos4Δclr4Δdcr1Δ+CD41}$'

t1d['log2'] = log_df(t1d, 2)

# when all three replicas are loaded,
# concatenate
tos4 = pd.concat([t1d, t2d, t3d])

tos4.sort_index(inplace=True)
tos4.drop(0, axis=1, inplace=True)
```

```
tos4_dict = tos4.groupby(['Gt'], sort=False)['log2'].apply(list).to_dict()

# calculate geometric mean
geom = []
for key, value in tos4_dict.items():
   geom.append([key, gmean(value)])

# In[ ]:


geom_df = pd.DataFrame(geom)
geom_df.rename(columns={0: 'Gt', 1: 'gmean'}, inplace=True)
```

Appendix C: Calibration curves and sample Python code to calculate primer efficiencies

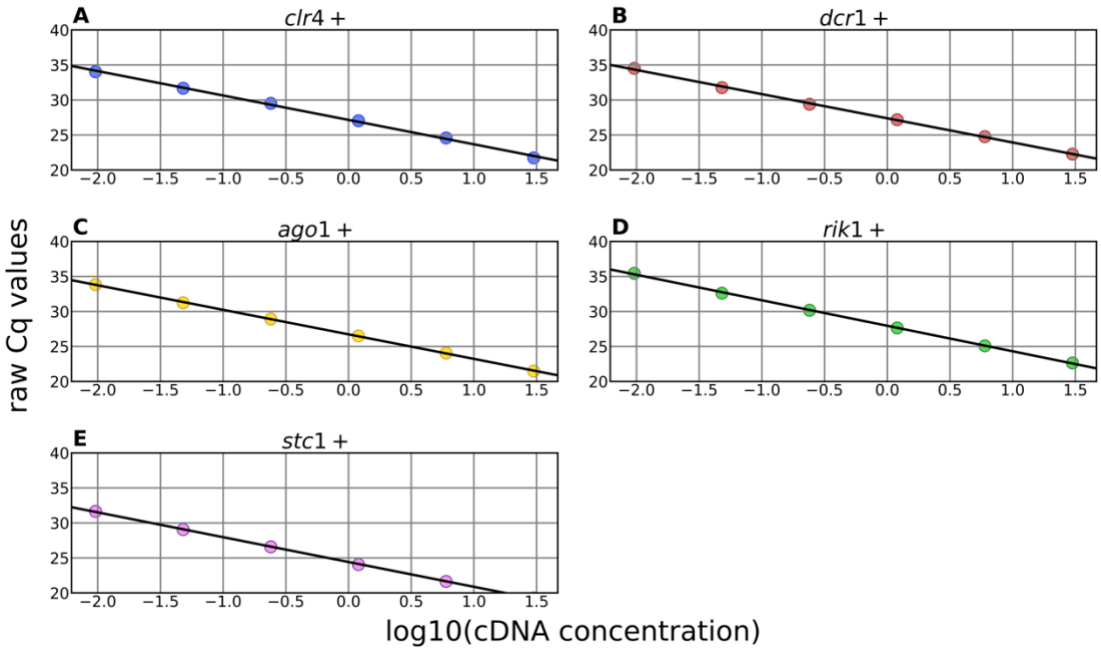

Figure C-1. Calibration curves for qPCR primer pairs listed in table 2-1 used to amplify (A) clr4+, (B) dcr1+, (C) ago1+, (D)rik1+ and (E)stc1+

```
# coding: utf-8


import pandas as pd
import numpy as np
import seaborn as sns
import matplotlib.pyplot as plt

get_ipython().run_line_magic('matplotlib', 'inline')
import math
from scipy import stats

eff = pd.read_excel('rnai_clrc_pr.efficiency_1907_annotatted.xlsx')

eff['log10'] = pd.DataFrame([math.log10(i) for i in eff['Concentration
(ng/ul)']])

# data for calculating clr4 primers efficiency
clr4 = eff[['log10', 'clr4']]
clr4.rename(columns={'clr4': 'Cq'}, inplace=True)


def primer_efficiency(f):
    f_mean = f.groupby('log10', sort=False).mean()  # average two replicas
    f_mean.reset_index(inplace=True)
    f_x = np.array(f_mean['log10'])
    f_y = np.array(f_mean['Cq'])
    f_reg = stats.linregress(f_x, f_y)
    eff = 10 ** (-1 / f_reg[0])  # calculated the efficiency using the
slope
    return {'Slope': round(f_reg[0], 3),
            'Efficiency': round(eff, 3),
            'Intercept': round(f_reg[1], 3),
            'R squared': round(f_reg[2] ** 2, 3),
            'R value': round(f_reg[2], 3),
            'P value': round(f_reg[3], 3),
            'Standard error': round(f_reg[4], 3)}


clr4_info = pd.DataFrame.from_dict(primer_efficiency(clr4),
orient='index')
clr4_info.rename(columns={0: 'Clr4'}, inplace=True)

# primer efficiences were calculated for all the primer pairs
primer_efficiencies = {'Clr4': 1.9357505401814168,
                       'Dcr1': 1.9487415097569485,
                       'Ago1': 1.928829676285554,
                       'Rik1': 1.8811063522834404,
                       'Stc1': 1.9152110916946998,
                       'Rdp1': 1.9449832094854238}
```

Appendix D: Raw Ct values for *act1*+ in figure 4 - 3

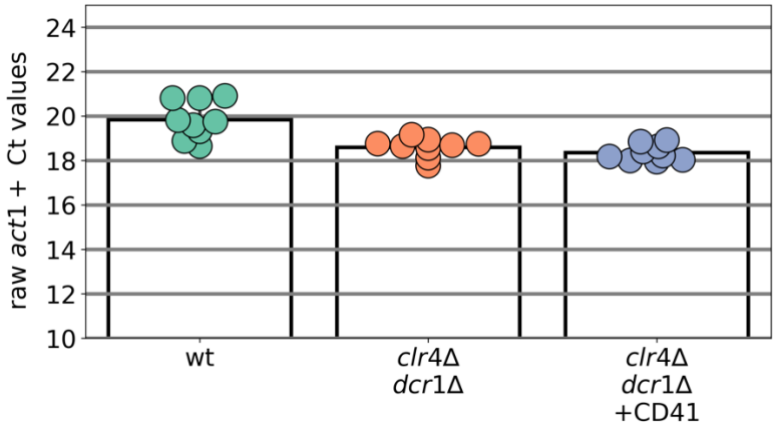

Figure D – 1: *act1*+ is stably expressed. Raw Ct values for *act1*+ amplification in figure 4 – 3.

Appendix E: Raw Ct values for *act1*+ in figure 4 – 4.

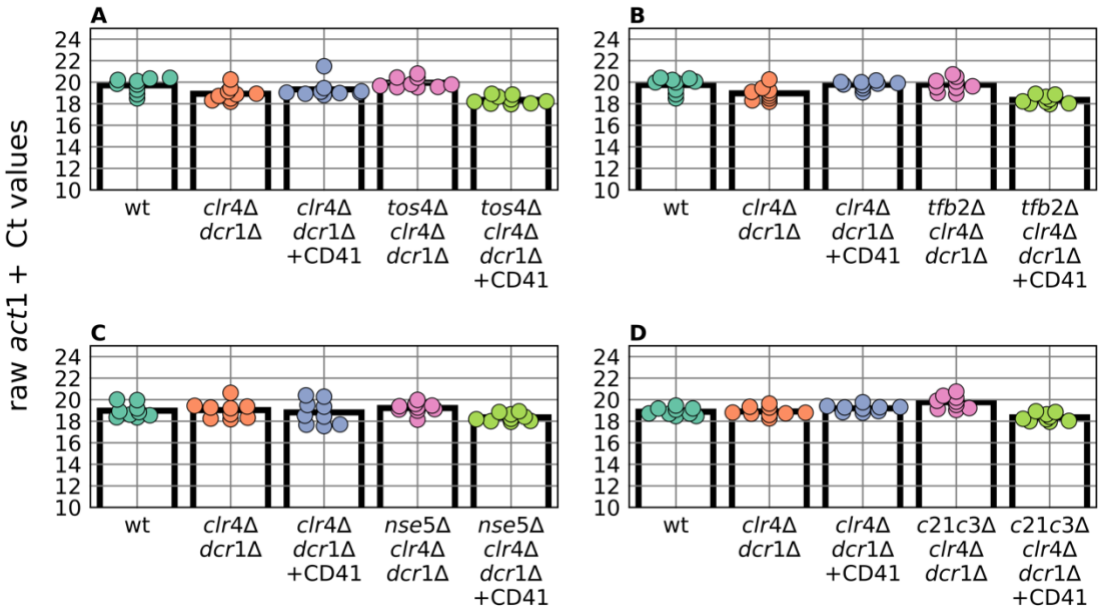

Figure E – 1: *act1*+ is stably expressed. Raw Ct values for *act1*+ amplification in figure 4 – 4.